Fire and Ice: the Geomorphic History of Middle Boulder Creek as Determined by Isotopic Dating Techniques, Colorado Front Range

by

Taylor F. Schildgen

A Thesis submitted in partial fulfillment

of the requirements for the Degree of Bachelor of Arts

with Honors in Geosciences

Williams College,

Williamstown, Massachusetts

2000

ACKNOWLEDGMENTS

First of all I would like to thank my thesis advisor and friend, David Dethier, for the guidance, inspiration, and help that he has provided me throughout my four years at Williams. David's care for and devotion to his students has been one of the most unexpected and valued features of my college career, and has made the whole process of writing this thesis one to be cherished. Thanks also to Paul Bierman at the University of Vermont, without whose help with cosmogenic isotope dating this thesis could not have been possible, and without whose easy-going, upbeat attitude the sample processing and long nights in Livermore, CA might have been drudgery. I cannot thank both David and Paul enough for endless editing scrawls that have contributed immensely to this thesis. Special thanks to Gordon Cook, Bob Anderson, and Philip Naysmith at Scottish Universities Environmental Research Centre (SUERC), who all contributed generously to the process of obtaining radiocarbon dates; Pete Birkeland for invaluable help and suggestions in the field, as well as help with charcoal collection; Jennifer Larson and Ben Copans for help with cosmogenic sample processing at the University of Vermont Cosmogenic Nuclide Extraction Laboratory; Marc Caffee for all of his time at Lawrence Livermore National Laboratory; my fellow 1999-2000 Geo thesis women -- Rebecca Atkinson, Carla Chokel, Patty Hines, and Cordy Ransom, who were always ready to lend advice, suggestions, and anything else to make the whole process a little bit easier, and to all the other people who helped guarantee an upbeat and lively working atmosphere in the geo computer lab. Thanks to Jeff Coe, Scott Elias, Tom Veblen, and Paul Carrara, who all helped in obtaining obscure and not-so-obscure papers and articles, and thanks to all the other people who contributed in some way, shape, or form: Malcolm Pringle, Laura Mallard and Simon, and the guy who flew the plane for us in Boulder. Finally, thanks to the entire Geosciences Department at Williams, of which I will always be proud and happy to have been a part.

ABSTRACT

Cosmogenic ^{26}Al, ^{10}Be, ^{14}C, and ^{36}Cl dating of fluvial fill terraces and other geomorphic surfaces along steep canyons of the Colorado Front Range provides a temporal framework for analyzing fluvial response to sediment budget perturbations. Fluvial terraces > 4 m above the Middle Boulder Creek channel (grade) record activity during late Pleistocene time. Terraces < 4 m above grade and alluvial fans preserve evidence for system responses to Holocene climate change. The fluvial processes that these surfaces record contributes to a comprehensive understanding of the long-term evolution of Front Range canyons.

Cosmogenic exposure ages of boulders on glacial moraines near Boulder Canyon are consistent with glacial chronologies derived from nearby regions. Samples from Bull Lake moraines have minimum average ^{10}Be and ^{26}Al ages of 101 ± 21 ka and 122 ± 26 ka, comparable to other age estimates of 150 to 100 ka for moraines at sites in Wyoming, southwest Montana, and other regions of Colorado. Pinedale moraines near Nederland have average model ^{10}Be and ^{26}Al ages of 16.9 ± 3.5 and 17.5 ± 3.6 ka, consistent with other cosmogenic exposure ages and ^{14}C estimates of 35 to 15 ka reported elsewhere in the Rocky Mountains. These new age estimates, considered together with field relationships, suggest that late Pinedale glaciers were nearly as extensive as those active during earlier Pinedale and Bull Lake advances.

The fluvial response to glaciation in the Front Range can be analyzed using regional and local late Pleistocene glacial chronology and cosmogenic exposure age estimates for fill terraces in Boulder Canyon. Results from Boulder Canyon show that terrace heights above grade can be divided into (1) Bull Lake (> ~100 ka) at 15 to 20 m above grade; (2) Pinedale (30 to10 ka) at 4 to15 m above grade; and (3) Holocene age at < 4 m above grade. Better-preserved terraces of latest Pleistocene age suggest that variations of height above grade reflect short-term fluctuations in the river profile during periods of rapidly changing stream load and power. Net river incision apparently occurred during transitions to interglacial periods. Soil development and stratigraphic position, used with limited cosmogenic and ^{14}C dating suggests that ~ 130 ka terraces in Boulder Canyon correlate with the Louviers or Slocum Alluviums , and that 32 to 10 ka fills in the Canyon correlate with the Broadway Alluvium on the High Plains east of the Front Range. Middle to late Pleistocene incision rates represented by high terraces in Boulder Canyon are higher than early Pleistocene rates, possibly as a result of east to west migration of a knickpoint on Middle Boulder Creek.

Low terraces (< 4 m above grade) and alluvial fans in Boulder Canyon record Holocene deposition resulting from forest fires related to climate change. Forest fires destabilized small (0.5-1.0 km^2) tributary catchments within the canyon during the early and late Holocene, producing episodes of alluvial deposition. Alluvial fans accumulated

TABLE OF CONTENTS

ACKNOWLEDGMENTS ii
ABSTRACT iii
TABLE OF CONTENTS v
LISTS OF FIGURES, TABLES, AND APPENDICES vii
INTRODUCTION 1
Geomorphology 4
Geomorphic record and glacial and nonglacial events 4
Incision rates and evolution of the river profile 14
Setting 16
Boulder Canyon and glaciated regions in north-central Colorado 16
Present and Holocene climate and vegetation in the Front Range 16
GEOLOGICAL HISTORY 21
Evolution of the Front Range 21
Glacial history 23
METHODS 27
Field mapping 27
Dating methods 30
Exposure-age dating using cosmogenic isotopes 30
Cosmogenic sampling 35
^{14}C dating 39
^{14}C sampling 43
Laboratory procedures 45
$^{26}Al/^{10}Be$ sample processing 45
^{14}C sample processing 50
GLACIATION IN THE COLORADO FRONT RANGE 53
Introduction 53
Cosmogenic exposure ages of Bull Lake and Pinedale Moraines 53
Discussion 55
FLUVIAL TERRACES OF BOULDER CANYON 58
Introduction 58
Boulder Canyon terraces 59
Morphology, correlation and weathering 59
Cosmogenic exposure ages 60
Soil profile 62
Discussion 62
Terrace heights and changing base levels 62

ABSTRACT

Cosmogenic ^{26}Al, ^{10}Be, ^{14}C, and ^{36}Cl dating of fluvial fill terraces and other geomorphic surfaces along steep canyons of the Colorado Front Range provides a temporal framework for analyzing fluvial response to sediment budget perturbations. Fluvial terraces > 4 m above the Middle Boulder Creek channel (grade) record activity during late Pleistocene time. Terraces < 4 m above grade and alluvial fans preserve evidence for system responses to Holocene climate change. The fluvial processes that these surfaces record contributes to a comprehensive understanding of the long-term evolution of Front Range canyons.

Cosmogenic exposure ages of boulders on glacial moraines near Boulder Canyon are consistent with glacial chronologies derived from nearby regions. Samples from Bull Lake moraines have minimum average ^{10}Be and ^{26}Al ages of 101 ± 21 ka and 122 ± 26 ka, comparable to other age estimates of 150 to 100 ka for moraines at sites in Wyoming, southwest Montana, and other regions of Colorado. Pinedale moraines near Nederland have average model ^{10}Be and ^{26}Al ages of 16.9 ± 3.5 and 17.5 ± 3.6 ka, consistent with other cosmogenic exposure ages and ^{14}C estimates of 35 to 15 ka reported elsewhere in the Rocky Mountains. These new age estimates, considered together with field relationships, suggest that late Pinedale glaciers were nearly as extensive as those active during earlier Pinedale and Bull Lake advances.

The fluvial response to glaciation in the Front Range can be analyzed using regional and local late Pleistocene glacial chronology and cosmogenic exposure age estimates for fill terraces in Boulder Canyon. Results from Boulder Canyon show that terrace heights above grade can be divided into (1) Bull Lake (> ~100 ka) at 15 to 20 m above grade; (2) Pinedale (30 to10 ka) at 4 to15 m above grade; and (3) Holocene age at < 4 m above grade. Better-preserved terraces of latest Pleistocene age suggest that variations of height above grade reflect short-term fluctuations in the river profile during periods of rapidly changing stream load and power. Net river incision apparently occurred during transitions to interglacial periods. Soil development and stratigraphic position, used with limited cosmogenic and ^{14}C dating suggests that ~ 130 ka terraces in Boulder Canyon correlate with the Louviers or Slocum Alluviums , and that 32 to 10 ka fills in the Canyon correlate with the Broadway Alluvium on the High Plains east of the Front Range. Middle to late Pleistocene incision rates represented by high terraces in Boulder Canyon are higher than early Pleistocene rates, possibly as a result of east to west migration of a knickpoint on Middle Boulder Creek.

Low terraces (< 4 m above grade) and alluvial fans in Boulder Canyon record Holocene deposition resulting from forest fires related to climate change. Forest fires destabilized small (0.5-1.0 km^2) tributary catchments within the canyon during the early and late Holocene, producing episodes of alluvial deposition. Alluvial fans accumulated at rates between 0.2 and 95 $Mgha^{-1}yr^{-1}$ depending on whether we assume constant or

episodic sediment accumulation rates. Alluvial deposition and associated forest fire occurrence in Boulder Canyon correlate with a late Holocene climate characterized by conditions drier than at present. Fire and deposition is also correlated with the warm and wet early Holocene climate which likely induced widespread vegetation growth to fuel extensive fires during occasional dry periods. Alluvial fans and fluvial terraces appear to be effective in preserving evidence of past climate change, and of processes that have contributed to the evolution of the Colorado Front Range.

TABLE OF CONTENTS

ACKNOWLEDGMENTS ii
ABSTRACT iii
TABLE OF CONTENTS v
LISTS OF FIGURES, TABLES, AND APPENDICES vii
INTRODUCTION 1
Geomorphology 4
Geomorphic record and glacial and nonglacial events 4
Incision rates and evolution of the river profile 14
Setting 16
Boulder Canyon and glaciated regions in north-central Colorado 16
Present and Holocene climate and vegetation in the Front Range 16
GEOLOGICAL HISTORY 21
Evolution of the Front Range 21
Glacial history 23
METHODS 27
Field mapping 27
Dating methods 30
Exposure-age dating using cosmogenic isotopes 30
Cosmogenic sampling 35
^{14}C dating 39
^{14}C sampling 43
Laboratory procedures 45
$^{26}Al/^{10}Be$ sample processing 45
^{14}C sample processing 50
GLACIATION IN THE COLORADO FRONT RANGE 53
Introduction 53
Cosmogenic exposure ages of Bull Lake and Pinedale Moraines 53
Discussion 55
FLUVIAL TERRACES OF BOULDER CANYON 58
Introduction 58
Boulder Canyon terraces 59
Morphology, correlation and weathering 59
Cosmogenic exposure ages 60
Soil profile 62
Discussion 62
Terrace heights and changing base levels 62
Long-profile evolution of Middle Boulder Creek 67

LIST OF FIGURES

Figure 1. Map showing Front and Sawatch Range, Colorado, and location of dated late Pleistocene sites discussed in the text: Sky Pond (Menounos and Reasoner, 1997); Butterfly Lake (Davis et al., 1992); upper Fraser River Valley (Nelson et al, 1979); and Echo Lake (Doerner,1994) 3

Figure 2. Schematic diagram showing how till of Pinedale, Bull Lake, and pre-Bull Lake age differs in position, topographic expression, and degree of weathering. Stronger soil development is expressed mainly in the B-horizon in the form of redder colors, greater clay content, and higher fine-clay to coarse-clay ratios (modified from Madole et al., 1998) 7

Figure 3. Maps showing late Pleistocene moraines and ice limits near Nederland (modified from Gable and Madole, 1976; Madole, 1976a; Madole et al., 1998) and at Twin Lakes Reservoir (modified from Nelson et al, 1984; Nelson and Shroba, 1998) and sites sampled for cosmogenic ages; scale: 1:24,000 8

Figure 4. Strath and fill terrace formation: a) formation of fill terraces from valley filling and subsequent incision, stranding alluvium as terraces on either side; b) formation of strath terraces from incision through bedrock channels, stranding the previous bedrock valley floor as terraces on either side (modified from Merritts et al., 1994) 9

Figure 5. Valley cross-section illustrating different types of fluvial terraces (modified from Bull, 1991); colluvium locally buries fill terrace 11

Figure 6. Alluvial fans at sites T41, T4, and T2; 1.0 m contours show height above reference point on Middle Boulder Creek; note: Middle Boulder Creek not drawn to scale; (a) alluvial fan at site T41; (b) alluvial fan near site T4; (c) alluvial fan near site T2 12

Figure 7. Drainage areas of Boulder Canyon alluvial fans; scale is 1:12,000 (1:24,000 map enlarged 200%); a) drainage area at site T2; total area = 1.02 km^2; b) drainage area at site T1; total area = 0.52 km^2; c) drainage area at site T41; area = 0.62 km^2; d) drainage area at site T6; area = 0.60 km^2 13

Figure 8. Map showing location of Middle Boulder Creek and nearby rivers in the Colorado Front Range, north central Colorado; Middle Boulder Creek catchment is shaded. Arrows show area sampled for cosmogenic exposure and ^{14}C dating 17

Figure 9. Profile of Middle Boulder Creek showing sample locations (sites are designated as dark triangles with the 99-T number plotted) and the surveyed reach in the inset window 18

Figure 10. Digital elevation model showing Pleistocene glacial limits in the northern Front Range (from Madole et al., 1998) 22

Figure 11. Depth profiles of ^{26}Al and ^{10}Be production rates in rock and sand. Profiles were created using the formula $P_x = P_o e^{-(x\rho/\Lambda)}$ where P_x = production rate at depth x; P_o = production rate; ρ = density of material; and Λ = attenuation length. For ^{26}Al, I assumed a production rate of 36.8 $atmg^{-1}yr^{-1}$ (Nishiizumi et al., 1989) multiplied by 2.4 to correct for altitude and latitude (2000 m, 40 degrees north). For ^{10}Be, I assumed a production rate of 6.0 $atmg^{-1}yr^{-1}$ (Nishiizumi et al., 1989) multiplied by 2.4 to correct for altitude and latitude. For rock, I assumed a density of 2.7 g/cm^3 (quartz-rich); for sand I assumed a density of 1.5 gcm^{-3}. I used an attenuation length of 160 gcm^{-2} (Lal, 1991; Brown et al., 1992).....31

Figure 12. Contour plots of altitude/latitude correction factors for cosmic ray flux and isotope production at Earth's surface based on data presented by Lal (1991) (from Bierman, 1994) 32

Figure 13. Boulders sampled from glacial moraines at Nederland and Lake Devlin; a) site 99-T75, boulder on Bull Lake moraine at Lake Devlin; length x width x height = 5 m x 3 m x 1 m; b) site 99-T76, boulder on Pinedale moraine at Lake Devlin; 4 m x 3.3 m x 1.5 m; c) boulder on Bull Lake moraine at Nederland; 2 m x 2 m x 1.5 m 36

Figure 14. Cosmogenic sample sites; a) site 99-T71-1, boulder 2m x 1.5 m x 0.8 m on 12 m terrace; sample collected from polished top surface; b) site 99-T71-1, cobbles collected from 30 cm below surface of 12 m terrace; c) site 99-T60-1, boulder 4.2 m x 2.8 m x 2.2 m, sample collected from where David Dethier sits; sample 5.0 m above Middle Boulder Creek 38

Figure 15. Cosmogenic sample sites; a) site 99-T26, sample collected from polished bedrock above pothole, 6.7 m above Middle Boulder Creek; b) site 99-T43, sample collected from terrace surface as shown, 7.5 m above Middle Boulder Creek; c) site 99-t10-1, cobbles collected from 65 cm below the surface of a 10 m terrace.....40

Figure 16. ^{14}C in the biosphere: radioactive carbon forms from the interaction of cosmic ray neutrons with nitrogen in the atmosphere. Following oxidation, ^{14}C is integrated into the biosphere through photosynthesis and thence through ingestion by animals (modified from Aitken, 1990) 41

Figure 17. Superficial deposits near Middle Boulder Creek on the Tungsten, CO 7.5' quadrangle; dashed regions show drainage areas for alluvial fans; charcoal sample sites are marked with dark triangles; graphic logs illustrate stratigraphic position of charcoal samples within soil pits 44

Figure 18. Flow chart of sample cleaning and quartz isolation 46

Figure 19. Flow chart of quartz dissolution 48

Figure 20. Flow chart of column separation of ^{10}Be and ^{26}Al 49

Figure 21. Flow chart of target preparation of samples 51
Figure 22. Cosmogenic exposure ages in soil profile at site T64 showing variation about a mean age of ~ 3 ka; all samples are from the soil profile except for the labeled rock sample 63
Figure 23. Terrace age versus height above grade, showing height range within glacial periods, and significant differences in height among different glacial periods. Bull Lake age deposition is thought to occur before ~100 ka, Pinedale deposition between ~10 and 30 ka, and Holocene age deposition between ~10 ka and today ..65
Figure 24. Rates of river incision based on age and terrace height above grade in Boulder Canyon and on the High Plains. Rates between data points are listed on graph. Long term incision rates are based on 20 m of canyon incision since 130 ka, and 7 m of Plains incision since 190 ka 66
Figure 25. Schematic cross-section of Boulder Canyon illustrating stratigraphic and age relationships of Holocene, Pinedale, and Bull Lake terraces 68
Figure 26. Profile of Middle Boulder Creek with terrace height above river exaggerated; 100 m is added to the elevation of Holocene age terraces, 200 m to late Pinedale terraces, 300 m to early Pinedale terraces, and 400 m to Bull Lake terraces, resulting in the offset appearance of terraces. Elevations of sites on Slocum and Broadway terraces are circled to distinguish them from Boulder Canyon terraces 69
Figure 27. Schematic cross-section of the inner canyon illustrating stratigraphic and age relationships of latest Pleistocene outwash, and Holocene alluvial fans and fluvial terraces on Middle Boulder Creek 75

LIST OF TABLES

Table 1. Quaternary time chart and provisional ages of glaciations (modified from Madole et al., 1998) 2
Table 2. Description and ages of High Plains alluvial surfaces 5
Table 3. Descriptions, soil characteristics, and age estimates of sample sites (Netoff, 1977) 28
Table 4. Model ages derived from cosmogenic isotope data for samples collected on glacial moraines near Nederland and Twin Lakes Reservoir, Colorado 54
Table 5. Cosmogenic isotope data for samples collected within Boulder Canyon 61
Table 6. Charcoal sample locations and ages 76
Table 7. Short and long term accumulation rates of alluvial fan material 78

LIST OF APPENDICES

Appendix A. Calibrated and uncalibrated ^{14}C ages 99
Appendix B. Cosmogenic isotope data for all glacial moraine and Boulder Canyon samples 100

INTRODUCTION

The remnants of river terraces and alluvial fans preserved in the deeply incised canyons of the Colorado Front Range reflect a history of long-term river incision, large scale Pleistocene sediment budget perturbations, and small scale Holocene perturbations. Relative dating techniques including the degree of soil development, landform shape, degree of rock weathering, and stratigraphic position have been used to draw broad correlations between the timing of terrace formation and glacial events (e.g., Netoff, 1977; Birkeland, personal communication) and to infer long-term evolution of longitudinal river profiles (e.g., Campbell, 1961). In this thesis I explore the relationship between glacial chronology of the Front Range and the fluvial responses to glacial events as preserved in Boulder Canyon through the use of ^{26}Al and ^{10}Be cosmogenic exposure age dating techniques. I also apply ^{14}C dating methods to determine ages of Holocene alluvial fans and terraces which indicate small-scale Holocene sediment budget perturbations within side channels of the canyon. The application of these field-based isotope dating techniques in Boulder Canyon represents the first attempt to quantitatively constrain the timing of multiple depositional and erosional events in a canyon draining the Colorado Front Range, and to correlate these events with climate change. Cosmogenic exposure age dating constrains the timing of middle and late Pleistocene glacial events in the region and provides a reasonable estimate of the incision rates of Middle Boulder Creek. ^{14}C dating provides new information concerning the Holocene history of Boulder Canyon, and the character of erosive processes in the canyon.

In this thesis, I explore the timing of two late Pleistocene glacial advances, and their effects on the fluvial dynamics of Middle Boulder Creek. The Bull Lake glaciation and the Pinedale glaciation (Table 1) brought lobes of ice out as far east as Barker Reservoir, Glacial Lake Devlin, and Twin Lakes Reservoir (Fig. 1). Middle Boulder

Table 1. Quaternary time chart and provisional ages of glaciations (modified from Madole et al., 1998)

FORMAL TIME DIVISIONS		INFORMAL TIME TERMS		GLACIATIONS	AGE (ka)
Quaternary Period	Holocene Epoch				
				Santanta Peak	10
	Pleistocene Epoch	late Pleistocene			~13
				Pinedale glaciation	
					~35
		middle Pleistocene	late	Bull Lake glaciation	~130
			middle	pre-Bull Lake glaciations	~300
			early		~620
		early Pleistocene			~788
					1800
Tertiary Period (part)	Pliocene Epoch				

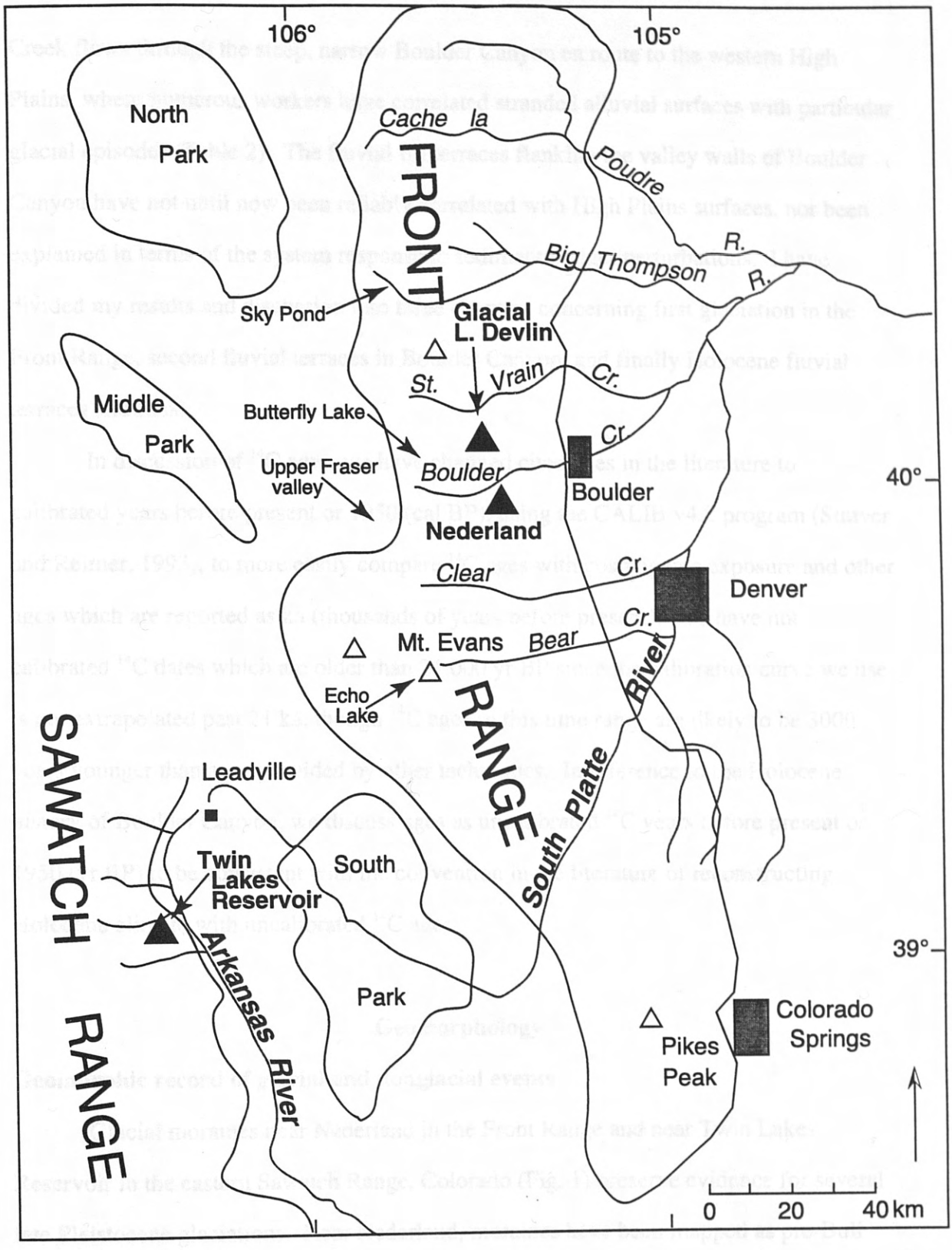

Figure 1. Map showing Front and Sawatch Range, Colorado, and location of dated late Pleistocene sites discussed in the text: Sky Pond (Menounos and Reasoner, 1997); Butterfly Lake (Davis et al., 1992); upper Fraser River Valley (Nelson et al., 1979); and Echo Lake (Doerner, 1994); Glacial Lake Devlin (Madole, 1986). (Modified from Steven et al., 1997).

Creek flows through the steep, narrow Boulder Canyon en route to the western High Plains, where numerous workers have correlated stranded alluvial surfaces with particular glacial episodes (Table 2). The fluvial fill terraces flanking the valley walls of Boulder Canyon have not until now been reliably correlated with High Plains surfaces, nor been explained in terms of the system response to sediment budget perturbations. I have divided my results and discussion into three chapters concerning first glaciation in the Front Range, second fluvial terraces in Boulder Canyon, and finally Holocene fluvial terraces and fans.

In discussion of ^{14}C ages, we have changed cited ages in the literature to calibrated years before present or 1950 (cal BP), using the CALIB v4.2 program (Stuiver and Reimer, 1993), to more easily compare ^{14}C ages with cosmogenic exposure and other ages which are reported as ka (thousands of years before present). We have not calibrated ^{14}C dates which are older than 21,000 yr BP since the calibration curve we use is not extrapolated past 21 ka, though ^{14}C ages in this time range are likely to be 3000 years younger than ages provided by other techniques. In reference to the Holocene history of Boulder Canyon, we discuss ages as uncalibrated ^{14}C years before present or 1950 (yr BP) to be consistent with the convention in the literature of reconstructing Holocene climate with uncalibrated ^{14}C ages.

Geomorphology

Geomorphic record of glacial and nonglacial events

Glacial moraines near Nederland in the Front Range and near Twin Lakes Reservoir in the eastern Sawatch Range, Colorado (Fig. 1) preserve evidence for several late Pleistocene glaciations. Near Nederland, moraines have been mapped as pre-Bull Lake (middle Pleistocene), Bull Lake (late Pleistocene), and Pinedale (latest Pleistocene), based on soil development, extent of boulder weathering, and moraine morphology (Fig.

Table 2: Description and ages of High Plains alluvial surfaces

Alluvium	Height above grade (m)[1]	Local height[2] (m)	Correlative glaciation[3]	Age estimate	Basis for age estimate	Reference
Nussbaum	~ 140		pre-Bull Lake	> 1.35 Ma	stratigraphy	
Rocky Flats	100 ± 10		pre-Bull Lake	1.35 Ma	soil development	Birkeland, 1999
Verdos	70 ± 5	20-25	pre-Bull Lake	640 ka	Lava Creek B ash	Hunt, 1954; Scott, 1963b
Slocum	6 - 30	7	Bull Lake	190 ± 50 ka	U-series bone	Scott and Lindvall, 1970; Szabo, 1980
Louviers	< 10	4 - 7	Bull Lake	129 ± 10 ka	U-series bone	Szabo, 1980
				86 ± 6 ka	U-series bone	
Broadway	< 9	4	Pinedale	< 38 ka	^{14}C	Machette, 1977
Piney Creek	< 5	< 4	Holocene	< 10 ka	^{14}C	

Notes:

1: Height above grade from Madole, 1991; Scott 1960, 1962,

2: Local height above grade from Boulder Quadrangle geology, Wruck et al., 1967.

3: From Birkeland et al., 1999; correlation derived from glacial chronology of the Front Range.

2; Gable, 1969; Gable and Madole, 1976; Madole, 1976a and unpublished data). Bull Lake and Pinedale-age deposits dominate the glacial record, but pre-Bull Lake deposits (Madole and Shroba, 1979) are present locally. In most of the upland Front Range mapped by Madole et al. (1998), Pinedale till and outwash fill broad valleys whereas Bull Lake till crops out in thin zones, between Pinedale moraines and high bedrock ridges. The upper reaches of alpine cirques preserve post-Pinedale glacial and glaciofluvial deposits locally, but far upvalley of pre-Bull Lake, Bull Lake, and Pinedale moraines (Davis et al. 1992). Near Twin Lakes, in the Sawatch Range, there is some uncertainty about assignment to the Bull Lake or Pinedale glaciations. Cosmogenic exposure ages of moraines near Nederland, Colorado and near Twin Lakes Reservoir should indicate the timing of maximum glaciation since the moraines in these locations are in close proximity to the farthest extent of glaciers in the region (Fig. 3).

If fill terrace formation is related to glacial events, then exposure ages of fluvial fill terraces in Boulder Canyon should also provide constraints on the timing of glacial events. Fluvial terraces, with upper strath surfaces 1 to12 m above the present level of Middle Boulder Creek, are common in the inner canyon, along with extensive areas of colluvial debris and localized alluvial fans. Fill terraces form by valley aggradation of alluvial material above a bedrock channel, followed by channel incision through the alluvium. A fill terrace may record aggradation in response to an increased sediment load followed by incision when the sediment load is removed (Merritts et al., 1994). In glaciated regions, widespread exposure of unconsolidated sediment during and immediately after glacial retreat led to high sediment loads transported by glacial meltwater and aggradation for some distance downstream (Madole et al., 1998). When the sediment supply diminished, meltwater cut down through the alluvium, stranding terraces (Fig. 4). However, subsequent erosion would generally prevent terraces from providing a complete, unambiguous record of geomorphic response to a glacial episode.

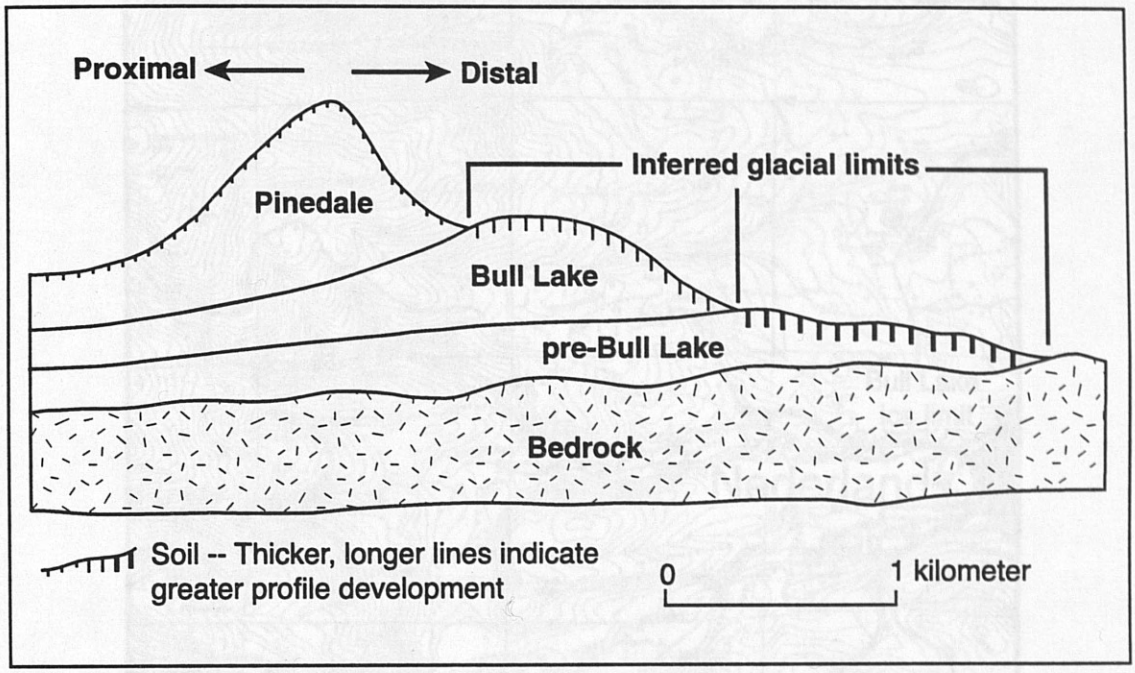

Figure 2. Schematic diagram showing how till of Pinedale, Bull Lake, and pre-Bull Lake age differs in position, topographic expression, and degree of weathering. Stronger soil development is expressed mainly in the B-horizon in the form of redder colors, greater clay content, and higher fine-clay to coarse-clay ratios (modified from Madole, 1998).

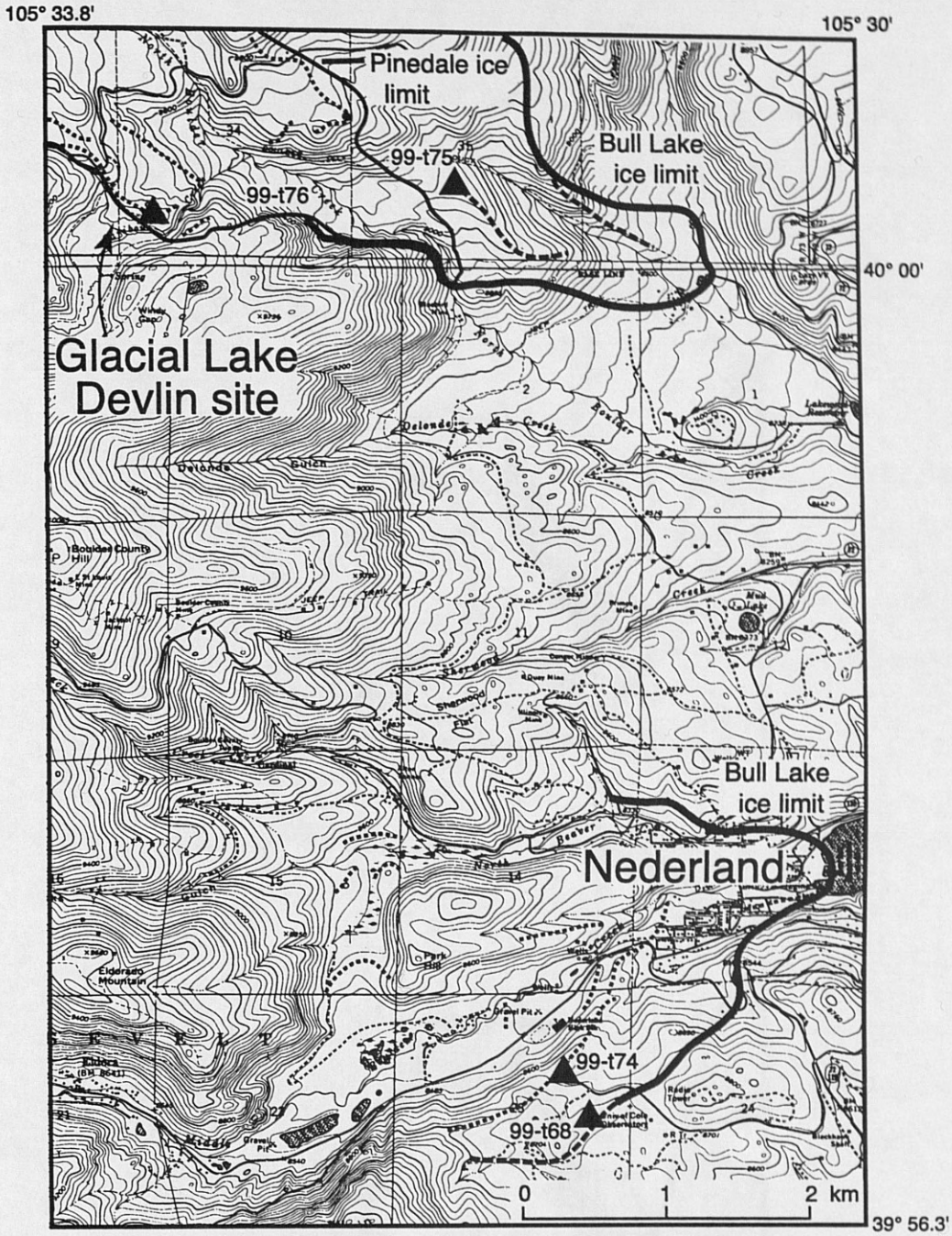

U. S. G. S. Nederland and Ward 7.5' quadrangles

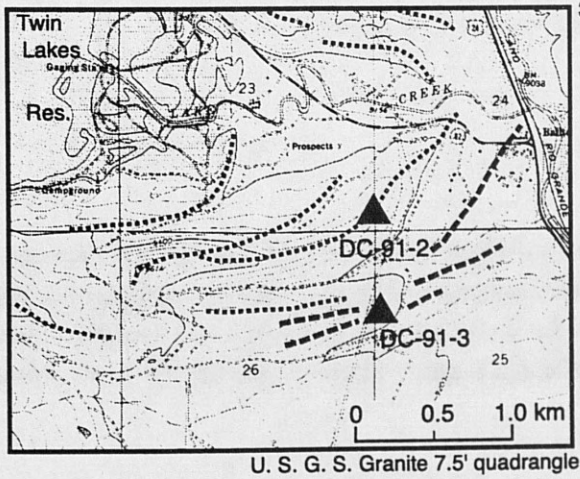

U. S. G. S. Granite 7.5' quadrangle

Figure 3. Maps showing late Pleistocene moraines and ice limits near Nederland (modified from Gable and Madole, 1976; Madole, 1976a; Madole et al., 1998) and Twin Lakes Reservoir (modified from Nelson et al., 1984; Nelson and Shroba, 1998) and sites sampled for cosmogenic dating; scale: 1:24,000.

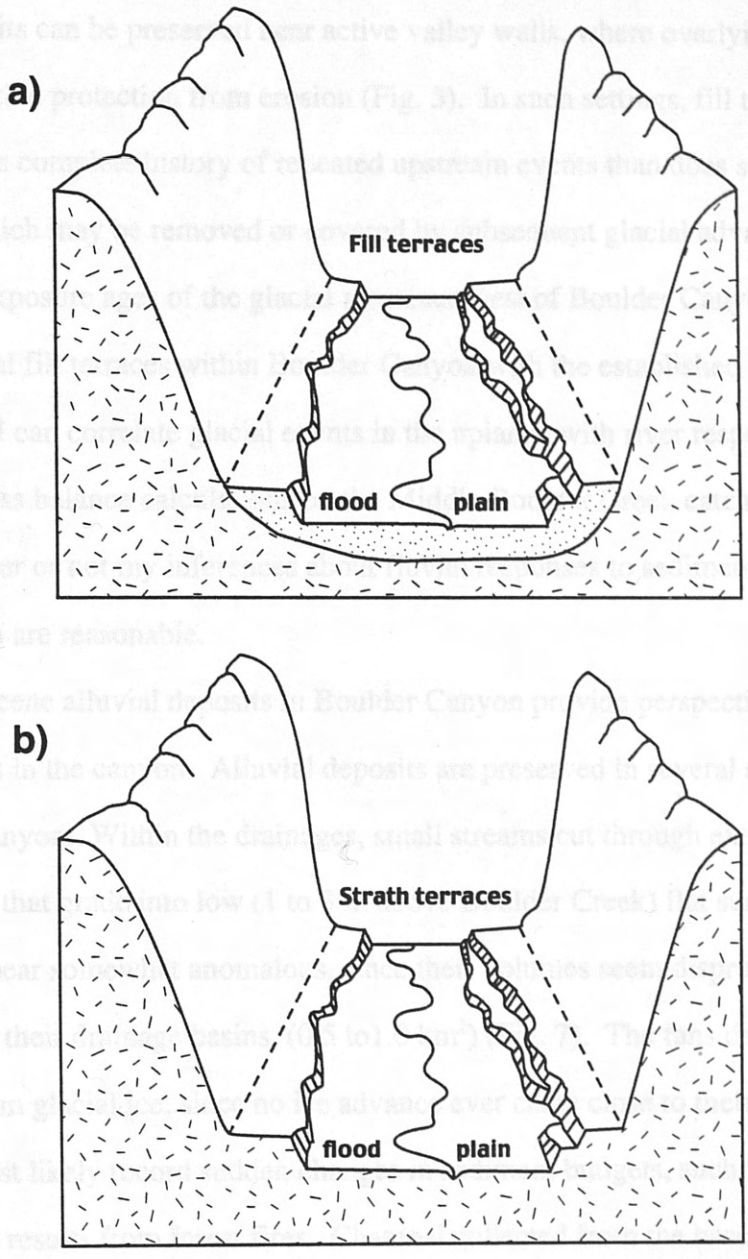

Figure 4. Strath and fill terrace formation: a) formation of fill terraces from valley filling and subsequent incision, stranding alluvium as terraces on either side; b) formation of strath terraces from incision through bedrock channels, stranding the previous bedrock valley floor as terraces on either side. (modified from Merritts et al., 1994).

Coarse glacial outwash is unstable and is preserved best where it is boulder rich or covered with coarse material such as colluvium. In a downcutting river system, older fluvial deposits can be preserved near active valley walls, where overlying colluvial deposits provide protection from erosion (Fig. 5). In such settings, fill terraces may record a more complete history of repeated upstream events than does source area evidence, which may be removed or covered by subsequent glacial advances. By comparing exposure ages of the glacial moraines west of Boulder Canyon and exposure ages of fluvial fill terraces within Boulder Canyon with the established regional glacial chronology, I can correlate glacial events in the uplands with river responses in Boulder Canyon. Mass balance calculations on the Middle Boulder Creek catchment can help to reveal whether or not my inferences about fluvial responses to sediment budget perturbations are reasonable.

Holocene alluvial deposits in Boulder Canyon provide perspective on relatively recent events in the canyon. Alluvial deposits are preserved in several side drainages within the canyon. Within the drainages, small streams cut through extensive terraced alluvial fans that grade into low (1 to 3 m above Boulder Creek) flat surfaces (Fig. 6). The fans appear somewhat anomalous, since their volumes seem disproportionately large compared to their drainage basins (0.5 to1.0 km^2) (Fig. 7). The fans did not receive sediment from glacial ice, since no ice advance ever came close to their drainage basins. The fans most likely record sudden changes in sediment budgets, such as the loss in slope stability that results from forest fires. Charcoal collected from the base of fans and from fill terraces located downstream of the fans provides information concerning the timing of fan formation, and concerning the erosive character of the event(s) that led to fan development. Comparison of the timing of fan and low terrace formation with the Holocene climate record contributes to discussion about links between characteristic climate regimes and alluvial fan/fluvial terrace formation.

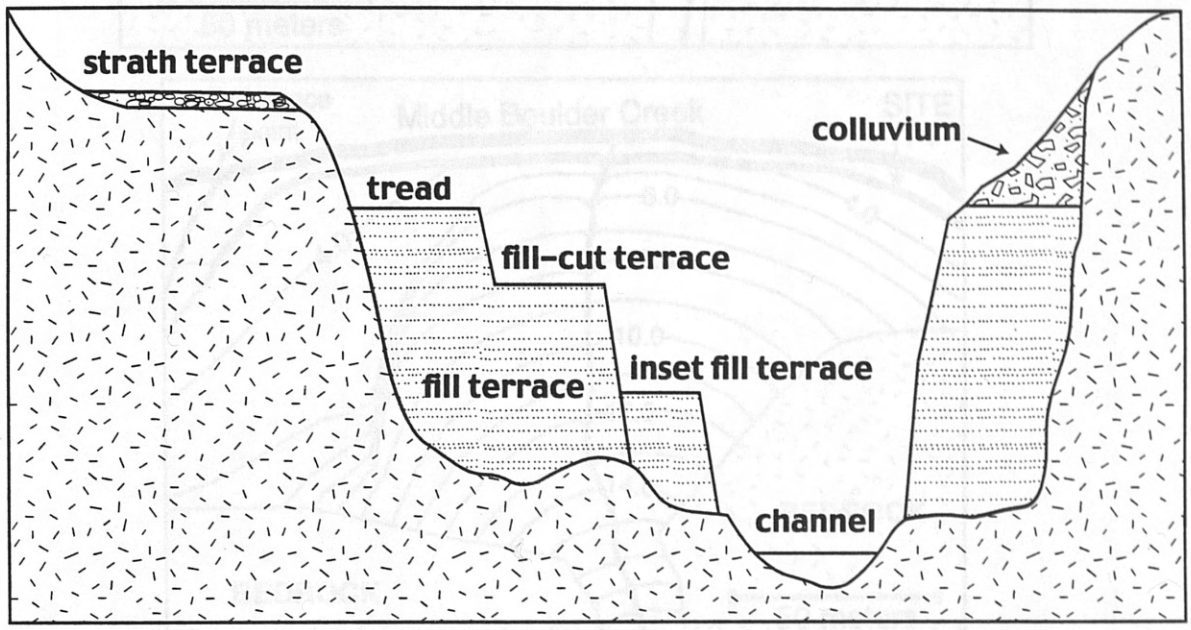

Figure 5. Valley cross-section illustrating different types of fluvial terraces; modified from Bull (1991); colluvium locally buries fill terraces.

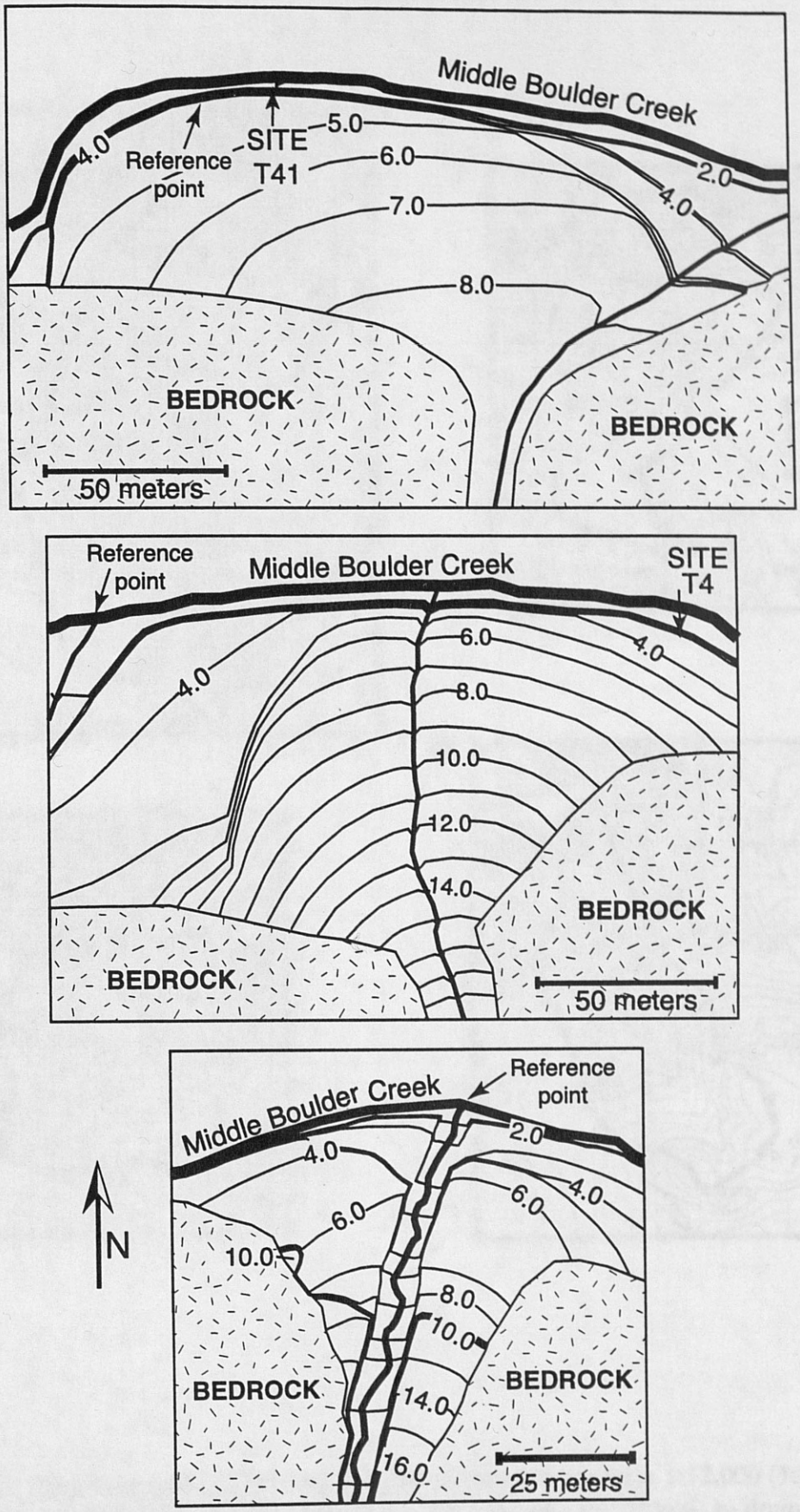

Figure 6. Alluvial fans at sites T41, T4, and T2; 1.0 m contours show height above reference point on Middle Boulder Creek; note: Middle Boulder Creek not drawn to scale; (a) alluvial fan at site T41; (b) alluvial fan near site T4; (c) alluvial fan near site T2.

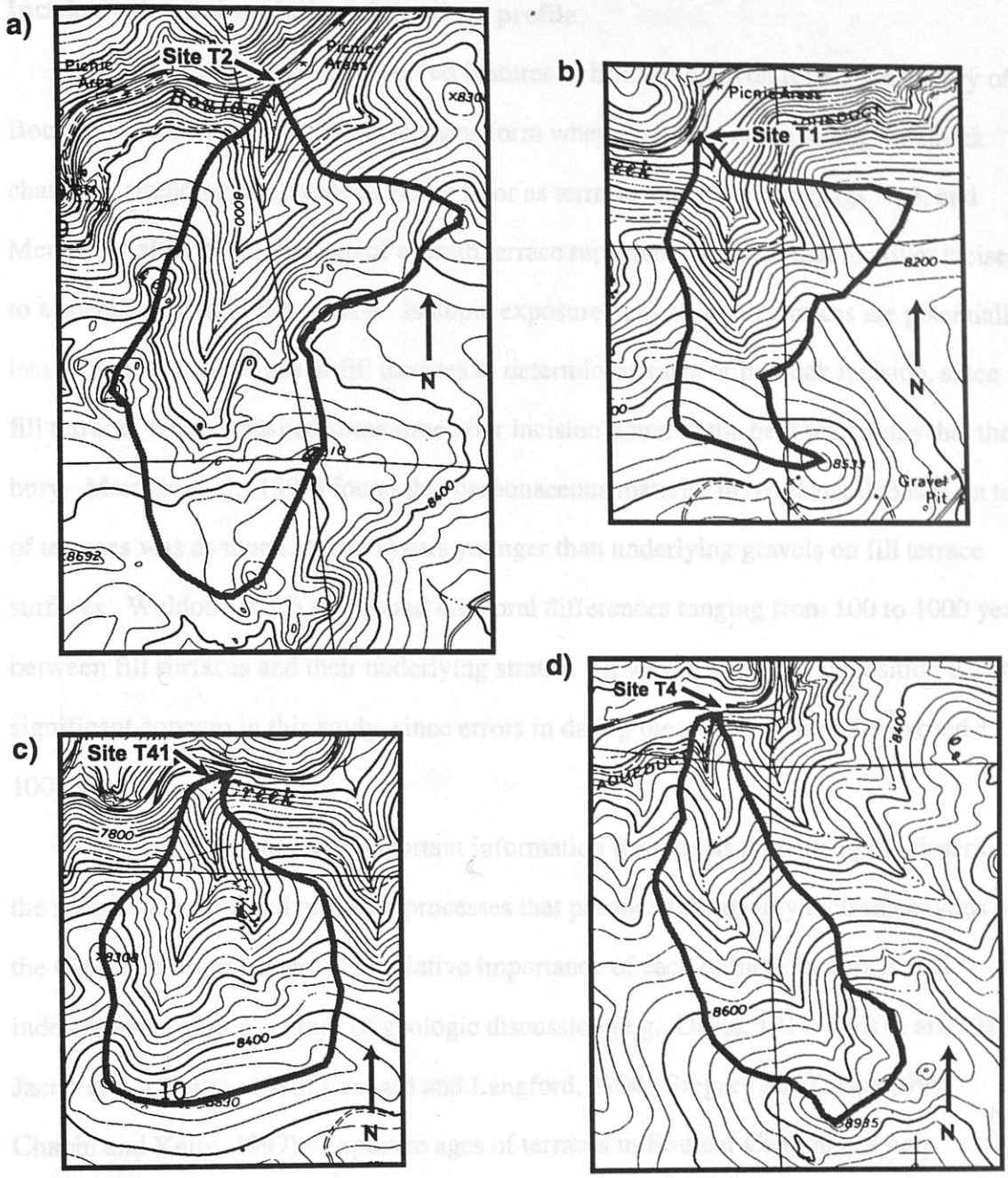

Figure 7. Drainage areas of Boulder Canyon alluvial fans; scale is 1:12,000 (1:24,000 map enlarged 200%); a) drainage area at site T2; total area = 1.02 km^2; b) drainage area at site T1; total area = 0.52 km^2; c) drainage area at site T41; area = 0.62 km^2; d) drainage area at site T4; area = 0.60 km^2.

Incision rates and evolution of the river profile

The exposure ages of preserved features in Boulder Canyon reflect the history of Boulder Canyon incision. Strath terraces form when rivers cut down through bedrock channels, stranding the previous valley floor as terraces on either side (Figs. 4, 5, and Merritts et al., 1994). The age of a strath terrace represents the time that the river incised to a specific depth in the canyon. Isotopic exposure ages of strath terraces are potentially less ambiguous than ages of fill terraces in determining rates of bedrock incision, since fill terraces were deposited some time after incision down to the bedrock straths that they bury. Merritts et al. (1994) found that carbonaceous material in overbank deposits on top of terraces was as much as 3000 years younger than underlying gravels on fill terrace surfaces. Weldon (1986) also found temporal differences ranging from 100 to 1000 years between fill surfaces and their underlying straths. However, overbank deposition is not a significant concern in this study, since errors in dating the surface can easily exceed ± 1000 yrs.

Incision rates provide important information for models that attempt to describe the roles of climatic and orogenic processes that produced the deeply incised canyons of the Colorado Front Range. The relative importance of each of these factors is still indeterminate after a century of geologic discussion (e.g., Davis, 1911; Epis et al., 1980; Jacob and Albertus, 1985; Leonard and Langford, 1994; Gregory and Chase 1994; Chapin and Kelly, 1997). Exposure ages of terraces in Boulder Canyon can help determine a rate of incision for the most recent river incision. However, poor preservation of deposits and of polished bedrock above a height of 20 m above the present valley floor hampers measuring incision rates for most of the 200 to 300 meter depth of the canyon. If I extrapolate my measured rate of incision through the rest of the canyon, I can approximate a time of the initiation of downcutting. How well this age

correlates with the presumed initiation of downcutting indicates whether or not the Pleistocene/Holocene rate of incision is faster or slower than incision rates of the past.

Finally, there is much to be learned from analyzing present and past geometrical characteristics of the river channel and valley. Longitudinal river profiles ("long profiles") are plots of river length against elevation. Terraces preserved along valley walls above the active valley bottom record a history of past long profiles. Long profiles can reflect characteristics of a drainage basin including variations in bedrock lithology, variations in resistance due to weathering or fracturing/faulting, and/or show a snapshot of one stage of a river's response to a change in base level (Pazzaglia et al., 1998). The shape of a river valley also reflects rates of incision and bedrock resistance. Rapid incision and resistant bedrock favor the formation of steep, narrow valleys, while slow incision and erodable rock types favor wide valleys (Pazzaglia et al., 1998). In a single long profile, regions of more resistant bedrock often exhibit steeper gradients. In studying coastal rivers, Pazzaglia et al. (1998) found that when incision rates are controlled by tectonic uplift, long profiles exhibit a strongly concave-upward shape due to the river's rapid response to changing base level. Tectonically active settings are characterized by high stream powers that are able to keep up with or exceed the rapid rates of rock uplift, producing relatively smooth concave-upward profiles. However, in tectonically stable regions, stream power tends to be limited. As a result, climate and bedrock characteristics are the dominant factors in controlling long profile shape after a change in base level. Profiles from stable regions tend to exhibit knickpoints, especially in regions of resistant bedrock. Knickpoints are localized convexities in an otherwise concave long profile. The longitudinal profile of Middle Boulder Creek preserves information about the tectonic, lithologic, and incision history of the Front Range region.

Setting

Boulder Canyon and glaciated regions in north-central Colorado

The 347 km^2 Middle Boulder Creek catchment extends through the glaciated regions east of the Continental Divide through the Colorado Front Range and to the city of Boulder (Fig. 8). The glaciated portion of the catchment alone is 93 km^2 measured at Nederland, which represents the easternmost terminus of several late Pleistocene glaciations. East of Barker Reservoir in Nederland, Middle Boulder Creek flows through Boulder Canyon, a steep, deeply incised canyon typical of those that cut through the gently undulating upland surface of the Colorado Front Range. The canyon drops 785 m in 25 km, from 2425 m at Barker Reservoir in Nederland down to 1640 m west of the city of Boulder (Fig. 9). The average gradient of 0.032 steepens in places to 0.085 and the canyon is locally as deep as 300 m and as narrow as 50 m at the valley floor. North Boulder Creek joins Middle Boulder Creek 12.5 km west of Boulder. Boulder Canyon meets the western High Plains in the city of Boulder, at the eastern edge of the Front Range.

Cosmogenic isotope, uranium-trend, and ^{14}C dating techniques from regions in and near the Colorado Front Range help to constrain glacial events and climate changes during the late Pleistocene and Holocene in Colorado. Age estimates of glacial moraines from Glacial Lake Devlin and Santanta Peak north of Nederland, the upper Fraser Valley to the west, Twin Lakes Reservoir to the southwest, and Mt. Evans to the south (Fig. 1) all provide data for regional correlation of events in the Middle Boulder Creek catchment.

Present and Holocene climate and vegetation in the Front Range

Local topography strongly influences aspects of the modern climate and vegetation of the Front Range. Prevailing westerly winds generally result in air mass

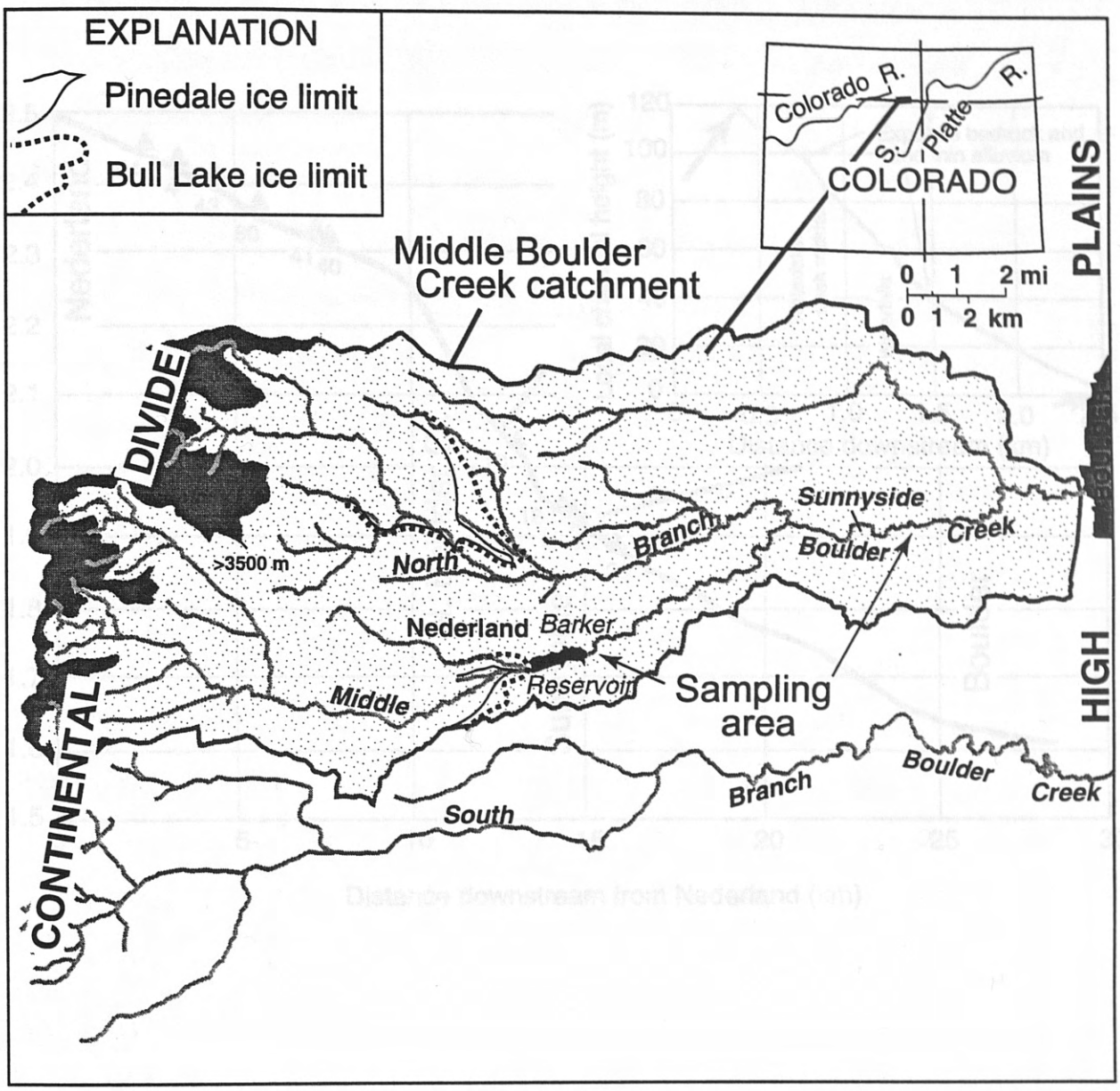

Figure 8. Map showing location of Middle Boulder Creek and nearby rivers in the Colorado Front Range, north central Colorado; Middle Boulder Creek catchment is shaded. Arrows show area sampled cosmogenic exposure and ^{14}C dating.

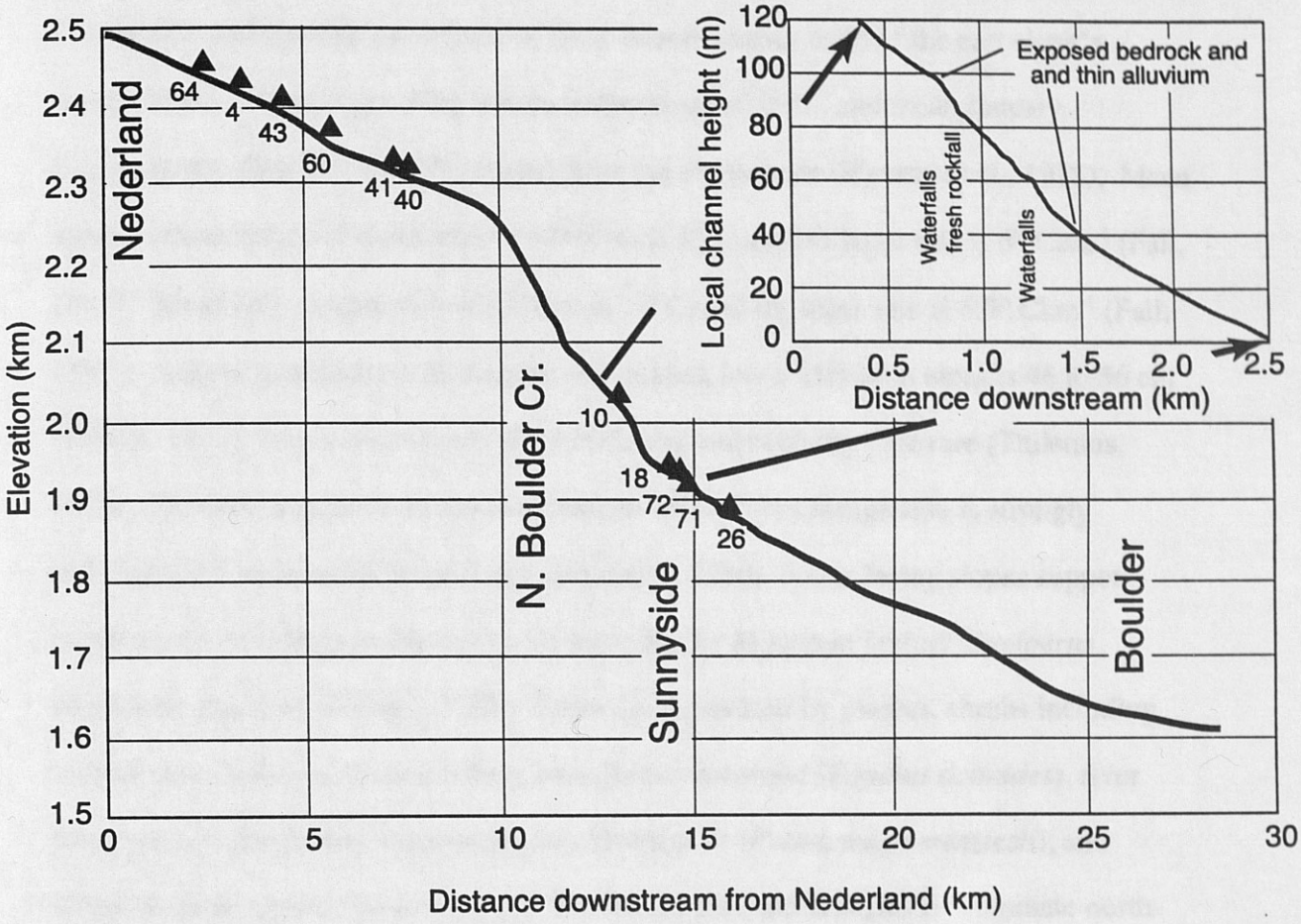

Figure 9. Profile of Middle Boulder Creek showing sample locations (sites are designated as dark triangles with the 99-T number plotted) and the surveyed reach in the inset.

movement from the north, west, and south. In the winter, cold fronts migrating from the north are often blocked from westward migration by the mountain front, so that temperatures in the plains can be lower than those in the mountains. In the spring, summer, and fall, Gulf air masses move into Colorado from the southwest and south. Convection and upslope movement of these masses causes most of the east slope's precipitation. A mean growing season temperature of 10°C, and mean January temperatures often below -11°C characterize the alpine zone (Hanson et al., 1978). Mean annual temperature for elevations of ~2500 m is 5°C, and the lapse rate is 6° Ckm^{-1} (Fall, 1997). Mean July temperature at 2500 m is 15°C, and the lapse rate is 6.9° Ckm^{-1} (Fall, 1997). Annual precipitation in the pine-dominated, lower elevation areas is 46 to 56 cm (Netoff, 1977). Winds often reach 40 to 50 km/hr and calm days are rare (Thilenius, 1975). Modern vegetation in lower elevations of the Front Range also is strongly influenced by slope orientation (Legg and Baker, 1980). South-facing slopes support ponderosa pine (*Pinus ponderosa*) with some Rocky Mountain juniper (*Juniperus virginiana* ssp. *scopulorum*). Valley floors are dominated by grasses, shrubs including willow (i.e., *Salix irrorata*) and trees including cottonwood (*Populus deltoides*), river birch (*Betula fontinalis*), ponderosa pine, Douglas fir (*Pseudotsuga menziesii*), and Colorado blue spruce (*Picea pugens*). Ponderosa pine and Douglas fir dominate north-facing slopes. In Boulder Canyon, lodgepole pine (*Pinus contorta*) and aspen (*Populus sp.*) are also present, most conspicuously in disturbed areas.

Pollen records indicating changes in upper and lower forest timberline elevations provide a proxy record of Holocene paleoclimatic regimes. Changes in lower timberline are primarily controlled by aridity whereas changes in upper timberline and forest composition are primarily controlled by temperature (Troll, 1973). Fall (1997) shows that prior to 11,000 yr B.P. in western Colorado, the subalpine forest dominated by spruce (*Picea*) and pine (*Pinus*) grew 300 to 700 m below the modern limit, indicating a

climate 2 to 5°C cooler with precipitation 7 to16 cm greater than today. The expanded range of the subalpine forest from 9000 to 6000 yr B.P. indicates mean July temperatures were 1 to 2°C warmer than today, with a wetter climate (8 to11 cm more precipitation). Upslope retreat of the lower timberline from 6000 to 4000 yr B.P. indicates drier conditions, and by 2000 yr B.P. the modern climate and vegetation patterns had been established. Fall (1997) notes that climatic records from the Front Range (i.e., Maher, 1972 and Short, 1985) can be interpreted to show similar trends as those seen in western Colorado, that is a warmer and wetter climatic regime for the early and middle Holocene. Temperature and precipitation trends noted by Fall are also correlated with: (1) palynological records from southern Colorado (Andrews et al., 1975; and Mehringer, 1976; Nichols, 1982); (2) pollen data and radiocarbon analyses from Lake Emma and Hurricane Basin in the San Juan Mountains, Colorado (Carrara et al. 1984); and (3) pollen and radiocarbon analyses from Lost Park, in the central Front Range (Vierling, 1997). Slightly earlier estimates of the timing of the onset of warmer-than-present conditions (~10,000 yr B.P.) are provided by (1) plant and insect microfossils in Lake Emma sediments (Elias et al., 1991); and (2) fossil beetle assemblages in the Rocky mountains from central Colorado to northern Montana (Elias, 1996; 1999). Elias (1999) furthermore notes a series of small-scale oscillations in the late Holocene (after 3000 yr B.P.). Pollen and beetle analyses from the Mary Jane site, 5 km west of the Continental Divide in central Colorado also found slightly different results than Fall, with cool and dry conditions prevailing from 13,800 to 12,300 yr BP (Short and Elias, 1987).

GEOLOGICAL HISTORY

Evolution of the Front Range

The Colorado Front Range exposes Precambrian metasedimentary and metaigneous rocks and several batholithic intrusions that stand in sharp relief against the High Plains of eastern Colorado (Fig. 10). The tectonic history spans a period of 1.8 billion years, first entailing uplift of Precambrian metamorphic and granitic rocks to form the Ancestral Front Range (Permian-Pennsylvanian) in the late Paleozoic through block-fault mountain building. Batholithic intrusions including the Boulder Creek granite were emplaced between 1700 and 1000 Ma. Uplift of the ancestral highlands in Pennsylvanian time created high topography that eroded and consequently was buried by 2400 m of marine sediment in the late Jurassic. The Laramide Orogeny (~70-65 Ma), elevated the modern Front Range over an area 180 miles north-south and 40 miles east-west in west central Colorado (Sonnenberg and Bolyard, 1997). Rock uplift may have continued into Pliocene time (e.g., Sonnenberg and Bolyard, 1997; Raynolds, 1997).

At some time prior to the start of river incision in the Front Range, a large area of gently undulating topography known as the "Rocky Mountain Erosion Surface," or the "Late Eocene Surface" had developed. The former name is preferred since it implies no specific time of formation. Sparse remnants of the hypothetical surface are separated from the High Plains of eastern Colorado by a 400 to 800 m east-facing escarpment. The change in climate or rock–uplift rates that initiated incision of the Colorado Front Range remains controversial after a century of geologic discussion. The dissected surface may have formed during the warm and equable late Eocene climate that smoothed topography through chemical weathering and relatively small storms (Gregory and Chase, 1994). According to Chapin and Kelly (1997), apatite fission track cooling ages from the Pike's Peak batholith in the southern Front Range argues against theories of significant post-Laramide rock uplift. They reason that the Rocky Mountain Erosion Surface must have

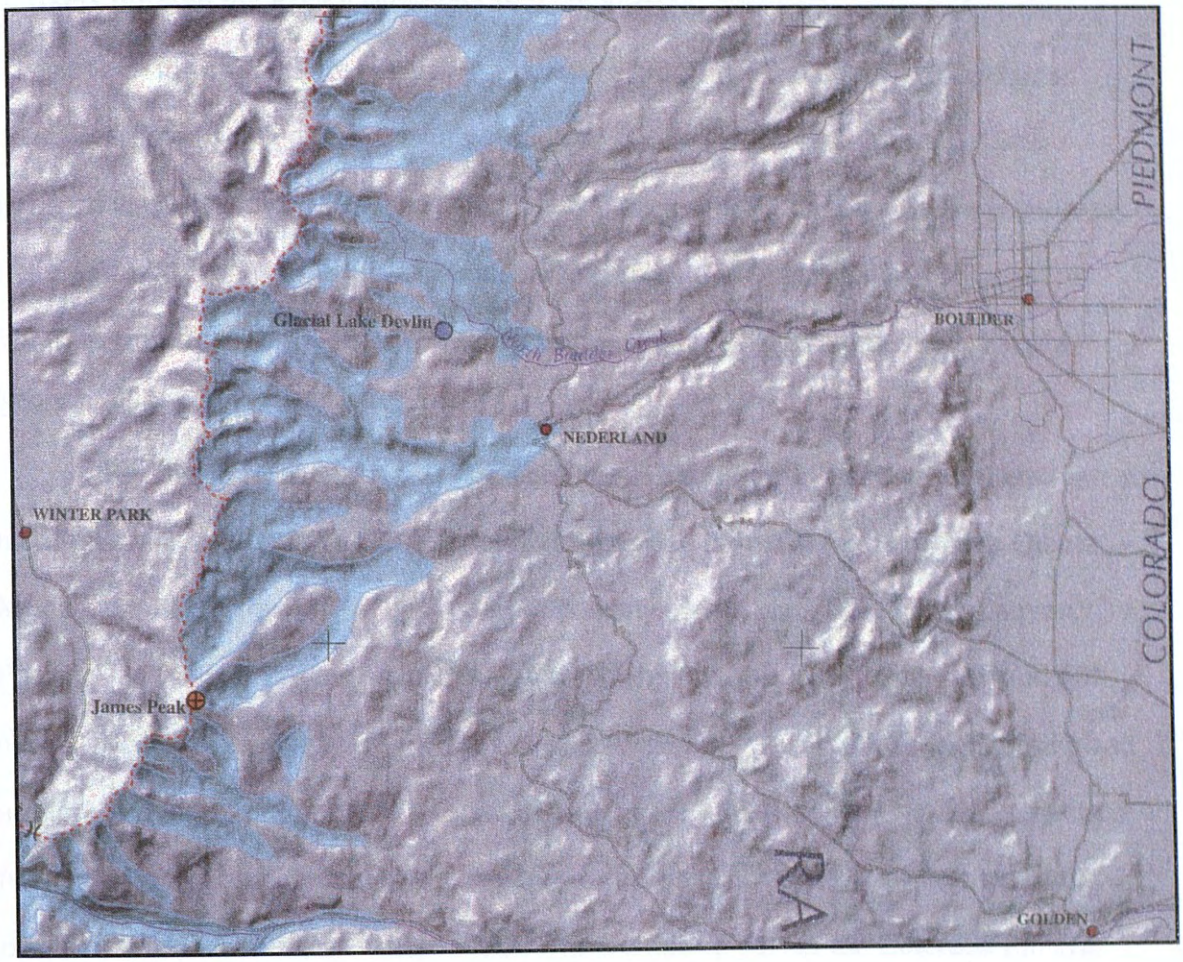

Figure 10. Digital elevation model showing Pleistocene glacial limits in the northern Front Range (from Madole et al., 1998).

been protected from incision prior to the Pliocene due to the presence of extensive alluvial aprons that extended from the Front Range to the High Plains. Chapin and Kelly (1997) hypothesize that the change to a much wetter, stormier climate in the early Pliocene led to excavation of the bordering alluvial aprons and subsequent downcutting of rivers through the Rocky Mountain Erosion Surface. They cite other studies that suggest erosion exposed an east-facing escarpment during exhumation of Laramide bedrock from beneath a thick mantle of sediments (e.g., Jacob and Albertus, 1985, Leonard and Langford, 1994, and Chapin and Cather, 1994). Similar evidence indicates that Laramide ranges in Wyoming stand in bold relief due to the removal of large volumes of sediment that filled Laramide basins (Love, 1960; Moore, 1960; Knight, 1990; Mears, 1993).

Boulder Canyon is cut into Boulder Creek Granodiorite, a strongly foliated fine to medium grained biotite- or biotite-hornblende-bearing intrusive. Silver Plume Quartz Monzonite dikes cross cut the granodiorite in many places north of Boulder Canyon. Foliation in the area strikes broadly east-west, with dips generally between 30 and 50° north. Faults strike dominantly to the east and northeast. West of Nederland, biotite and hornblende gneisses dominate the bedrock. Laramide intrusives ranging in composition from gabbro to quartz monzonite are also exposed upstream in the Middle and North Boulder Creek catchments. These rocks, which make up part of the Colorado mineral belt, are altered or deeply weathered and oxidized in many areas (Gable, 1969; 1972).

Pleistocene/Holocene glacial history

The Pleistocene pre-Bull Lake, Bull Lake, and Pinedale glaciations are not well dated in the Front Range, but regional correlations allows us to suggest probable ages (Table 1, Appendix A). Pre-Bull Lake deposits are the least well constrained, with a possible range between 230 and 750 ka. This range is supported by (1) a 660 ka exposure

age estimate based on ^{36}Cl and ^{10}Be ages of moraines in the Wind River Range, Wyoming (Chadwick et al., 1997); and (2) a minimum exposure age of 232 ka based on ^{36}Cl and ^{10}Be dating of boulders on moraines in the same region (Phillips et al., 1997). Bull Lake advance(s) and retreat(s) probably occurred between 150 and 100 ka at sites in Wyoming, southwest Montana and Colorado. Age control is provided by (1) ^{36}Cl and ^{10}Be dating of boulders in Wind River Range in Wyoming showing morainal deposition between the intervals 130 to 100 ka and 120 to 100 ka (Phillips et al, 1997); (2) obsidian rind thicknesses near West Yellowstone which provide a range of 130 to 155 ka for Bull Lake till (Pierce et al., 1976), an estimate which is broadly supported by the 114,500 yr age of a rhyolite flow that underlies the till, and oxygen-isotope data from marine sediments which indicate a period of glacial growth between 130 and 150 ka; and (3) uranium-trend ages of 130 ± 40 ka for Bull Lake till in the North St. Vrain drainage basin in the Colorado Front Range (Shroba et al., 1983). The timing of Pinedale events is relatively well known. Data from Colorado, southwest Montana, and Wyoming suggest glaciation between ~35 and 14 ka with most Pinedale maxima occurring between 23 and 16 ka. Limiting dates include: (1) ^{14}C dating of sediments from Glacial Lake Devlin, Colorado Front Range (Madole, 1986) which provides a glacial maximum estimate of 22,400 +1070/-1230 yr BP based on the first sediment that accumulated in the lake, and a 15,228-13,591 cal BP to 16,111-14339 cal BP estimate for ice retreat based on the youngest sediments from the lake; (2) ^{14}C dating of sediments from the Park Range west of the Continental Divide (Madole, 1980, 1986) which show that deglaciation of a glacier source area occurred between 16,768-16,075 cal BP and 13,470-12894 cal BP ; (3) ^{14}C dating of sediments from the Mary Jane site in the Upper Fraser River Valley of Colorado which provide a 30,480 +2800/-4300 yr BP and 30,050 ± 1200 yr BP estimate for a Pinedale glacier advance, and a 16,935-16,046 cal BP estimate for final retreat (Nelson et al., 1979); (4) 20 to 30 ka obsidian hydration ages of Pinedale till in West

Yellowstone (Pierce et al., 1976); (5) 16 to 23 ka cosmogenic-isotope exposure ages of Pinedale boulders in the Wind River Range, Wyoming (Gosse et al., 1995); and (6) a minimum limit for Pinedale retreat in the Front Range of 14,939-13,813 cal BP based on late glacial "Santanta Peak" readvances high in Front Range cirques (Benedict, 1973, 1981; Davis et al., 1992; Menounos and Reasoner, 1997).

The chronology of Holocene glacial fluctuations is not completely understood, but glaciers were probably never much larger than they are today. The Arapaho cirque in the North Boulder Creek drainage basin contains glacial and periglacial deposits dated as late Pleistocene and Holocene through radiocarbon techniques and relative-age techniques including lichenometry, soil development, and rock weathering (Benedict, 1967, 1968, 1973; Madole 1972; Mahaney, 1974). Benedict (1973, 1981) used minimum radiocarbon ages from 3236-2877 cal BP to 5916-5615 cal BP from till near Triple Lakes and lichenometry to suggest that glaciers extended as far as Triple Lakes during the Holocene (Fig. 8). Davis (1987) dated organic matter in sediments from a lake behind the till, however, he measured ages as old as 13,391-10,687 cal BP. This older minimum age for the till negates Benedict's claim of extensive glacial advance in the Holocene (Birkeland et al., 1987).

Some alluvial surfaces on the High Plains east of the Front Range have been correlated with Pleistocene glaciations or changed climate (Madole, 1991) and may correlate with terrace surfaces within Boulder Canyon. The stratigraphy of High Plains surfaces consists of late Pliocene Nussbaum Alluvium, early Pleistocene Rocky Flats Alluvium, middle Pleistocene Verdos Alluvium, middle Pleistocene Slocum Alluvium, late Pleistocene Louviers Alluvium, late Pleistocene Broadway Alluvium, and Holocene age pre-Piney Creek, Piney Creek, and post-Piney Creek deposits (Table 2). In the Boulder, CO 7.5' quadrangle, mapped heights of High Plains surfaces above grade are considerably lower than the height ranges suggested by Madole (1991) based on rivers in

the High Plains of eastern Colorado. This may be a result of differing characteristics of drainages that head in a glaciated catchment, or a result mismapping of local units.

METHODS

Field mapping

I mapped and sampled fluvial terraces with David Dethier along Middle Boulder Creek between Barker Reservoir at the west end of Boulder Canyon, and the city of Boulder, Colorado, at the east end of the canyon. I marked the location of each terrace remnant on 1:24,000 Tungsten, CO and Boulder, CO topographic maps. I used a hand level to measure the height of each terrace surface above the present river level. Errors in measurement are estimated at ± 1 m, largely as a result of large local variations in the river gradient. Changes in the river stage could have also led to errors not exceeding ± 0.5m. Where terraces were buried by colluvium, I used the highest occurrence of stream-rounded cobbles in a deposit to approximate terrace height. Whenever possible, I also recorded the height of each terrace above its bedrock strath surface. I also noted the degree of soil development, the degree of rock weathering, and stratigraphic relationships with other terraces, providing qualitative estimates of age. I consulted work by Netoff (1977) and Barber (1983) in Boulder Canyon for descriptions of terraces and soils (Table 3).

I found that no terrace remnants appear to exist > 21 m above Middle Boulder Creek, despite diligent searching along the upper reaches of the valley walls. The best preserved terraces are mainly covered by colluvium derived from adjacent valley walls, indicating that preservation potential of terraces was rather low except when they were buried soon after deposition. For this reason, exposures of younger terraces were far more abundant than exposures of older terraces. Bedrock straths were also rare due to rapid weathering of bedrock surfaces, although accordant remnant toeslopes on valley walls may indicate past river positions. In four weeks of mapping, I believe that I located all sizable terrace exposures in the canyon.

Table 3. Descriptions, soil characteristics, and age estimates of sample sites.

Sample	Distance from Nederland gaging station (km)	Terrace height (m)	Soil Characteristics			Age estimate	Reference[1]
			Profile thickness (cm)	Maximum color	Soil Horizons		
99-T11	13.9	21				Bull Lake	this study
99-T18	14.4	12	203	10YR 4/4	Bt/BC	Pine/B. Lake	BC-12 (N)
99-T10	13.2	10		Oxidized around boulders		late Pinedale	this study
99-T64	2.6	9	180+	10YR 5/8	A/BC	Pinedale	this study
99-T43	4.1	7	127	10YR 4/6	A/B/BC	late Pinedale	BC-8 (N)
99-T45	4.5	7	80	Oxidized near surface		late Pinedale	this study
99-T60	5.9	5			A/Bw/BC	Pinedale	this study
	4.3	6.2	89	10YR 4/3	A/B/BC	Pinedale	BC-9 (N)
	5.4	5	216		A/B/BC	Pinedale	BC-10 (N)
99-T41	7.7	4.5	87		A/BC	early Holocene	this study
99-T40	7.6	2	70		A/C	Holocene	this study
99-T4	3.9	2.5	69		A/C	Holocene	this study

Notes:
1: (N) refers to Netoff (1977).

I created a longitudinal profile of Middle Boulder Creek by measuring the length of the channel between 40-foot contour intervals on 1:24,000 topographic maps (Fig. 9). In constructing the profile, I used the thalweg distance in the long profile rather than the shorter "valley-bottom" length which is measured along the floodplain. I surveyed a ~2.2 km profile along the steepest part of Middle Boulder Creek using compass, tape, and hand level, measuring the distance between every 1.5 m rise in the river elevation (Fig. 9, inset).

We mapped alluvial fans in small side drainages within Boulder Canyon using hand level, compass and tape, measuring 20 to 50 points on each of these 2,600 – 11,000 m^2 surfaces (Fig. 6). In estimating the volume of alluvial material, we assumed that fans T4 and T41 overlie horizontal surfaces defined by the bottom contour of each fan and that fan T2 overlies a sloping surface defined by the base of the ravine that incises the fan. I cut out pieces of paper traced over each 1-meter closed contour on a fan. I also weighed a square that was scaled to 20m x 20 m (400 m^2). Since each piece of paper represented a wedge of sediment 1 m in thickness, I divided the total weight of the paper by the weight per 400 m^3 to determine total volume. Errors in the volume result primarily from inaccurate assumptions about the surface underlying the alluvial material and surveying errors. We did not map or calculate the volume of fan T1 but it likely falls within the range calculated from the other fans. I measured drainage areas by first scanning 1:24,000 topographic maps and opening them as images in ArcView version 3.1. I drew polygons around the drainage areas and converted them to shapefiles to determine the area of each drainage area. I double checked this measurement by manually drawing drainage boundaries on 1:24,000 topographic maps and finding the areas of polygons placed inside the boundaries (Fig. 7).

Dating methods

Previous work in Boulder Canyon has been based on qualitative estimates of the ages of terraces and glacial moraines. I used ^{14}C, ^{36}Cl, ^{10}Be and ^{26}Al dating techniques to quantitatively constrain the timing of terrace and alluvial fan formation in Boulder Canyon. Age estimates for these geomorphic features refine the chronology of glacial and non-glacial events in Boulder Canyon, and give more information on the fluvial response to sediment budget perturbations in Boulder Canyon.

Exposure age dating using cosmogenic isotopes

We used interpretive models to determine exposure ages of terraces by measuring accumulation of cosmogenic isotopes ^{10}Be and ^{26}Al, and by measuring isotopic ratios of ^{36}Cl (Bierman et al., 1995). Cosmogenic isotopes are produced in situ primarily by neutron spallation resulting from interactions of secondary cosmic ray particles (neutrons) with surface materials (Bierman, 1994). The production rate of cosmogenic isotopes (P_x) at depth (x) in material of density (ρ) is given by the equation

$$P_x = P_o * e^{-(x\rho/\Lambda)} \qquad (1)$$

where (P_o)is the production rate at the surface and (Λ) is the attenuation length for fast neutrons, which is typically 150-170 g/cm^2 (Kurz, 1986,; Lal, 1991; Brown et al., 1992; Sarda et al., 1993). This relationship yields an exponentially declining abundance of isotopes with increasing depth (Fig. 11). Surface production rates were corrected for variations resulting from altitude and latitude (Fig. 12, Lal, 1991; Clapp and Bierman, 1995). For samples which had been buried, we corrected for the lower accumulation rates below the surface assuming a sediment density of 1.5 g/cm^3 in equation (1). We also corrected accumulation rates for horizon shielding and slope of the surface based on scaling factors calculated by Dunne et al. (1999). For cosmic ray intensity given by

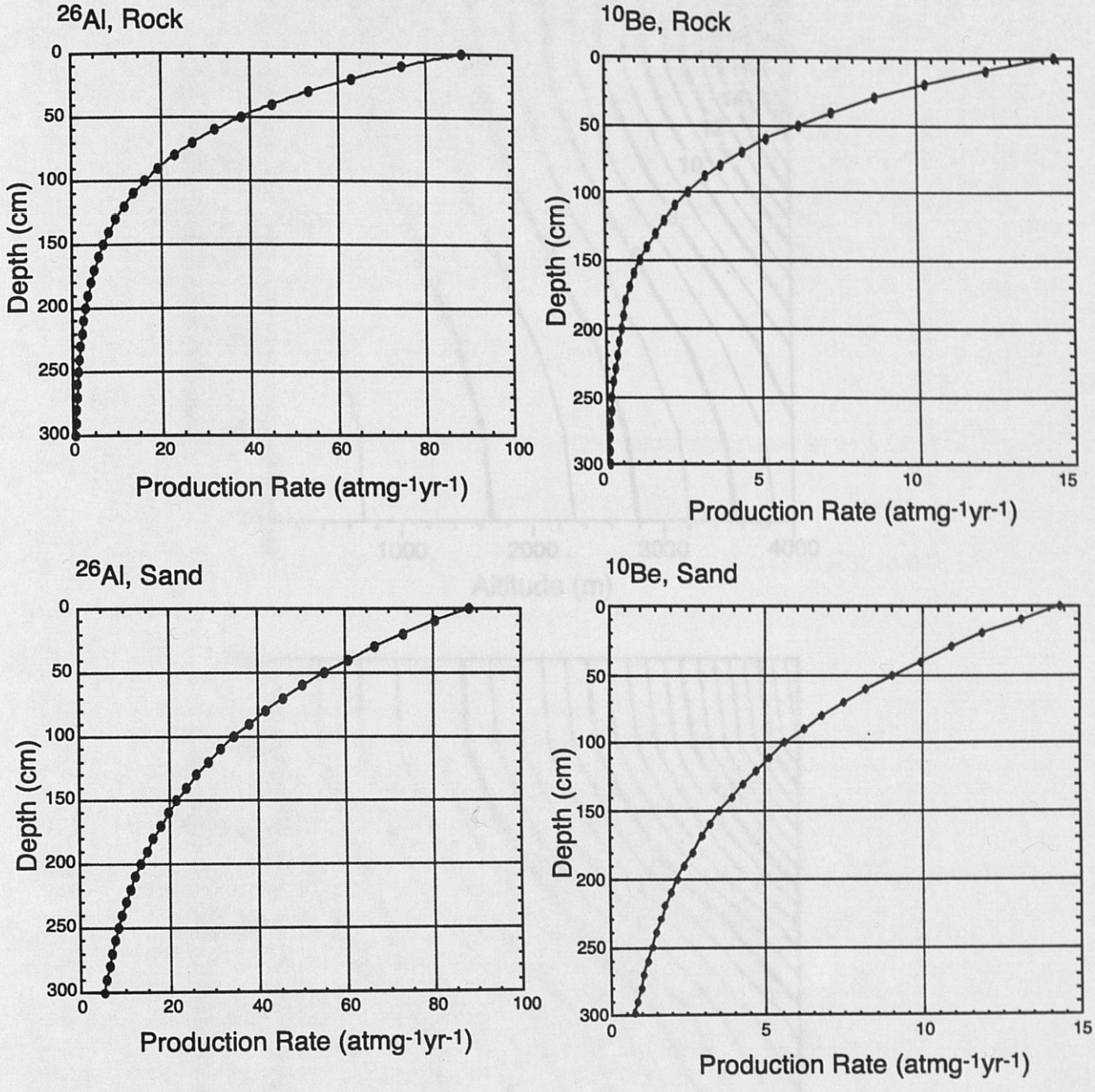

Figure 11. Depth profiles of ^{26}Al and ^{10}Be production rates in rock and sand. Profiles were created using the formula $P_x = P_0 e^{-(x\rho/L)}$ where P_x = production rate at depth x; P_0 = production rate; ρ = density of material; and L = attenuation length. For ^{26}Al, I assumed a production rate of 36.8 $atmg^{-1}yr^{-1}$ (Nishiizumi et al., 1989) multiplied by 2.4 to correct for altitude and latitude (2000 m, 40 degrees north). For ^{10}Be, I assumed a production rate of 6.0 $atmg^{-1}yr^{-1}$ (Nishiizumi et al., 1989) multiplied by 2.4 to correct for altitude and latitude. For rock, I assumed a density of 2.7 gcm^{-3} (quartz-rich); for sand I assumed a density of 1.5 gcm^{-3}. I used an attenuation length of 160 gcm^{-2} (Lal, 1991; Brown et al., 1992).

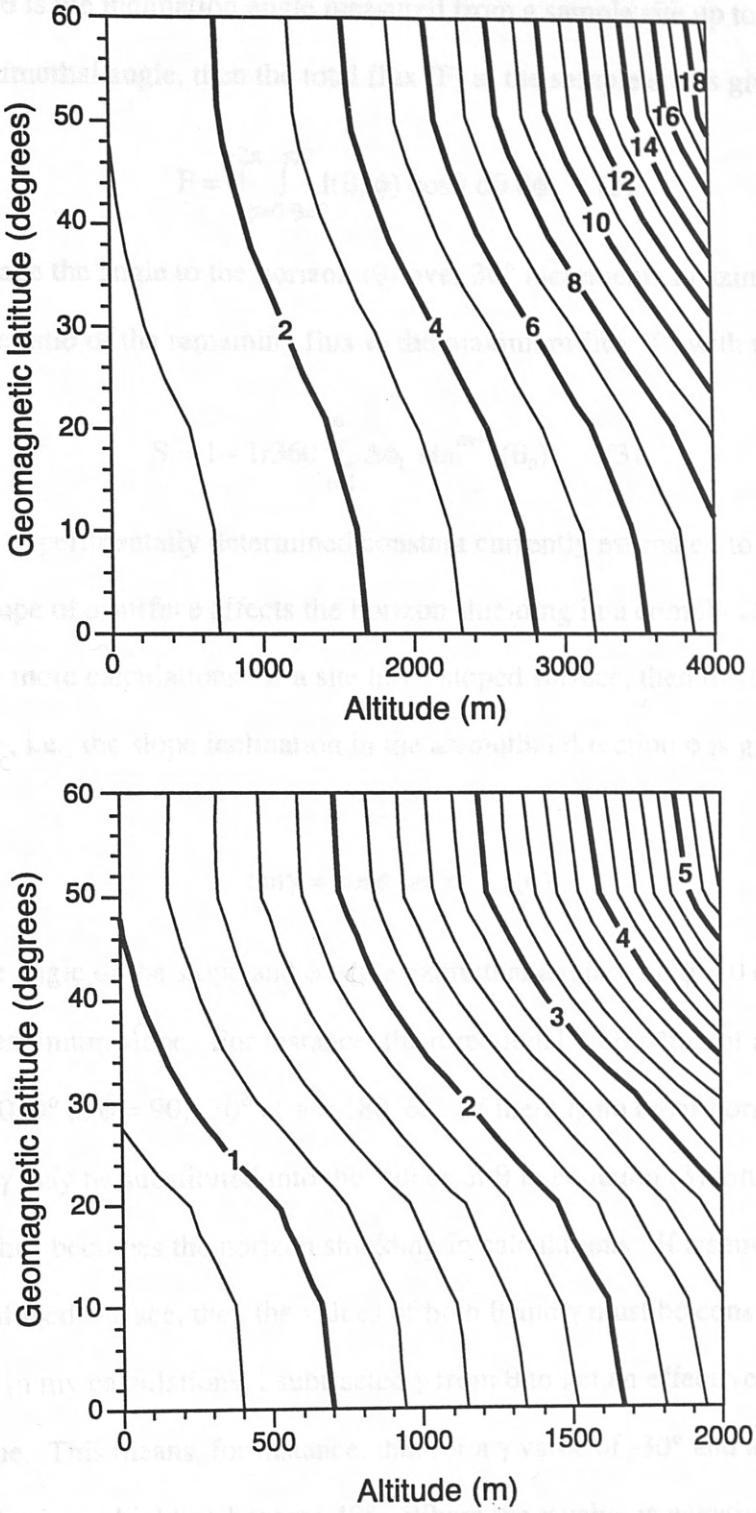

Figure 12. Contour plots of altitude/latitude correction factors for cosmic ray flux and isotope production at Earth's surface based on data presented by Lal (1991) (from Bierman, 1994).

$I(\theta, \phi)$, where θ is the inclination angle measured from a sample site up to the horizon, and ϕ is the azimuthal angle, then the total flux (F) at the sample site is given by

$$F = \int_{\phi=0}^{2\pi} \int_{\theta=0}^{\pi/2} I(\theta, \phi) \cos\theta \, d\theta \, d\phi \qquad (2)$$

Since we average the angle to the horizon (θ) over 30° increments in azimuth (ϕ), we determined the ratio of the remaining flux to the maximum flux (S) with the equation

$$S = 1 - 1/360° \sum_{i=1}^{n} \Delta\phi_I \sin^{m+1}(\theta_0) \qquad (3)$$

where m is an experimentally determined constant currently estimated to be 2.3.

The slope of a surface affects the horizon shielding in a complicated way, and requires a few more calculations. If a site has a sloped surface, then the directional inclination (γ) , i.e., the slope inclination in the azimuthal direction ϕ is given by the relationship

$$\tan\gamma = \cos\phi \tan\alpha \qquad (4)$$

where α is the angle of the slope and ϕ is the azimuthal angle with $\phi = 0$ defined as the direction of maximum slope. For instance, the directional inclination of a 30° slope will be 30° at $\phi = 0$, 0° at $\phi = 90$, -30° at $\phi = 180$, etc. If there is no other horizon shielding, the values of γ may be substituted into the values of θ in equation (3). Shielding created by the slope thus becomes the horizon shielding in calculations. If a sample site has both $\theta > 0°$ and a sloped surface, then the values of both θ and γ must be considered at each increment ϕ. In my calculations, I subtracted γ from θ to get an effective horizon shielding value. This means, for instance, that for a γ value of -30° and a θ value of 10°, the effective horizon shielding became 40°. Where the γ value is negative (sloping below the horizon), the effective horizon shielding is increased, but where the γ value is positive, the effective horizon shielding is decreased. I determined the flux by

substituting these effective horizon shielding values for θ into equation (3). Only one of my samples (99-T26) required the combination of slope and horizon shielding corrections.

After making flux corrections, uncertainties in production rate remain. Changes in magnetic field intensity produce variations in the rate of surface production of approximately 10-20% for early Holocene and late Pleistocene samples (Bierman, 1994). Reedy et al. (1983) suggest changes in atmospheric ^{10}Be production of ± 30% over 100 ka periods, and 10% over 200 ka. Several other workers have noted significant variations in production rates over time (i.e., Raisbeck et al, 1985). In our calculations, we have assumed a conservative production rate uncertainty of ± 20%. Presumably, older samples will fall toward the lower end of this range since the damping effect is stronger when there is more time over which to average the changing production rates. Cosmogenic exposure ages of the samples presented here thus may change as production rates are refined in the future, but the relative ages of the samples will not change.

Since the measured abundance of cosmogenic isotopes is a result of isotopes accumulated since deposition, as well as any isotopes acquired prior to deposition ("inherited" isotopes), we must make the assumption of zero or constant inheritance in order to determine the exposure age of a sample. An assumption of zero is best justified in settings where a sample is either continually eroded or buried just prior to deposition. As a result, glacially-derived sediment is probably reliable for cosmogenic exposure age dating. Examining the relationship between Al and Be ages, as well as examining the ratio of measured isotopes give us opportunities to verify this assertion.

Cosmogenic exposure age dating techniques require either the continuous exposure of a sample after deposition, or a known depth of burial since deposition. Assumptions concerning burial history are difficult to make unless the ratio of two different isotopes can be analyzed. Since ^{10}Be and ^{26}Al have different decay rates (half-

lives of 0.7 and 1.4 My, respectively), isotope ratios can be viewed as a function of erosion rate, time of burial after cosmogenic ray exposure, or exposure age (Lal, 1991). Assuming a simple exposure history since deposition, the isotopic ratio ^{10}Be / ^{26}Al starts near 6 and decreases over time. Erosion of the surface will depress the expected ratio near the upper end of the time line, since the loss of both isotopes enhances the effect of the differing decay rates. Post-exposure burial of the sample will cause the ratio to drop, since ^{26}Al decay will cause the ratio to drop and cosmogenic accumulation will stop.

Cosmogenic Sampling

D. Dethier and I collected samples from several large boulders on glacial moraines near Nederland in the Front Range and Dethier sampled boulders near Twin Lakes Reservoir in the eastern Sawatch Range, Colorado (Fig. 1) to be dated using ^{26}Al and ^{10}Be exposure age techniques. Stringent criteria must be applied for selecting samples in the field to best assure that reasonable results can be obtained. We used a hammer, cold chisel, and portable rock drill to remove surface samples from the largest and flattest boulders we could find from each moraine crest to maximize the chances that the boulder crests have been exposed since the time of deposition, and to minimize the chances that the boulders have rolled since the time of deposition. At Nederland and at Glacial Lake Devlin north of Nederland, we collected two samples from boulders on moraines mapped as "Bull Lake," and two from boulders on moraines mapped as "Pinedale" (Fig. 3, Gable, 1969; Gable and Madole, 1976; Madole, 1976a and unpublished data). At the Front Range sites, boulders sampled from Bull Lake moraines were approximately 1 meter high and had an average diameter of 2 to 4 m, while boulders sampled from Pinedale moraines were approximately 1.5 m high and had an average diameter of 3.5 to 4 m (Fig. 13). As noted by Phillips et al., (1997), typical rates of till erosion in the Wind River Range of Wyoming are 1 cm/ka for matrix, and 1 mm/ka

a)

b)

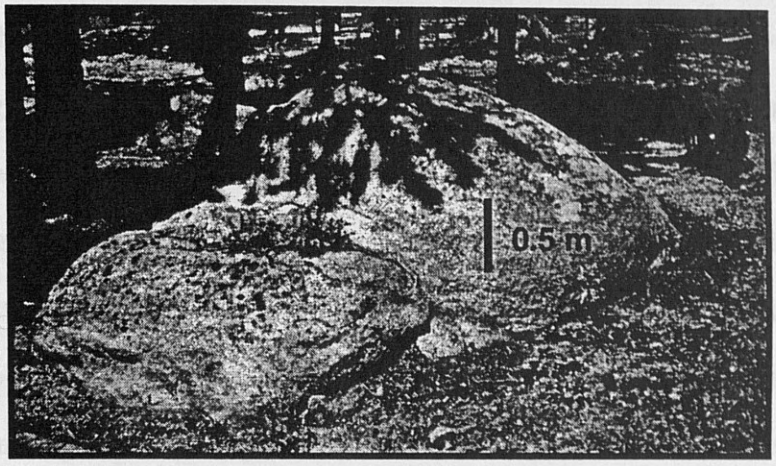

c)

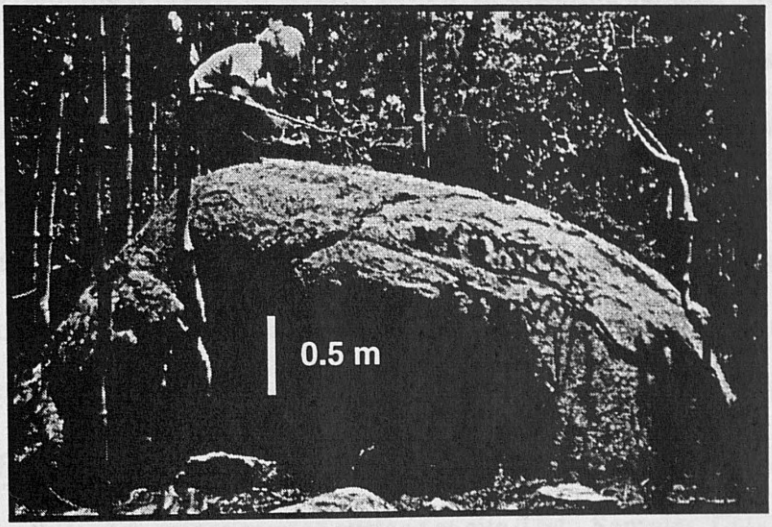

Figure 13: Boulders sampled from glacial moraines at Nederland and Lake Devlin; a) sample T75, boulder on Bull Lake moraine at Lake Devlin; l*w*h = 5 m x 3 m x 1 m; b) sample T76, boulder on Pinedale moraine at Lake Devlin; l*w*h = 4 m x 3.3 m x 1.5 m; c) sample T68, boulder on Bull lake moraine at Nederland; l*w*h = 2m x 2 m x 1.5 m.

for boulders (for their work, mostly banded gneiss, with some granite and diorite). Based on this rate of erosion, the top surfaces of the Bull Lake (if 110,000 ka or less) and Pinedale boulders should have been exposed since the time of deposition. Near Twin Lakes, in the Sawatch Range, Dethier sampled 2 sites on moraines described in detail by previous workers (Shroba, 1977; Nelson et al., 1984; Nelson and Shroba, 1998), but where there is some uncertainty about assignment to the Bull Lake or Pinedale glaciations (Fig. 2). In cooperation with Bierman, he sampled the outer Pinedale moraine at Stop #3 and the Bull Lake moraine from Stop #4 at localities described by Nelson et al. (1984). Large granodiorite boulders were common on the moraines, but granite, biotite gneiss, and other lithologies were present locally. At each site, we measured (1) horizon geometry, (2) sample thickness, (3) strike and dip of the sample surface, and (4) surface characteristics such as grain relief, evidence of spalling, or glacial polish/striations.

I also collected samples from six fluvial terraces and two other locations within Boulder Canyon (Fig. 9), including several sites where age had been estimated from the degree of soil development (Table 3, Netoff, 1977). In selecting samples, we chose the largest boulders from a surface to maximize chances that the rock had been stable and been exposed since deposition. Other selection criteria included clear evidence of river transport (exotic lithology and extensive rounding), and no evidence of former burial (oxidation). In the absence of appropriate boulders, or where terraces were buried by colluvium, we sampled cobbles from the B-horizon beneath the terrace, noting the depth and density of cover material. The samples at T64 represent a soil profile collected in 20 cm increments from a single exposure a few hundred meters east of Barker Dam. Sample T64-r is a rock collected from the terrace surface at site T64. Samples T71-1 and T71-2 represent samples collected within the same fill terrace, with the former collected from a polished boulder on the terrace surface, and the latter consisting of cobbles collected from 30 cm below the surface (Fig. 14). T71 is located at Sunnyside, only 0.2 km downstream

a)

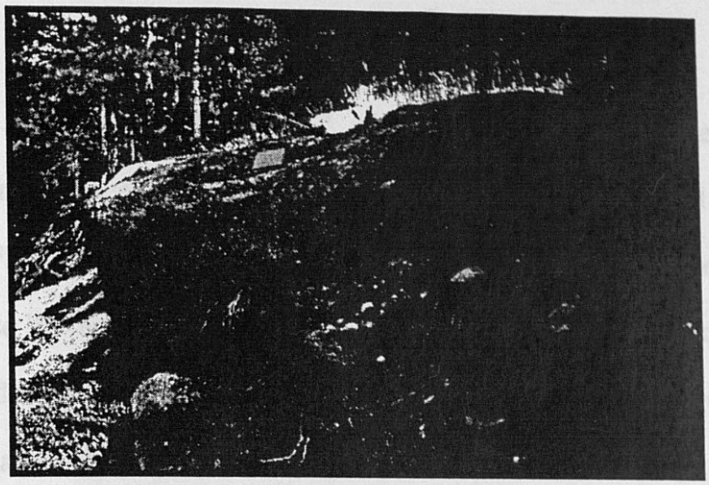

b)

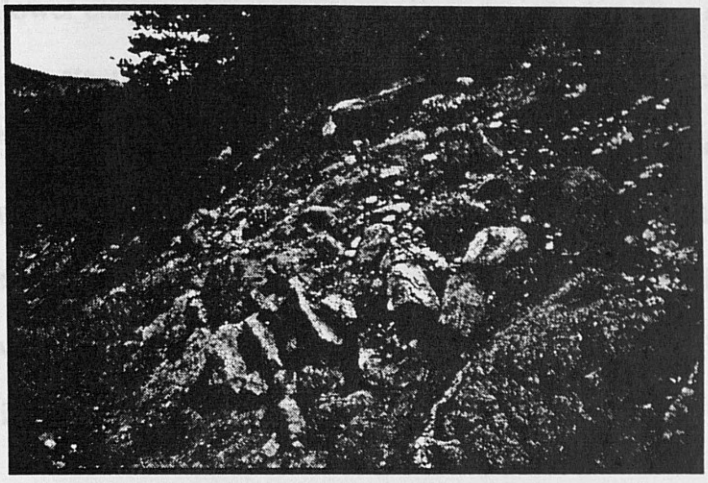

c)

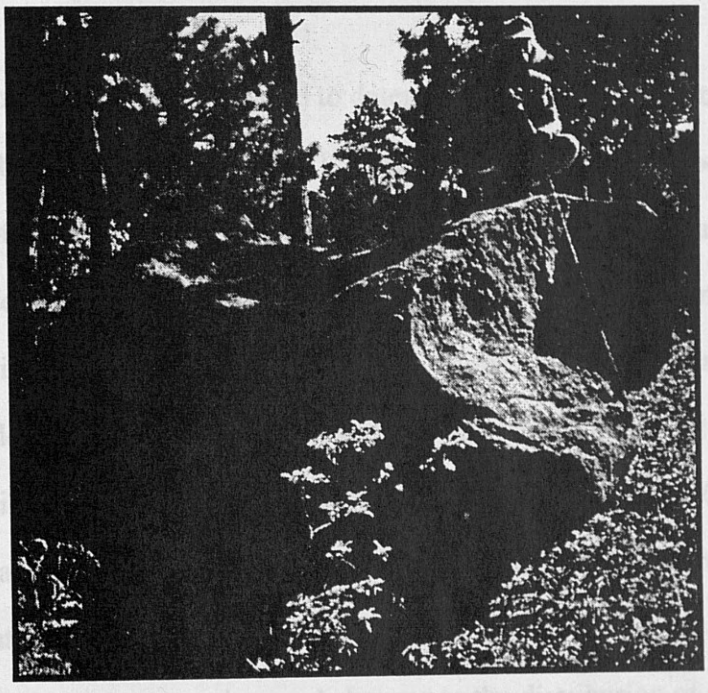

Figure 14: Cosmogenic sample sites; a) site 99-T71-1, boulder 2 m x 1.5 m x 0.8 m on 12 m terrace; sample collected from polished top surface; b) site 99-T71-2, cobbles collected from 30 cm below surface of 12 m terrace; c) site 99-T60-1, boulder 4.2 m x 2.8 m x 2.2 m, sample collected from where David Dethier sits; sample 5.0 m above Middle Boulder Creek

of the terrace sample sites T18 and T72, which are < 50 m apart. The sample at T43 was collected from a terrace surface, and the sample at T10 was collected from 65 cm below the surface (Fig. 15). In addition to terrace samples, we collected one sample from a boulder whose lithology and shape (Fig. 14) suggested that it fell into the late Pleistocene Middle Boulder Creek from a nearby cliff and was sculpted in place (99-T60-1), and one sample from a polished edge of a pothole (99-T26) (Fig. 15). Despite thorough searches on upper and lower canyon walls, we found terrace remnants >10 m above grade only near the base of a steep reach of Middle Boulder Creek, approximately 14 km downstream from the gaging station at Nederland. In this region where high terraces are preserved, low (0.5 to 3 m) terraces are uncommon. With the exception of 99-T60-1, all samples had smoothed or polished surfaces, indicating minimal erosion since deposition. At each site we measured (1) horizon geometry, (2) strike and dip of the sample surface, (3) sample thickness, and (4) sample depth.

^{14}C Dating

^{14}C isotope dating can be used to determine the age of deposits if they contain preserved carbonaceous material. ^{14}C is a radioactive isotope of carbon formed through interactions of cosmic ray neutrons with ^{14}N in the atmosphere. ^{14}C atoms are chemically identical to the stable ^{12}C and ^{13}C isotopes; therefore ^{14}C moves through the carbon cycle in a similar fashion as the stable isotopes. Stable and unstable forms of carbon dioxide form in the atmosphere and are taken up by plants through photosynthesis. Stable and unstable forms of the bicarbonate ion (HCO_3^-) are dissolved in water and are incorporated into carbonaceous material (Fig. 16). Variations in the production rate of ^{14}C in the atmosphere have resulted from changes in the paleomagnetic intensity over time and changes in the distribution of carbon in our system. A stronger magnetic pole deflects cosmic rays away from the Earth, resulting

a)

b)

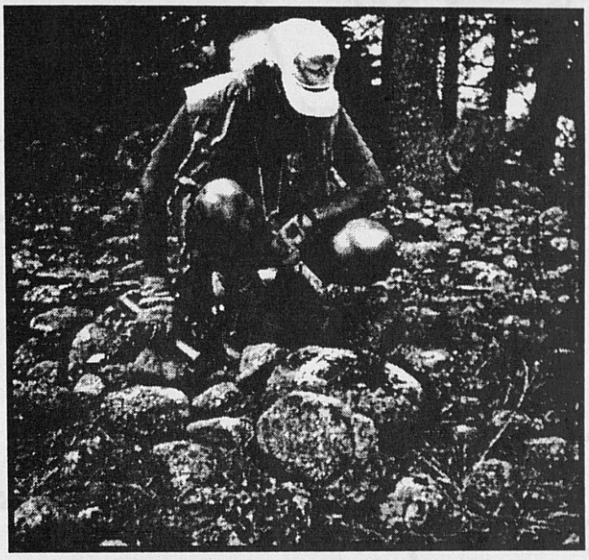

c)

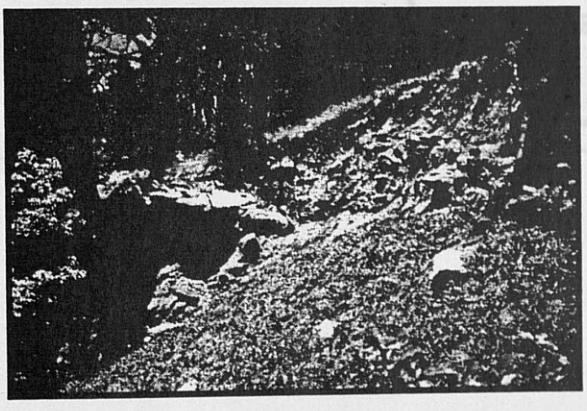

Figure 15: Cosmogenic sample sites; a) site 99-T26, sample collected from polished bedrock above pothole, 6.7 m above Middle Boulder Creek; b) site 99-T43, sample collected from terrace surface as shown, 7.5 m above Middle Boulder Creek; c) site 99-T10-1, cobbles collected from 65 cm below the surface of a 10 m terrace.

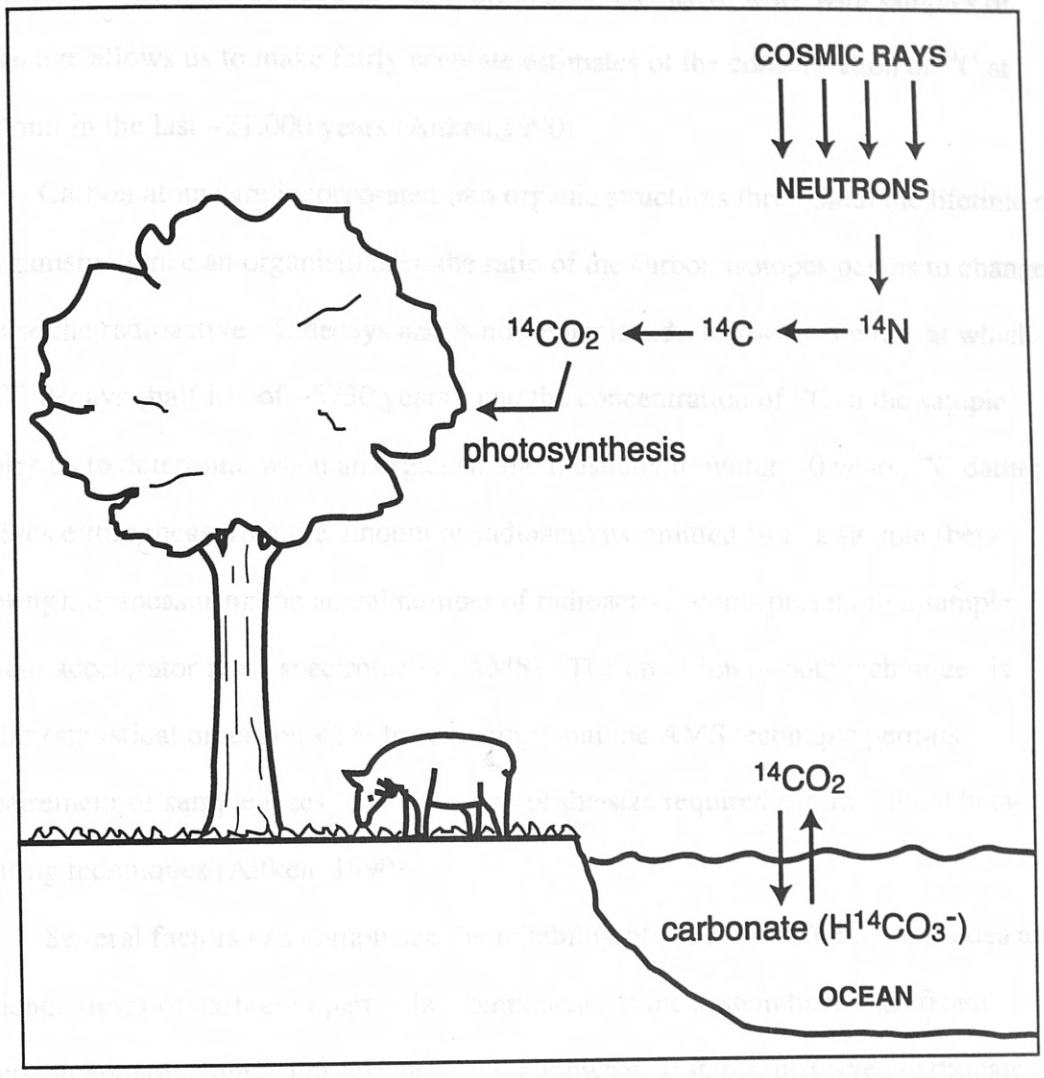

Figure 16. ^{14}C in the biosphere: radioactive carbon forms from the interaction of cosmic ray neutrons with nitrogen in the atmosphere. Following oxidation, ^{14}C is integrated into the biosphere through photosynthesis and thence through ingestion by animals (modified from Aitken, 1990).

in a lower production rate of ^{14}C. There is no significant latitudinal variation due to the rapid mixing of ^{14}C atoms in the atmosphere. Changes in the distribution of carbon in the system, such as placing "old carbon" in the atmosphere by burning fossil fuels, results in a lower concentration of ^{14}C. Fortunately, extensive work with samples of known age allows us to make fairly accurate estimates of the concentration of ^{14}C at any point in the last ~21,000 years (Aitken,1990).

Carbon atoms are incorporated into organic structures throughout the lifetime of an organism. Once an organism dies, the ratio of the carbon isotopes begins to change, because the radioactive ^{14}C decays and is not replenished. Knowing the rate at which the ^{14}C decays (half life of ~5730 years), and the concentration of ^{14}C in the sample enables us to determine when an organism died, usually to within 50 years. ^{14}C dating involves either measuring the amount of radioactivity emitted from a sample (beta-counting), or measuring the actual number of radioactive atoms present in a sample through accelerator mass spectrometry (AMS). The precision of both techniques is similar (statistical precision <1% for counting), but the AMS technique permits measurement of sample sizes only a fraction of the size required for traditional beta-counting techniques (Aitken, 1990).

Several factors can complicate the reliability of ^{14}C dates. The mixing rates and residence times of carbon in particular components of the system have significant effects on apparent ages. For instance, in groundwater systems, dissolved carbonate may not be in contact with the atmosphere for several hundreds to several thousands of years. Radioactive carbon in this system will decay without replenishment. If "old water" has contaminated a sample surface, the carbonate contamination can be removed with acid pretreatment. However, if the old carbon has been incorporated into organic structures through photosynthesis, no pretreatment can remedy the problem. Another significant problem is that very low concentrations of ^{14}C in old samples make them

highly susceptible to the effects of contamination with young material. Fortunately, since my samples are of Holocene age, contamination with "zero-age" material is not as significant a concern as it would be for older samples. Other contaminants that might affect sample ages such as modern humic acids or root hairs can be removed through sample pretreatment.

^{14}C Sampling

I collected charcoal samples from three locations in two terraces downstream of alluvial fans, and from the base of one alluvial fan. Sampled terraces ranged from 1.5 to 4.5 m above grade. I measured stratigraphy and described soil profiles for each sampling site (Fig. 17). The charcoal did not appear to have an anthropogenic origin, as it was generally located in concentrated horizontal layers or was dispersed throughout a narrow zone approximately one meter beneath the surface of the terrace. Layers of charcoal were continuous for at least several meters in the locations sampled. Sedimentary layers above and below the charcoal-rich layers did not appear to have been disturbed, nor was there field evidence of a hiatus between the time of deposition of the charcoal and deposition of the one meter of sand above the charcoal (i.e., no buried O/A horizons). The charcoal can be characterized as "chunk" charcoal. In one location the charcoal chunks were well rounded, most likely due to transport. As Madole (1986) noted the Boulder Canyon area is entirely within the crystalline core of the Front Range, and is far removed from areas of sedimentary rocks. As such, it is unlikely that the ^{14}C ages will be influenced by either hard-water effects or by redeposition of organic matter eroded from older rocks. The high concentration of charcoal from our sample sites indicates rapid deposition from a nearby source of charcoal.

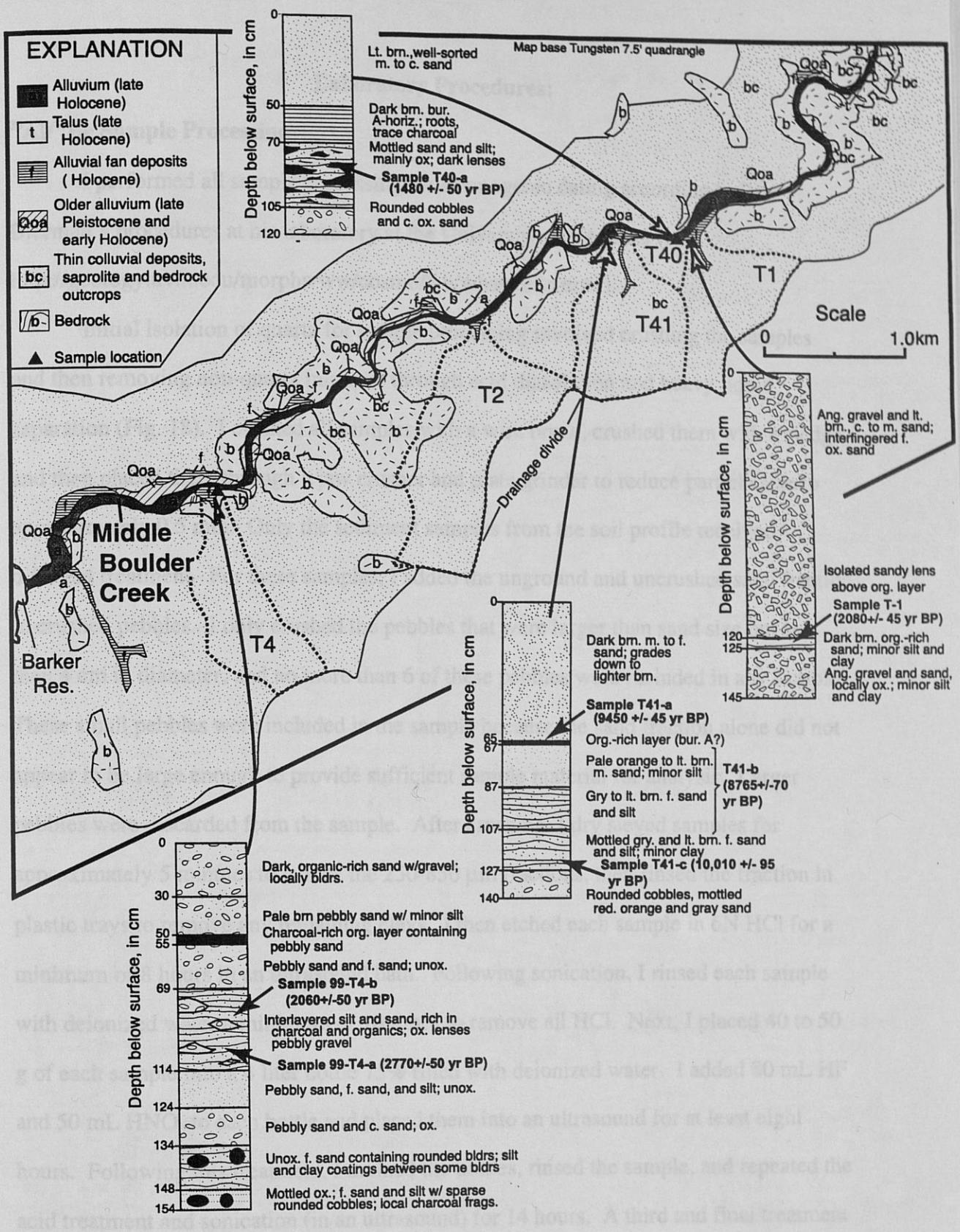

Figure 17. Superficial deposits near Middle Boulder Creek on the Tungsten, CO 7.5' quadrangle; dashed regions show drainage areas for alluvial fans; charcoal sample sites are marked with dark triangles; graphic logs illustrate stratigraphic position of charcoal samples at each sample site.

Laboratory Procedures:

$^{26}Al/^{10}Be$ Sample Processing

I performed all sample processing for cosmogenic dating according to Paul Bierman's procedures at his laboratory at the University of Vermont (see http://geology.uvm.edu/morphwww/cosmo/lab/whatwedo.html).

Initial isolation of quartz for sample processing involved crushing the samples and then removing non-quartz minerals through acid dissolution and heavy liquid separation (Fig. 18). I cleaned all samples with a wire brush, crushed them with a sledge, and then placed them through a jaw crusher and plate grinder to reduce particle size to approximately 0.5 mm. Only the sediment samples from the soil profile received different treatment. For these samples, I added the unground and uncrushed sand fraction to crushed pebbles. I only crushed the pebbles that were larger than sand size but less then 4 cm in diameter, and no more than 6 of these pebbles were included in any sample. These small pebbles were included in the sample because the sand fraction alone did not appear to be large enough to provide sufficient sample material for analysis. Larger pebbles were discarded from the sample. After crushing, I dry sieved samples for approximately 5 minutes to isolate the 250-850 μm fractions, then rinsed the fraction in plastic trays to remove any remaining clays. I then etched each sample in 6N HCl for a minimum of 8 hours in an ultrasound bath. Following sonication, I rinsed each sample with deionized water a minimum of 10 times to remove all HCl. Next, I placed 40 to 50 g of each sample into a 4 liter bottle 75% filled with deionized water. I added 80 mL HF and 50 mL HNO_3 to each bottle and placed them into an ultrasound for at least eight hours. Following this treatment, I drained the bottles, rinsed the sample, and repeated the acid treatment and sonication (in an ultrasound) for 14 hours. A third and final treatment consisted of the same acid treatment and 24 hours of sonication. This treatment served to purify 29 to 40 g of quartz so that the purified material contained 11 to 79 μg g^{-1} of ^{27}Al

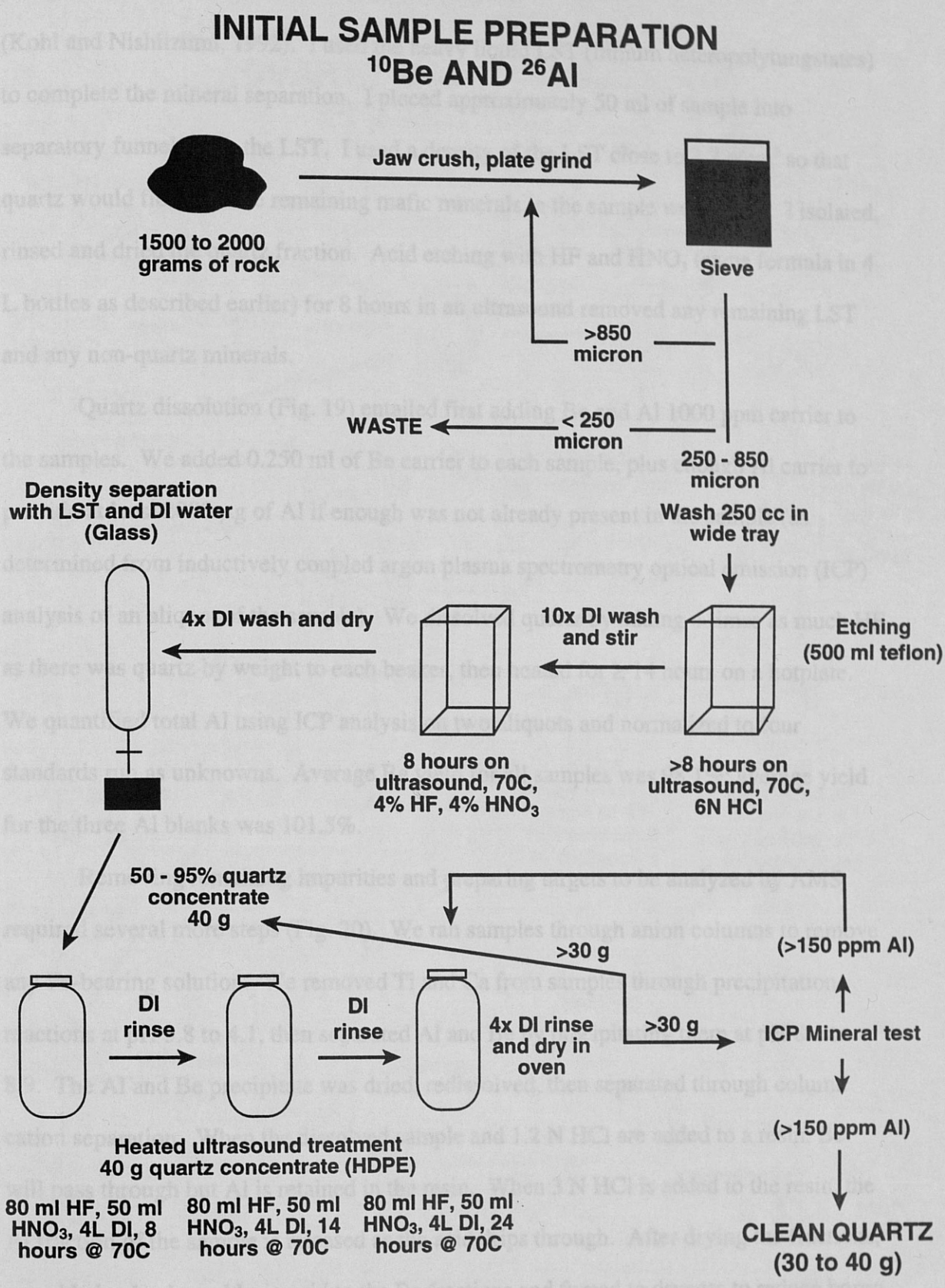

Figure 18. Flow chart of sample cleaning and quartz isolation.

(Kohl and Nishiizumi, 1992). I used the heavy liquid LST (lithium heteropolytungstates) to complete the mineral separation. I placed approximately 50 ml of sample into separatory funnels with the LST. I used a density of the LST close to 2.7 g/cm^3 so that quartz would float and the remaining mafic minerals in the sample would sink. I isolated, rinsed and dried the quartz fraction. Acid etching with HF and HNO_3 (same formula in 4 L bottles as described earlier) for 8 hours in an ultrasound removed any remaining LST and any non-quartz minerals.

Quartz dissolution (Fig. 19) entailed first adding Be and Al 1000 ppm carrier to the samples. We added 0.250 ml of Be carrier to each sample, plus enough Al carrier to provide at least 2000 µg of Al if enough was not already present in the sample (as determined from inductively coupled argon plasma spectrometry optical emission (ICP) analysis of an aliquot of the sample). We dissolved quartz by adding 4 times as much HF as there was quartz by weight to each beaker, then heated for ≥ 14 hours on a hotplate. We quantified total Al using ICP analysis on two aliquots and normalized to four standards run as unknowns. Average Be yield for all samples was 98.1%; average yield for the three Al blanks was 101.5%.

Removing remaining impurities and preparing targets to be analyzed by AMS required several more steps (Fig. 20). We ran samples through anion columns to remove any Fe-bearing solution. We removed Ti and Ca from samples through precipitation reactions at pH 3.8 to 4.1, then separated Al and Be by precipitating them at pH 8.1 to 8.9. The Al and Be precipitate was dried, redissolved, then separated through column cation separation. When the dissolved sample and 1.2 N HCl are added to a resin, Be will pass through but Al is retained in the resin. When 3 N HCl is added to the resin, the Al fraction of the sample is released as the acid drips through. After drying the fractions, we added < 1 ml perchloric acid to the Be fractions and fumed to dryness to reduce boron in the sample. We then dissolved samples in 1.2 normal HCl, and adjusted pH to 8.1 to

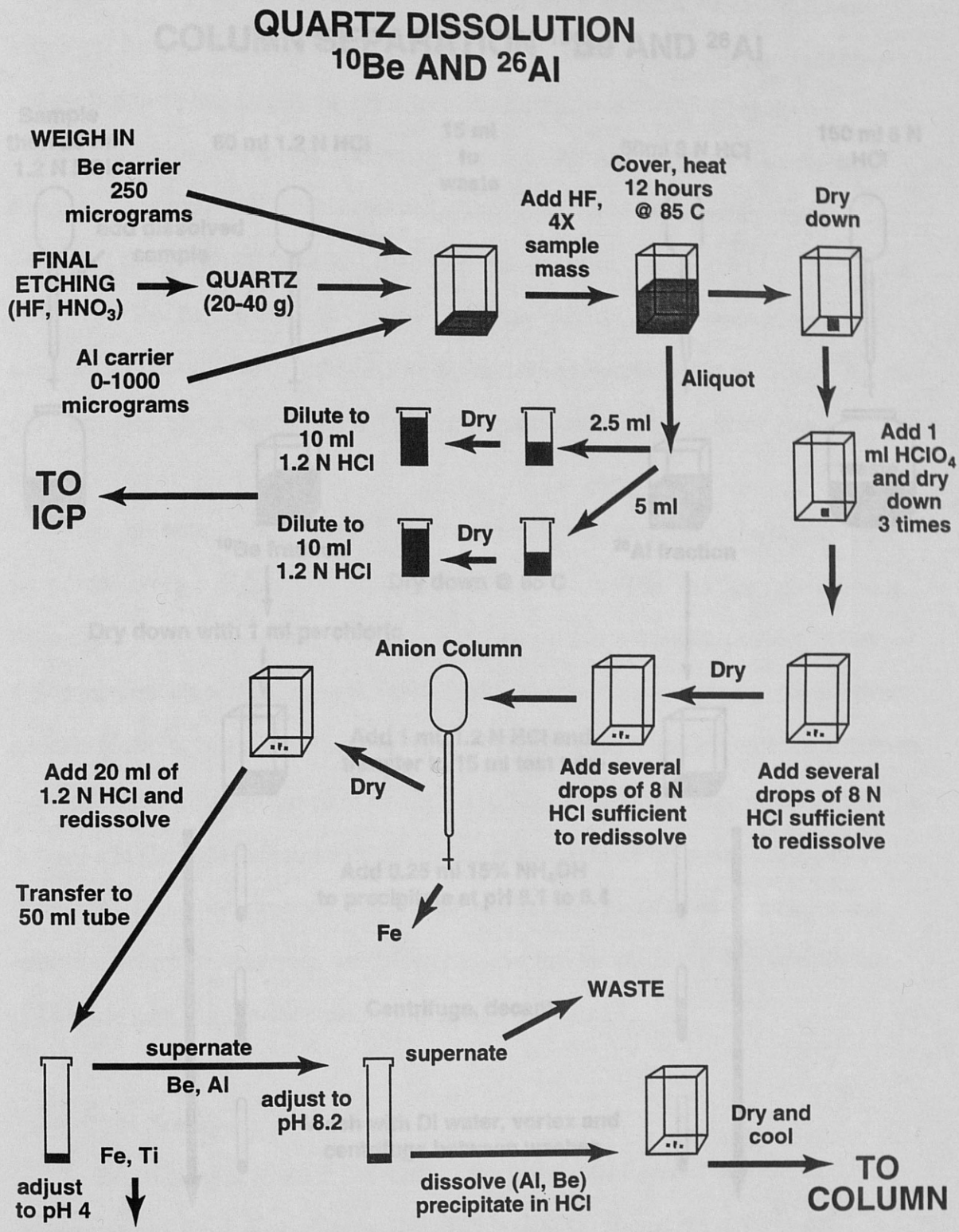

Figure 19. Flow chart of quartz dissolution.

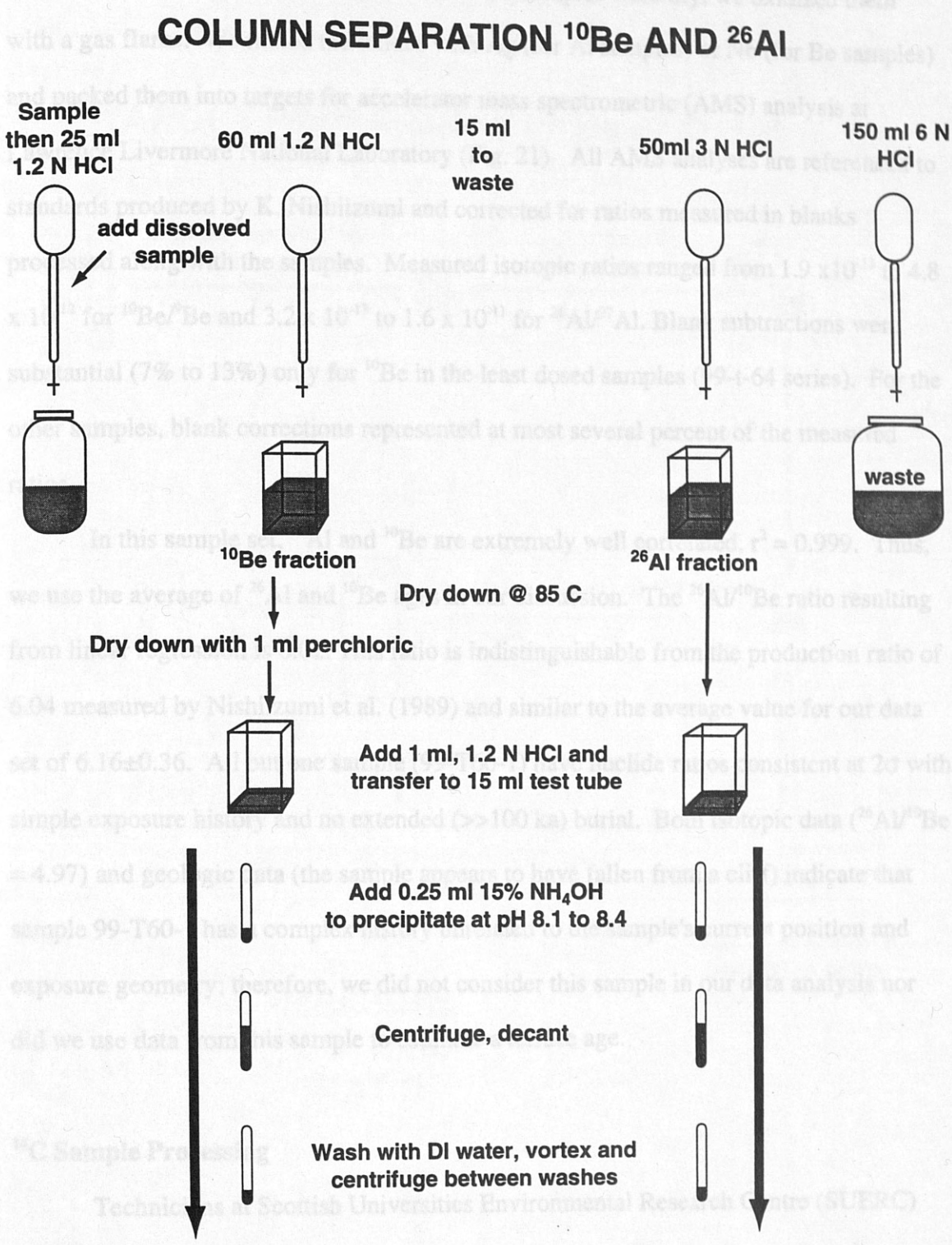

Figure 20. Flow chart of column separation of ^{10}Be and ^{26}Al.

8.9 to again precipitate the Al and Be. After the samples were dry, we oxidized them with a gas flame. We mixed the oxides with Ag (for Al samples) or Nb (for Be samples) and packed them into targets for accelerator mass spectrometric (AMS) analysis at Lawrence Livermore National Laboratory (Fig. 21). All AMS analyses are referenced to standards produced by K. Nishiizumi and corrected for ratios measured in blanks processed along with the samples. Measured isotopic ratios ranged from 1.9×10^{-13} to 4.8×10^{-12} for $^{10}Be/^{9}Be$ and 3.2×10^{-13} to 1.6×10^{-11} for $^{26}Al/^{27}Al$. Blank subtractions were substantial (7% to 13%) only for ^{10}Be in the least dosed samples (99-t-64 series). For the other samples, blank corrections represented at most several percent of the measured ratios.

In this sample set, ^{26}Al and ^{10}Be are extremely well correlated, $r^2 = 0.999$. Thus, we use the average of ^{26}Al and ^{10}Be ages in our discussion. The $^{26}Al/^{10}Be$ ratio resulting from linear regression is 6.02. This ratio is indistinguishable from the production ratio of 6.04 measured by Nishiizumi et al. (1989) and similar to the average value for our data set of 6.16±0.36. All but one sample (99-T60-1) have nuclide ratios consistent at 2σ with simple exposure history and no extended (>>100 ka) burial. Both isotopic data ($^{26}Al/^{10}Be$ = 4.97) and geologic data (the sample appears to have fallen from a cliff) indicate that sample 99-T60-1 has a complex history unrelated to the sample's current position and exposure geometry; therefore, we did not consider this sample in our data analysis nor did we use data from this sample to estimate a terrace age.

^{14}C Sample Processing

Technicians at Scottish Universities Environmental Research Centre (SUERC) and I prepared charcoal samples for dating by both conventional radiometric and accelerator mass spectrometry (AMS) methods. Pretreatment consisted of first heating samples to 80°C in 1 molar hydrochloric acid (HCl) for 3 to 4 hours. After rinsing and

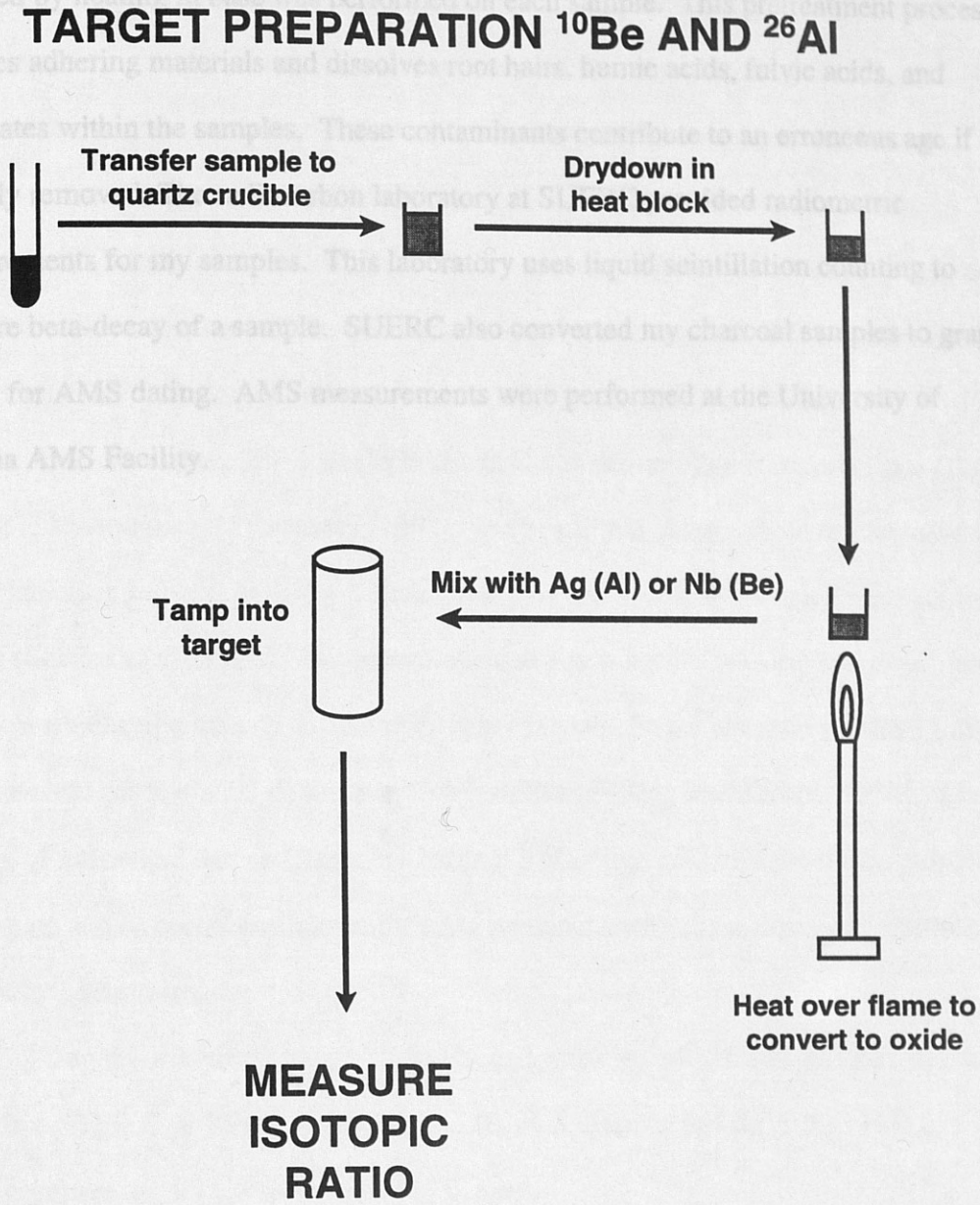

Figure 21. Flow chart of target preparation of samples.

metal sieving, samples were heated to 80°C in 2% weight/volume sodium hydroxide (NaOH) for 3 to 4 hours. After more rinsing, at least one more cycle of heating in acid followed by heating in base was performed on each sample. This pretreatment process removes adhering materials and dissolves root hairs, humic acids, fulvic acids, and carbonates within the samples. These contaminants contribute to an erroneous age if not properly removed. The radiocarbon laboratory at SUERC provided radiometric measurements for my samples. This laboratory uses liquid scintillation counting to measure beta-decay of a sample. SUERC also converted my charcoal samples to graphite targets for AMS dating. AMS measurements were performed at the University of Arizona AMS Facility.

GLACIATION IN THE COLORADO FRONT RANGE

Introduction

Measurement of cosmogenic isotopes produced *in-situ* presents new possibilities for determining ages of landforms such as moraines and for accurately reconstructing glacial chronologies, particularly in areas where organic matter is sparse or where deposits are too old for radiocarbon dating. Numerical age estimates for glacial landforms in Colorado are sparse, particularly for older deposits. For example, the age of deposits from the most recent Pinedale glaciation in northern Colorado is constrained only locally by ^{14}C dating of sediment in glacially-dammed lakes (Nelson et al., 1979; Madole, 1986; Doerner, 1994) and in lakes and bogs downvalley from moraines (Davis et al., 1987; Menounos and Reasoner, 1997). The age of the older and more extensive Bull Lake glaciation is constrained in Colorado only by a uranium trend age from a single soil profile (Shroba et al., 1983). In contrast, there is a rich literature using soil development and rock-weathering criteria to date relatively Pinedale, Bull Lake, and pre-Bull Lake moraines and other glacial deposits in Colorado (see Nelson and Shroba, 1998). The paucity of numerical age estimates has made it difficult to calibrate the relative-dating techniques and to correlate Colorado glacial sequences with those described elsewhere in the Rocky Mountains.

^{14}C ages have been changed to calibrated years before present (cal BP) when possible (< 21,000 yr BP) through the CALIB v4.2 (Stuiver and Reimer, 1993) to more easily compare model exposure ages to ^{14}C ages.

Cosmogenic exposure ages of Bull Lake and Pinedale moraines

My cosmogenic age estimates support previous age estimates based on soils and geomorphic relations (Madole et al., 1998) and are consistent with relative age relationships (Table 4, Appendix B). Using the production rates of Nishiizumi et al.

Table 4: Model ages derived from cosmogenic isotope data for samples collected on glacial moraines near Nederland and Twin Lakes Reservoir, Colorado.

Sample	Quadrangle	Elevation (km)	^{36}Cl model age (ka)	^{10}Be model age[1] (ka)	^{26}Al model age[2] (ka)	Average age[3] (ka)	^{10}Be/^{26}Al
99-t75	Ward	2.77		99.5 ± 20.5	102.9 ± 22.3	101.2 ± 21.4	6.04 ± 0.32
99-t68	Nederland	2.50		124.3 ± 25.8	119.4 ± 26.1	121.8 ± 25.9	5.69 ± 0.31
DC-91-3	Granite	2.81	30	15.9 ± 0.6			
99-t76	Ward	2.98		16.8 ± 3.4	16.9 ± 3.5	16.9 ± 3.5	6.04 ± 0.32
99-t74	Nederland	2.65			17.5 ± 3.6	17.5 ± 3.6	
DC-91-2	Granite	2.85	30	16 ± 0.6			

Notes:

1: Calculated using Nishiizumi et al. (1989) production rate estimates of ^{10}Be = 6.03 atomsg^{-1}yr^{-1}; ^{26}Al = 36.8 atomsg^{-1}yr^{-1}; also rock density = 2.7 gcm^{-3}; latitude = 40° N; attenuation length = 165 gcm^{-2}.

2: Elevation and latitude corrections made using Lal (1991) considering only neutrons.

3: Average (weighted) calculated considering uncertainty of each measurement

(1989), boulders on the prominent Pinedale moraines in the Boulder Creek drainage, in the Middle Boulder Creek drainage near Nederland, and near Twin Lakes Reservoir have average exposure ages that cluster about 17 ka; using the lower production rate estimates of Larsen et al. (1995) or Stone et al (1998) would generate model ages closer to 20 ka.

Two of three Bull Lake samples have considerably higher nuclide abundances than the Pinedale samples and thus I interpret them as having longer exposure ages. I averaged ^{10}Be and ^{26}Al exposure ages to determine that demonstrably eroded boulders on Bull Lake moraines have been exposed for >100 ka near the Glacial Lake Devlin site (Fig. 3), and >120 ka south of Nederland. The measured ^{26}Al/^{10}Be ratios of ~ 6, and thus the close relationship between ^{26}Al and ^{10}Be exposure ages for Bull Lake samples 99-T75 and 99-T86, and Pinedale sample 99-T76, are consistent with simple exposure histories that include no long term burial during or prior to initial exposure (Nishiizumi et al., 1991; Bierman et al., 1999).

The ^{10}Be exposure age of 15.9 ± 0.6 ka for the Bull Lake moraine south of the Twin Lakes Reservoir is the same as that for the nearby Pinedale moraine (16.8 ± 3.4 ka) and is thus inconsistent with the subdued moraine morphology, rock weathering criteria, and soils data. ^{36}Cl exposure ages calculated using the model of Bierman et al. (1995a) for both moraines are comparable (~ 30 ka), but nearly twice as old as the ^{10}Be exposure ages.

Discussion

Our cosmogenic exposure ages are consistent with the sparse suite of radiometric dates for glaciations in Colorado. Exposure ages (^{10}Be and ^{26}Al) from outer Bull Lake moraines near Nederland (Fig. 3) are consistent with a Bull Lake glaciation before 120 ka (Nishiizumi et al., 1989, production rates) or 140 ka (Larsen et al., 1995, production rates). Thus, our data are compatible with the only other radiometric age for Bull Lake

glaciation in Colorado: a uranium-trend age of 130±40 ka for Bull Lake till from the North St. Vrain catchment (Shroba et al., 1983). Elsewhere in the Rocky Mountains, ages of Bull Lake advance(s) and retreat(s) are estimated at 150 to 100 ka from cosmogenic exposure ages in Wyoming (Phillips et al., 1997; Hancock et al., 1999), and at 155 to 130 ka, based on obsidian rind thicknesses near West Yellowstone (Pierce et al.,1976).

In contrast, the ^{10}Be and ^{36}Cl model ages for a boulder on a Bull Lake moraine at Twin Lakes Reservoir (DC-91-3) are indistinguishable from those of a boulder on the adjacent Pinedale moraine (DC-91-2). The boulder we sampled on the Bull Lake moraine might have fallen from the Pinedale-age glacier, but the boulder's cracked and stained appearance and adjacent well-developed soil profiles (Nelson and Shroba, 1998) suggest the moraine is considerably older. The consistent ^{36}Cl model ages argue for similar exposure histories for DC-91-2 and -3 and against complicated scenarios involving burial, rolling, or exhumation. The nearly two-fold difference in exposure ages between ^{36}Cl and ^{10}Be in both samples is most likely the result of violating the assumptions of no-erosion or no-burial. Small amounts of erosion or burial by snow pack (cm to dm) could more than double effective thermal neutron stopping rates, inflating ^{36}Cl model ages by similar amounts (Bierman et al., 1995b). In this application, the ^{10}Be data are likely more reliable estimators of age.

Our cosmogenic exposure ages for the Front and Sawatch Ranges indicate that outer Pinedale-age moraines stabilized at about 17 ka at three different locations in Colorado. Our cosmogenic data are consistent with others measured in the Rocky Mountains. North of Colorado, cosmogenic-isotope dating of boulders on Pinedale moraines in the Wind River Range, Wyoming, indicates ages (using Nishiizumi et al., 1989, production rates) between about 23 and 16 ka (Gosse et al., 1995; Chadwick et al.,

1997). Thus, Pinedale glaciation in southwest Montana and Wyoming was broadly synchronous with glaciation in the Front and Sawatch Ranges of Colorado.

Studies of Pinedale-age deposits in Colorado and Wyoming based on ^{14}C and obsidian hydration ages have suggested that moraines were constructed between about 35 and 15 ka (i.e., Madole, 1976; Nelson et al., 1979; Davis et al., 1992; Doerner, 1994; Pierce et al., 1976). Most germane to our study is Madole's (1986) conclusion that the Pinedale maximum occurred at 23,500 and 21,000 yr BP (uncalibrated) based on radiocarbon analysis of dispersed carbon in Glacial Lake Devlin sediments (Fig. 3). If Madole's ages and interpretations are correct, then the production rates of Larsen et al. (1995) or Stone et al. (1998) appear to generate more accurate ages for our study than those of Nishiizumi et al. (1989). Geologic and dating evidence shows that Bull Lake glaciers were similar in extent to the maximum extent of Pinedale ice in the Front and Sawatch Ranges. Our results and previous research in the Front and Sawatch Ranges suggests that that maximum extent of Pinedale glaciers occurred before ~ 17 ka, perhaps as early as 23 ka. Pinedale ice retreated back into Front Range cirques before 14,939-13,813 cal BP (12,040 ± 60 yr BP)(Benedict, 1973, 1981; Menounos and Reasoner, 1997) based on late glacial "Santanta Peak" readvances high in Front Range cirques. Additional research combining detailed mapping and exposure-age dating may allow a precise evaluation of Pinedale-age glacier fluctuations in the Colorado Rocky Mountains.

FLUVIAL TERRACES IN BOULDER CANYON

Introduction

Fluvial fill terraces in Boulder Canyon, Colorado Front Range record late Quaternary downcutting, punctuated by periods of aggradation that likely reflect glaciation of the upper reaches of Boulder Creek (Madole, 1991). Terraces thus register perturbations of the catchment sediment budget in a system driven by incision since at least Pliocene time (Epis et al., 1980; Scott and Taylor, 1986; Gregory and Chase, 1994). The distribution of terraces and underlying deposits reflects temporal changes in base level and evolution of the longitudinal profile of Middle Boulder Creek. In the Boulder Creek catchment and in other large Front Range catchments, millennial-scale changes in sediment budgets likely record the effects of advancing and retreating glaciers and other major shifts in climate (Madole, 1991), whereas decadal-scale changes may reflect forest fires and large storms.

Previous studies of fluvial terraces in Boulder Canyon analyzed stratigraphy, soil development and clast weathering to derive qualitative age estimates (Netoff, 1977; Barber, 1983). The paucity of organic matter and thus the inability to constrain deposit ages by ^{14}C dating limited the use of terraces as a tool for studying river dynamics over time. However, recent advances in the use of *in situ* produced cosmogenic isotopes such as ^{26}Al and ^{10}Be provide a basis for determining exposure ages of terraces and other landforms (e.g. Burbank et al., 1996; Chadwick et al.,1997; Phillips et al.,1997). These isotopes allow us to: (1) correlate terraces with upstream moraines; (2) calculate rates of incision; and (3) provide calibration for age estimates based primarily on the degree of soil development.

The change in climate or rock–uplift rates that initiated incision of the Colorado Front Range remains controversial after a century of geologic discussion (e.g., Davis, 1911; Epis et al., 1980; Jacob and Albertus, 1985; Leonard and Langford, 1994; Gregory

and Chase 1994; Chapin and Kelly, 1997). The evolution of longitudinal river profiles, mirrored by terraces and correlated surfaces, can contribute to this discussion since persistent convex-upward portions of the longitudinal profile, or "knickpoints," (e.g., Merritts, 1994; Pazzaglia et al., 1998) characterize tectonically stable regions. Dated terraces and correlation with the broad alluvial surfaces of the western High Plains (Madole, 1991) allow us to study the evolution of Middle Boulder Creek's longitudinal profile.

Boulder Canyon terraces

Morphology, correlation and weathering

Fluvial terraces, with upper strath surfaces 1 to12 m above the present level of Middle Boulder Creek, are common in Boulder Canyon, along with extensive areas of colluvial debris and localized alluvial fans. Terraces are best preserved upstream of the confluence with North Boulder Creek. The paucity of terraces and fans downstream may reflect a change in river dynamics that decreases the probability of terrace formation or preservation, or may result from human manipulation of deposits during road, railroad, and pedestrian path construction. Exposed bedrock slopes and cliffs are common on steep valley walls of Boulder Canyon, but thin colluvial debris with local bedrock outcrops predominate where slopes are < 30 °. In the gently rolling upland, bedrock is deeply weathered, grussified and readily eroded where exposed.

Fluvial deposits show decreased preservation and increased degree of soil development as height above grade increases. Low terraces (0.5 to 3 m above grade) form surfaces up to 50 m wide and hundreds of meters long in the broadest portions of the valley and are continuous for up to several kilometers in the upper canyon. In the lower canyon, low terraces are more difficult to identify, since many have been extensively disturbed by development. Holocene terraces and adjacent fans show

minimal soil development (Table 3, Netoff, 1977). Terrace remnants 4 to ~9 m above grade are also common and are best-preserved in the upper canyon. They have weakly developed B-horizons that suggest latest Pinedale age (Netoff, 1977). Terraces ~9 to 14 m above grade are exposed within about 2 km of Sunnyside (Fig. 8) and display better-developed Bt-horizons, suggesting an early Pinedale or Bull Lake age. Near Sunnyside we mapped 3 exposures of terraces 14-21 m above grade, each consisting of a layer of stream-transported cobbles in an oxidized, coarse-grained matrix. Topographic position of these exposures above inset Pinedale (?) terraces suggests a pre-Pinedale age.

Cosmogenic exposure ages

The fluvial fill terraces of Boulder Canyon give cosmogenic exposure age estimates (Table 5, Appendix B) that are broadly consistent but younger than previous age estimates for terraces based on soil development, clast weathering, and stratigraphic position (Table 3, Netoff, 1977). The single sample from a Bull Lake age terrace 16 m above grade has an age estimate of 130 ± 27.5 ka, consistent with the 101 ± 21 ka and 122 ± 26 ka age estimates of two Bull Lake moraines near Nederland (Table 4). Terrace remnants are dominated by Pinedale cosmogenic exposure ages ranging from 29 to about 11 ka. Several terraces noted as "early Wisconsinan/Bull Lake" in age based on soil development and stratigraphic position (Table 3, Netoff, 1977) appear to be of early Pinedale age. Terraces ~9 to 14 m above grade have early Pinedale exposure ages (29 to 16 ka) whereas terraces 4 to ~9 m above grade have late Pinedale exposure ages of 14 to10.5 ka. We assume that all samples give reliable exposure ages except for sample 99-T60-1 and the samples at site T64, which are discussed below.

Table 5. Cosmogenic isotope data for samples collected within Boulder Canyon

Sample[1]	Age Estimate[2]	Terrace height (m)	Elevation (km)	Location (UTM)	$^{10}Be/^{26}Al$	^{10}Be model age[3] (ka)	^{26}Al model age[3] (ka)	Average age[4] (ka)
99-t64-r	Pinedale	9.5	2.451	4424200 N, 459200 E	6.64 ± 0.57	3.8 ± 0.8	4.2 ± 0.9	4.0 ± 0.8
99-t64-0	Pinedale	9.5	2.451	4424200 N, 459200 E	6.01 ± 0.42	2.8 ± 0.6	2.8 ± 0.6	2.8 ± 0.6
99-t64-20	Pinedale	9.5	2.451	4424200 N, 459200 E	6.32 ± 0.79			
99-t64-40	Pinedale	9.5	2.451	4424200 N, 459200 E	ND			
99-t64-60	Pinedale	9.5	2.451	4424200 N, 459200 E	5.92 ± 0.41			
99-t64-80	Pinedale	9.5	2.451	4424200 N, 459200 E	6.53 ± 0.48			
99-t64-100	Pinedale	9.5	2.451	4424200 N, 459200 E	6.86 ± 0.51			
99-t64-120	Pinedale	9.5	2.451	4424200 N, 459200 E	6.21 ± 0.37			
99-t10-1	late Pinedale	10	2.024	4427800 N, 466700 E	5.59 ± 0.35	19.9 ± 4.0	18.3 ± 3.8	19.1 ± 4.0
99-t18	Pinedale/B.L.	12.5	1.951	4428100 N, 467600 E	6.19 ± 0.36	15.9 ± 3.2	16.2 ± 3.4	16.0 ± 3.2
99-t26-1	Pinedale	6.7	1.878	4428000 N, 469000 E	ND	13.8 ± 2.8	ND	ND
99-t43	late Pinedale	7.5	2.415	4424600 N, 460400 E	6.01 ± 0.42	11.9 ± 2.4	11.8 ± 2.5	11.8 ± 2.4
99-t60-1	Pinedale	4	2.354	4425600 N, 461500 E	4.97 ± 0.28	39.8 ± 8.1	32.7 ± 6.8	35.6 ± 8.1
99-t71-1	Pinedale	12	1.939	4428100 N, 467800 E	6.20 ± 0.34	22.4 ± 4.5	22.9 ± 4.8	22.6 ± 4.5
99-t71-2	Pinedale	12.0	1.939	4428100 N, 467800 E	5.69 ± 0.33	31.1 ± 6.3	29.7 ± 6.2	30.4 ± 6.3
99-t72	Bull Lake	16.0	1.951	4428100 N, 467650 E	6.03 ± 0.35	132.9 ± 27.8	138.7 ± 30.6	135.5 ± 27.8

Notes:

1: For 99-t64 profile samples, last number is depth below surface in cm; sample 99-T64-r is a rock on the surface.

2: From relative soil development.

3: Calculated using Nishiizumi et al. (1989) production rate estimates of ^{10}Be = 6.03 atomsg^{-1} yr^{-1}; ^{26}Al = 36.8 atomsg^{-1}yr^{-1}; also samples at 40° N; density = 2.7 gcm^{-3}(rock), 1.5 gcm^{-3} (soil); latitude = 40° N; attenuation length = 165 gcm^{-2}.

4: Average (weighted) calculated considering uncertainty of each measurement.

Soil profile

Cosmogenic isotope abundance in the soil profile at site T64 and in a rounded clast on the terrace indicate that the surface does not cap a late Pleistocene deposit that has been exposed since deposition. Model ages show no clear depth relationship (Fig. 22) and what appears to be noise about a mean of ~ 3 ka. We consider two possible explanations for the ages, though field data do not help to constrain a solution. First, the deposit could have accumulated rapidly during the late Holocene, and noise in the profile reflects low and somewhat variable inheritance. Construction of a ~9 m terrace in the wide valley east of Barker Reservoir requires extensive sediment transport, an event for which we observed no evidence in other areas. Second, until recently the terrace could have been buried by a few meters of sediment which would have restricted cosmogenic isotope accumulation. Sediment was probably not derived from a side drainage, since the deposit is rich in large, rounded boulders, typical of upstream sources. As a result of this ambiguity, we do not use these cosmogenic ages in further discussion. The low and limited range of cosmogenic ages, however, does demonstrate minimal cosmogenic inheritance within the fill, and perhaps within fill terraces throughout Boulder Canyon.

Discussion

Terrace heights and changing base levels

Cosmogenic age estimates for terraces in Boulder Canyon and correlation with surfaces in the adjacent High Plains allow us to reconstruct late Pleistocene fluvial dynamics along Middle Boulder Creek. Base level defined by Middle Boulder Creek was ~ 20 m higher than today at 130 ka. By ~ 20 ka, incision of alluvium and bedrock dropped base level to between ~9 and 14 m above present grade. Before ~12 ka, terraces formed 4 to ~9 m above Middle Boulder Creek and during the past 10 ka, base level has been as much as 3 m above grade. There is no preserved record of alluvium older than

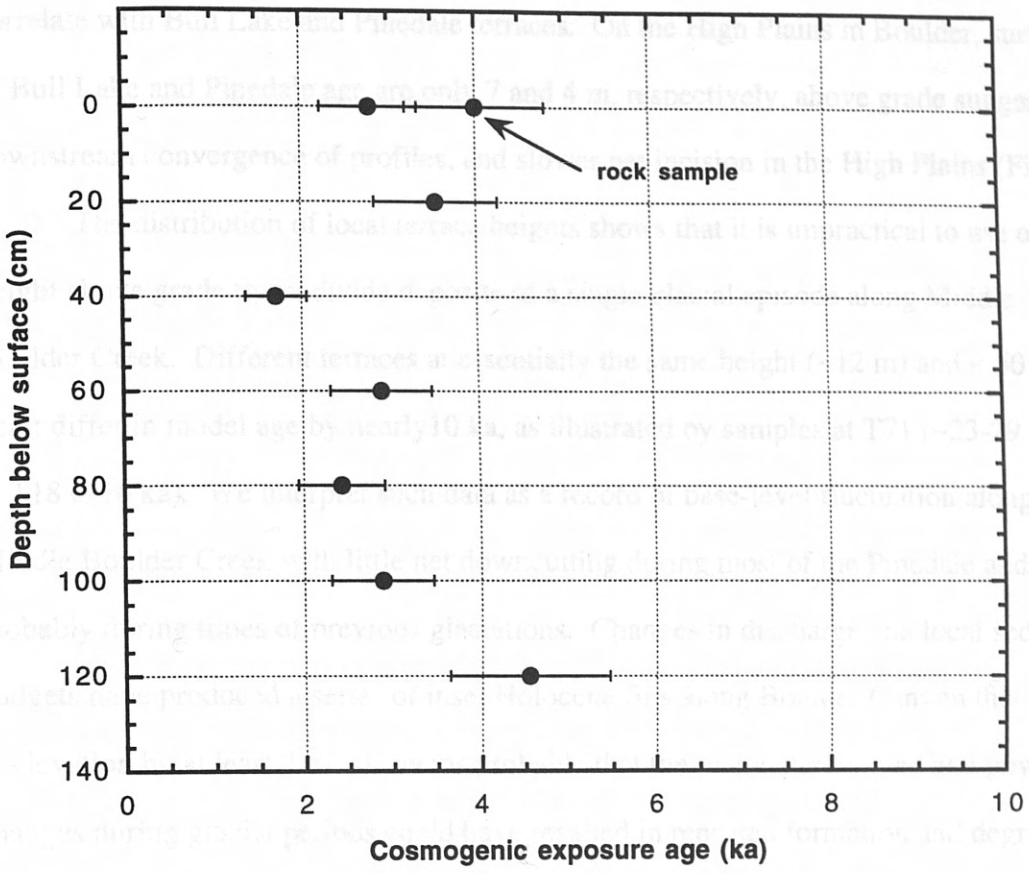

Figure 22. Cosmogenic exposure ages in soil profile at site T64 showing variation about a mean of ~ 3 ka; all samples are from soil profile except for the labeled rock sample.

~130 ka in Boulder Canyon (Fig. 23). The range of heights represented by terraces within Boulder Canyon contrasts markedly with those of High Plains surfaces thought to correlate with Bull Lake and Pinedale terraces. On the High Plains in Boulder, surfaces of Bull Lake and Pinedale age are only 7 and 4 m, respectively, above grade suggesting a downstream convergence of profiles, and slower net incision in the High Plains (Fig. 24).

The distribution of local terrace heights shows that it is impractical to use only height above grade to subdivide deposits of a single glacial episode along Middle Boulder Creek. Different terraces at essentially the same height (~12 m) and < 50 m apart differ in model age by nearly10 ka, as illustrated by samples at T71 (~23-29 ka) and at T18 (~16 ka). We interpret such data as a record of base-level fluctuation along Middle Boulder Creek with little net downcutting during most of the Pinedale and probably during times of previous glaciations. Changes in discharge and local sediment budgets have produced a series of inset Holocene fills along Boulder Canyon that range in elevation by at least 3 m. It seems probable that the major stream load and power changes during glacial periods could have resulted in repeated formation and degradation of fill terraces within ~10 m of a relatively constant base level. Consider that filling a 10 m deep valley of triangular cross section 75 m in average width and 12.5 km in length (distance between Boulder Dam and the confluence with North Boulder Creek) would require approximately $4.7*10^6$ m^3 of sediment. Assuming a density of 1.5 gcm^{-3}, the fill volume would be ~ $7*10^6$ Mg. Assuming a sediment production rate of 0.5 $Mgha^{-1}yr^{-1}$ from the 347 km^2 drainage basin of Middle Boulder Creek at Nederland (~ 3x background sedimentation rate), it would take only 1500 years to construct such a fill. During episodes of aggradation, considerable material may be transported through the canyon, but it seems probable that fills 10 m thick could accumulate and erode several times within a glacial period. Based on the pattern of incision reflected by terraces (Fig. 24), we believe net incision likely occurs during the transition to interglacial periods,

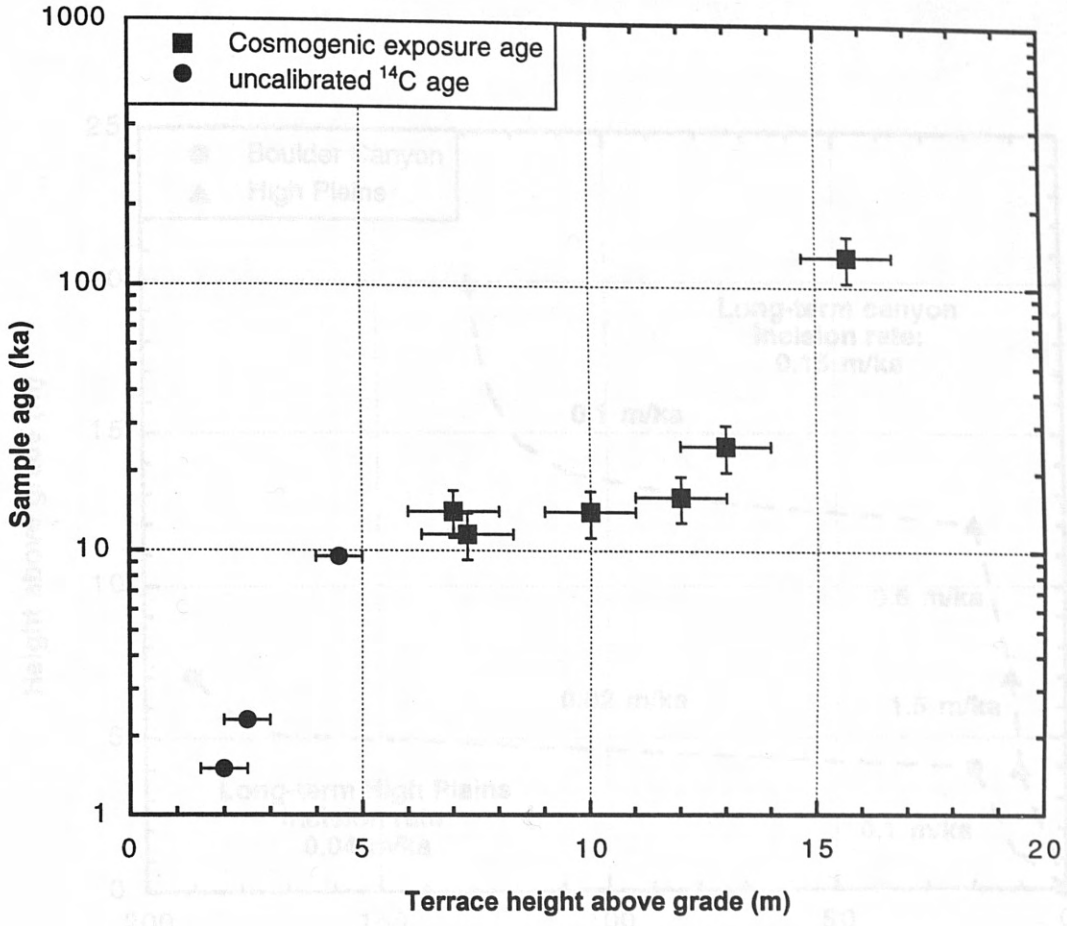

Figure 23. Terrace age versus height above grade, showing height ranges within glacial periods, and significant differences in height among different glacial periods. Bull Lake age deposition is thought to occur before ~100 ka, Pinedale age depostion between ~10 and 30 ka, and Holocene age deposition between ~10 ka and today.

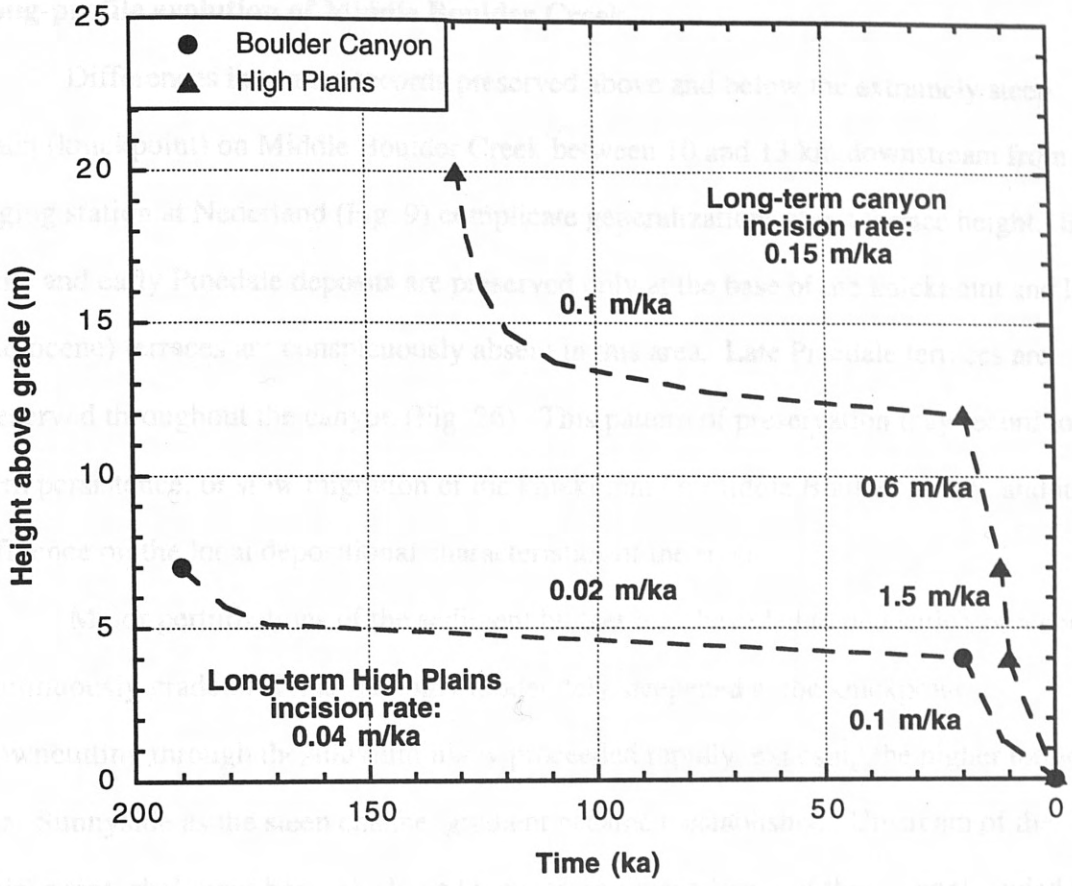

Figure 24. Rates of river incision based on age and terrace height above grade in Boulder Canyon and on the High Plaines. Rates between data points are listed on graph. Long term incision rates are based on 20 m of canyon incision since 130 ka, and 7 m of Plains incision since 190 ka.

when available sediment decreases concurrent with continued periods of peak discharge. The geomorphic result is a series of inset terrace remnants within approximately 10 m of a base level characteristic for each glacial period (Fig. 25).

Long-profile evolution of Middle Boulder Creek

Differences in terrace records preserved above and below the extremely steep reach (knickpoint) on Middle Boulder Creek between 10 and 13 km downstream from the gaging station at Nederland (Fig. 9) complicate generalizations about terrace height. Bull Lake and early Pinedale deposits are preserved only at the base of the knickpoint and low (Holocene) terraces are conspicuously absent in this area. Late Pinedale terraces are preserved throughout the canyon (Fig. 26). This pattern of preservation may record long-term persistence, or slow migration of the knickpoint on Middle Boulder Creek, and its influence on the local depositional characteristics of the river.

Major perturbations of the sediment budget may have led to deposition of a nearly continuously graded fill that was only moderately steepened at the knickpoint. Downcutting through the alluvium likely proceeded rapidly, exposing the higher terraces near Sunnyside as the steep channel gradient became reestablished. Upstream of the knickpoint, shallower bedrock slowed incision and meandering of the channel tended to erode the fill. This may be the reason that the highest terraces are only preserved at the base of the knickpoint. Alternatively, preservation of the high terraces could simply be a result of the sharp meander and confluence with a stream from a large tributary catchment at Sunnyside, which may have aided in preservation of extensive early and late Pinedale terraces. Preservation of both Bull Lake and Pinedale terraces, and absence of Holocene deposits suggests that only during glacial periods did river dynamics permit deposition on this steep meander of Middle Boulder Creek.

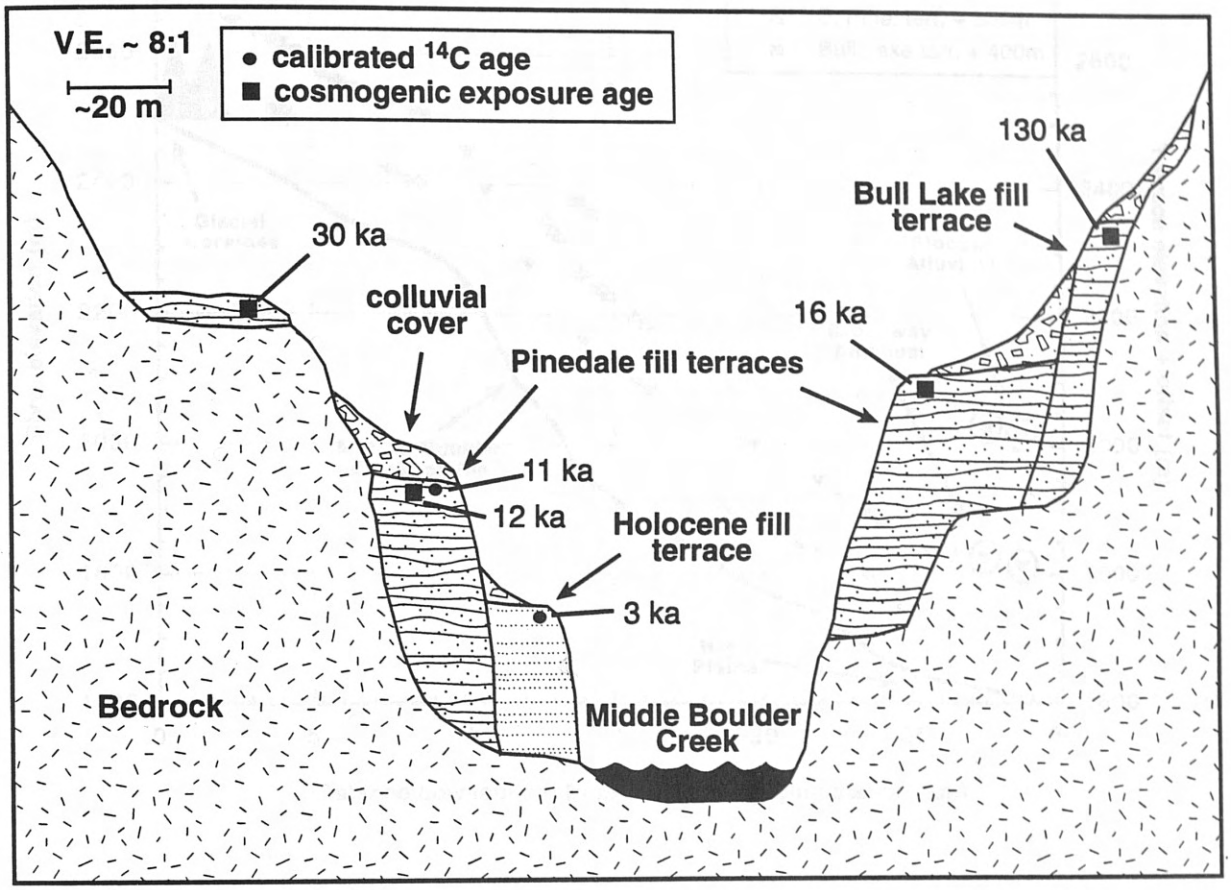

Figure 25. Schematic cross-section of Boulder Canyon illustrating stratigraphic and age relationships of Holocene, Pinedale, and Bull Lake terraces.

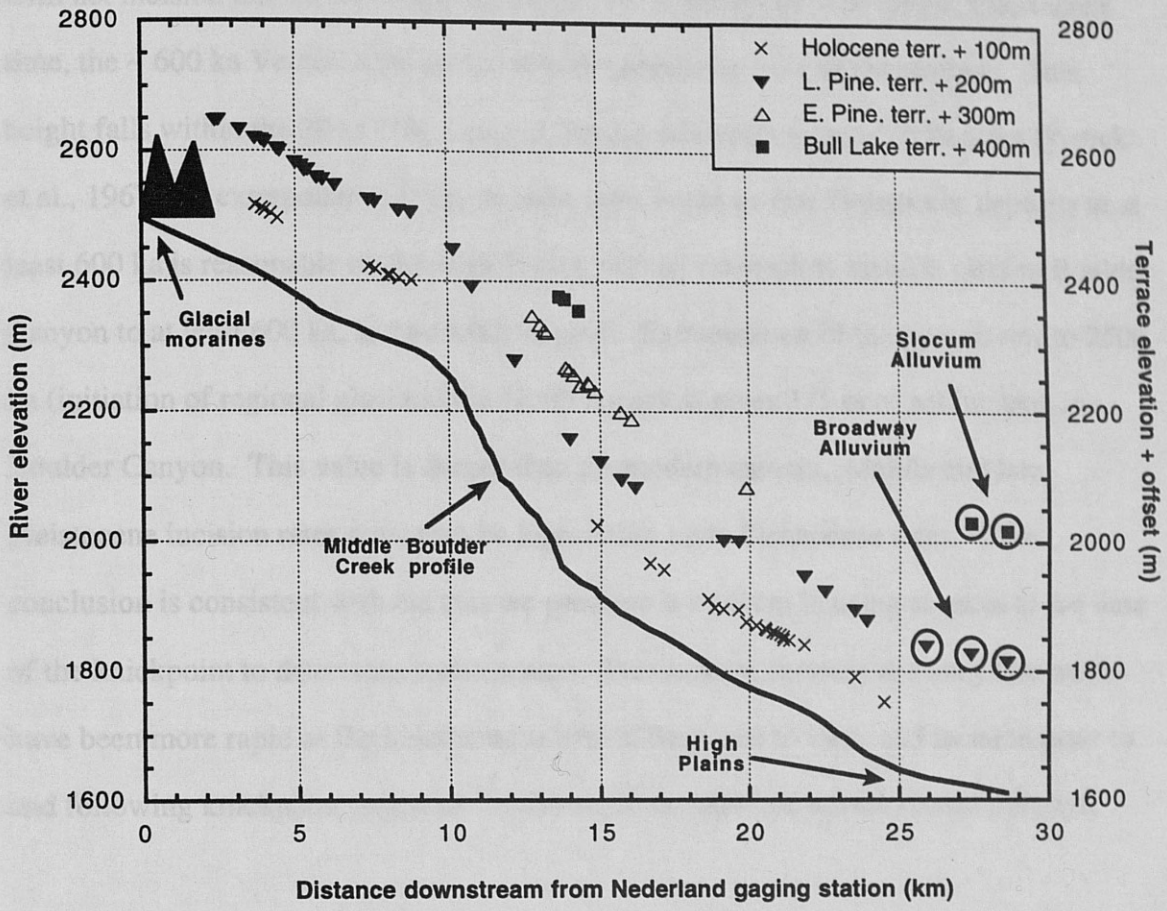

Figure 26. Profile of Middle Boulder Creek with terrace height above grade exaggerated; 100 m is added to the elevation of Holocene terraces, 200 m to late Pinedale terraces, 300 m to early Pinedale terraces, and 400 m to Bull Lake terraces, resulting in the offset appearance of terraces. Elevations of sites on Slocum and Broadway terraces are circled to distinguish them from Boulder Canyon terraces.

Heights of older surfaces on the High Plains suggest that short-term incision rates calculated using late Pleistocene deposits in Boulder Canyon and on the High Plains (Fig. 24) approximate downcutting rates for middle Pleistocene time to present. If the long term net incision rate on the High Plains (Fig. 24) is extrapolated to middle Pleistocene time, the ~ 600 ka Verdos Alluvium in Boulder should be ~ 21 m above grade. This height falls within the 20 to 25 m range of Verdos Alluvium mapped in Boulder (Wruck et al., 1967). If extrapolation of net incision rates based on late Pleistocene deposits to at least 600 ka is reasonable on the High Plains, we can extrapolate incision rates in Boulder Canyon to at least 600 ka, and possibly beyond. Extrapolation of the canyon rate to 2500 ka (initiation of regional glaciation in North America) gives 375 m of net incision in Boulder Canyon. This value is deeper than the modern canyon. Middle and late Pleistocene incision rates must thus be higher than early Pleistocene rates. This conclusion is consistent with the bias we presume is inherent in using terraces at the base of the knickpoint to determine incision rates. Presumably, incision at Sunnyside would have been more rapid as the knickpoint migrated from east to west, and incision prior to and following knickpoint migration would be slower than the terrace record portrays.

Relationship between fill terrace deposition and glaciation

Our terrace exposure age estimates show a close relationship with the late Pleistocene glacial chronology of the Colorado Front Range. Most preserved terraces within Boulder Canyon are < 8 m above grade. We can correlate these terraces with the 11.5 (± 2.5) ka fill terrace at site T43, which is 7 m above grade, and the13.8 (± 2.8 ka) polished bedrock at site T26, which is also 7 m above grade. These results suggest that most deposits preserved within Boulder Canyon are <13 ka. These ages are younger than the 14,939-13813 cal BP limiting age estimate of Pinedale ice retreat from the Colorado Front Range, based on late glacial "Santanta Peak" readvances in Front Range

high cirques (Benedict, 1973, 1981; Davis, 1987; Menounos and Reasoner, 1997) and on deglaciation at Lake Emma in the San Juan Mountains (Elias et al., 1991). The age estimates of fill terraces in Boulder Canyon thus suggest a peak in terrace formation following Pinedale ice retreat from the Boulder Creek drainage. Our single age estimate of a Bull Lake age terrace (130 ± 27.5 ka) is imprecise, but well within the range of estimated regional retreat of Bull Lake ice (~100-150 ka). Fill terraces in Boulder Canyon probably formed at times of high water and sediment availability, i.e., when ice retreat exposed widespread unconsolidated sediment and provided considerable meltwater for sediment transport. Uncertainties in cosmogenic production rates prevent us from making precise revisions to the late glacial chronology of the local area, but our results suggest that fluvial fill terraces may be used to limit the timing of major glacial retreats.

HOLOCENE ALLUVIAL FANS AND TERRACES

Introduction

Analysis of Holocene geomorphic change provides tools for understanding present geomorphic processes and the effects of climate change on past sediment storage and flux. In Boulder Canyon, Colorado (Fig. 8), alluvial fans from side drainages and fluvial terraces along the Middle Boulder Creek record deposition and the changing position of the canyon floor. Fluvial terraces integrate the local sediment budget in the 347 km^2 main catchment (measured where Middle Boulder Creek enters the city of Boulder, CO, U.S. Geological Survey unpublished data), whereas alluvial fans show the effects of processes within smaller (0.6 to 1.0 km^2) tributary catchments. Regional evidence suggests that fluvial reworking of Pinedale (latest Pleistocene) glacial deposits and forest fires play a significant role in the Holocene record of Boulder Canyon. Retreat from Pinedale maximum positions occurred before ~12 ka at Glacial Lake Devlin (Fig. 1; Madole, 1986; and Fig. 10, Madole et al., 1998), and before ~13 ka in the upper valley of the Colorado River on the west side of the Front Range (Madole,1976a). Only tiny glacial remnants, confined to the alpine portions of the Boulder Creek catchment, remained by ~ 11.5 ka (Davis et al, 1987). In nearby unglaciated areas, erosion and transport of sediment after fires (Moses, 1982; Jarrett, 1999) demonstrates that vegetation loss from steep Front Range slopes makes soil and grussified bedrock susceptible to rapid erosion. We hypothesize that forest fires generated alluvial fans in several side drainages within Boulder Canyon, and also contributed to the development of fluvial fill terraces downstream from the fans.

Modern erosion rates and erosional response to fire in the Rocky Mountain region

Background values of erosion and transport provide a basis for examining rapid rates of catchment erosion that occur after fires. Bovis (1974) noted that 80% of the

variance in annual soil loss from the subalpine Front Range was explained by bare soil area, slope, grain size parameters of surficial deposits, and infiltration rates. He reported soil loss rates of 5 to 10 $gm^{-1}yr^{-1}$ in dense stands of sub-alpine spruce-fir and that rates reached a maximum of 900 $gm^{-1}yr^{-1}$ near 8500 ft elevation. Assuming a drainage density of approximately 10 km/km^2, Bovis' upper limits yield 0.2 $Mgha^{-1}yr^{-1}$ and his lower limits 0.002 $Mgha^{-1}yr^{-1}$. Higher rainfall intensities during convective storms and larger areas of bare ground suggest that areas at lower elevation experience higher rates of soil movement. Stream sediment loads integrate catchment soil loss and channel erosion, both influenced by anthropogenic activity. At Clear Creek, Colorado Front Range, the measured suspended sediment load of ~ 0.77 $Mgha^{-1}yr^{-1}$ can be doubled to ~ 1.5 $Mgha^{-1}yr^{-1}$ to approximate total sediment load (from http://co.water.usgs.gov/sediment/). These data provide an upper limit for the present rate of erosion in the catchment since they are influenced by anthropogenic disturbance of both sediment and water budgets.

Fire events drive surface erosion, but the relationship is complex because both catchment characteristics and fire intensity are variable. Factors that control surface erosion include reduced cover and soil strength, raindrop impact, shallow overland flow, concentrated flow (rill erosion), reduced infiltration, and reduced evapotranspiration (Moses, 1982; Meyer, 1999; Robichaud, 1999). Rates of surface erosion after fire can vary from 0.1 to greater than 50 $Mg*ha^{-1}yr^{-1}$, often decreasing by orders of magnitude each year after the fire (Robichaud, 1999). Moses (1982) noted that in the Front Range, erosion rates in one-year old burns was an order of magnitude higher than rates in 2- to 4-year old burns.

Forest fire frequency is closely related to changes in climate and vegetation (Whitlock, 1999, Millspaugh et al., 2000). Since 1600 A.D., widespread forest fires in the Colorado Front Range have been strongly associated with warm and dry spring-summers (Veblen et al., 2000 in press). Regional fire frequency was high in early

Holocene time, but areas of high monsoonal precipitation in the early Holocene, perhaps including the Front Range, experienced higher fire frequencies in the middle and late Holocene (Whitlock and Bartlein, 1993; Whitlock et al., 1995; Whitlock, 1999). Fire events recorded in wildfire-flood sequences, lake sediments, and vegetation change indicate a high frequency of fire events in localities in Idaho and Colorado during the middle and late Holocene (Meyer, 1999; Jarrett, 1999; Keattch, 1994; Madole,1995; Fall,1985). However, forest fire evidence in the Front Range is not exclusive to the middle and late Holocene. Coe (1998) reported that alluvial fans from small side drainages (< 0.5 km^2) to Clear Creek, Colorado Front Range, show multiple late Holocene fan-building events, but late Holocene accumulation rates (0.2 to 0.4 mm/yr) are lower than early Holocene accumulation rates (0.4-0.6 mm/yr). Coe (1999) suggests a link between fan accumulation and fire events based on the abundance of preserved charcoal in alluvial material. We infer from these studies that fan accumulation is related to climate-induced fire events, and these events take place throughout several periods within the Holocene.

Geomorphic relations and ages of Holocene fans and terraces in Boulder Canyon

Fluvial terraces and alluvial fans of Holocene age dominate valley-floor deposits in Boulder Canyon west of the confluence with North Boulder Creek. Field relationships suggest a genetic connection between many of the alluvial fans and adjacent fluvial terraces. The alluvial fans we surveyed (Fig. 6) grade into, overlie and/or are incised into low fluvial terraces along the main channel (Fig. 27). The most extensive terrace remnants (50 m wide and over 100 m long) are adjacent to and downstream from alluvial fans. We mapped low terrace remnants at other locations along Middle Boulder Creek, but none rival the extent of the terraces abutting alluvial fans. Charcoal dates from low terraces and fans (Table 6) allow us to estimate deposit age and to determine the time

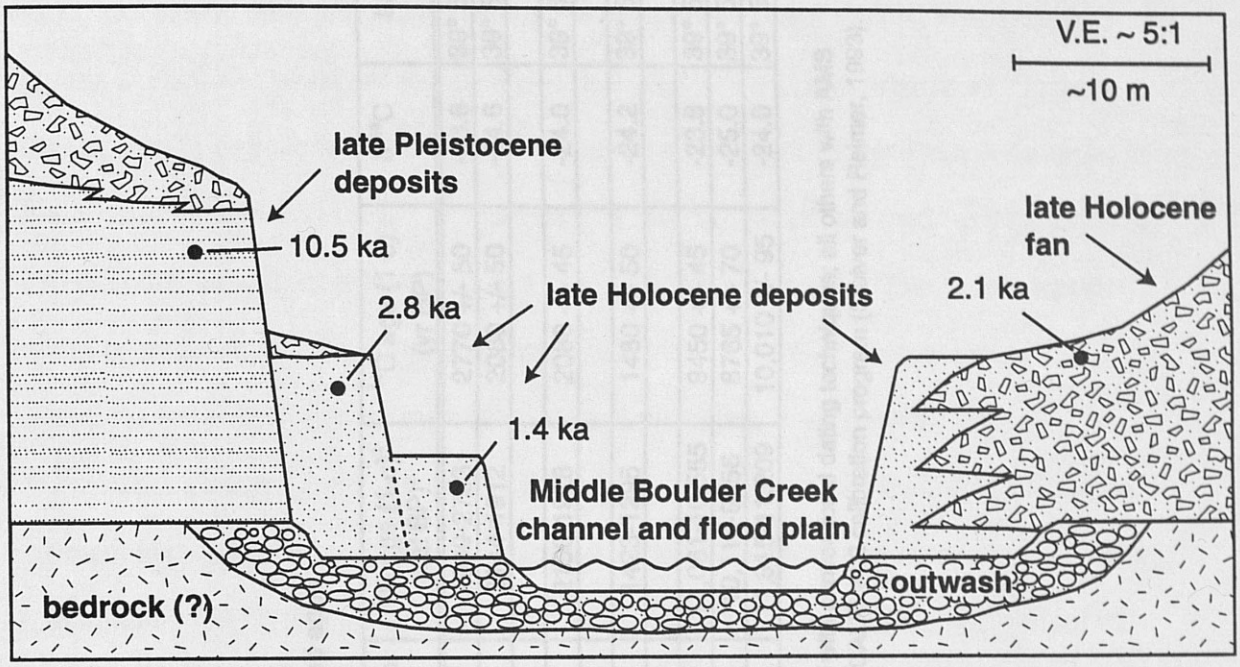

Figure 27. Schematic cross-section of the inner canyon illustrating stratigraphic and age relationships of late Pleistocene outwash, and Holocene alluvial fans and fluvial terraces on Middle Boulder Creek.

Table 6. Charcoal sample locations and ages.

Sample	Distance from Barker dam (km)	Elevation (m)	^{14}C age (1 σ)[1] (cal BP)[2]	^{14}C age (1 σ) (yr BP)	δ ^{13}C	Latitude, Longitude
99-T4a	1.9	2414	2969-2763	2770 +/- 50	-23.6	39° 58.3' N, 105° 28.0' W
99-T4b	1.9	2414	2144-1912	2060 +/- 50	-24.6	39° 58.3' N, 105° 28.0' W
99-T1	6.5	2304	2150-1928	2080 +/- 45	-24.0	39° 59.3' N, 105° 25.7' W
99-T40	6.0	2316	1423-1295	1480 +/- 50	-24.2	39° 59.3' N, 105° 26.0'W
99-T41a	5.8	2316	11,061-10,555	9450 +/- 45	-23.6	39° 59.3' N, 105° 26.0'W
99-T41b	5.8	2316	10,110-9556	8765 +/- 70	-25.0	39° 59.3' N, 105° 26.0'W
99-T41c	5.8	2316	11,915-11,209	10,010 +/- 95	-24.0	39° 59.3' N, 105° 26.0'W

Notes:

1: Samples 99-T4a and 99-T40 measured with conventional dating techniques; all others with AMS

2: Calibrated ranges determined from the CALIB v4.2 calibration program (Stuiver and Reimer, 1993).

period over which fan material accumulated. The approximate volume of each alluvial fan provides a minimum estimate of material eroded from the study catchments (Table 7). Poor exposure and sparse charcoal limited direct ^{14}C dating to one fan, but the relationship between fans and adjacent alluvial fills suggests that alluvial ages closely constrain fan ages.

Terrace and fan deposits are rich in sand, gravelly sand and gravel, and expose weakly developed soils and mottled zones. We measured and described stratigraphic sections at each site where we sampled charcoal (Fig. 17) and in nearby areas. Terrace deposits locally expose layers of fine sand and silt and we noted buried soil A-horizons in several alluvial fan exposures. The basal unit of each fluvial terrace tends to be composed of round cobbles with oxidized rinds in a sandy, oxidized matrix. Clasts in fan deposits tend to be more angular than those in terrace alluvium. Layers of charcoal were continuous for at least several meters laterally in the deposits we sampled but concentrations ranged from charcoal-rich alluvium to small, widely separated fragments. Sediment above and below the charcoal-rich layers did not appear to have been disturbed. Gradational contacts and the absence of buried B-horizons suggest that deposition of the layers was relatively rapid. The upper 0.6 to 1.0 m of most terrace remnants near side channels appear to be composed of fan and main-channel alluvium.

Charcoal fragments generally were concentrated in horizontal layers or dispersed throughout a narrow zone approximately one meter beneath terraces. The high concentration of charcoal suggests rapid deposition from a nearby source of charcoal. The charcoal was mainly cm-scale "chunks," but at site T40 the charcoal chunks were rounded, most likely due to transport. Our samples did not appear to have an anthropogenic origin: we found no evidence of fire pits, cracked rocks or cultural material associated with the laterally extensive charcoal-rich layers. The Boulder Canyon

Table 7. Short and long term accumulation rates of alluvial fan material.

Fan	Catchment area ($km^{2)}$	Fan volume[1] (m^3)	Total thickness removed (cm)[2]	Long-term accum. rate ($Mgha^{-1}yr^{-1}$)	Short-term accum. rate ($Mgha^{-1}yr^{-1}$)
T4	0.6	46,100	7.7	> 0.27	> 39
T41	0.6	43,700	7.0	> 0.35	> 35
T2	1.0	7,200 (13,000)	0.7 to 1.3	nd	nd
T1	0.5	< 50,000	< 9.6	< 0.45	< 96

Notes:

1: Fan volume for T2 shows estimate for base defined by the base of the ravine, and in parentheses the volume determined by assuming a horizontal base.

2: Calculated by dividing fan volume by catchment area; represents thickness of soil removed from catchment area.

area is entirely within the crystalline core of the Front Range, and is far removed from areas of sedimentary rocks (Madole, 1986). As such, it is unlikely that the ^{14}C ages are influenced by either hard-water effects or by redeposition of organic matter eroded from older rocks.

Radiocarbon ages of charcoal samples show that that the 4 m terrace (T-41) is of latest Pleistocene/earliest Holocene age and that two low terraces (T4 and T40) and the upper part of one alluvial fan (T1) are of late Holocene age (Table 6). Samples collected from beneath the 4.0 m terrace at T41 range in age from 10,010 to 8765 yr BP. The three ages within the profile are not in stratigraphic order, perhaps as a result of differences in the ages of wood prior to burning or mixing of charcoal of different ages in the sediment (Madole, 1995). At site T4 in the upper canyon, the 2.0 m terrace has an apparent time gap of ~850 years in the 20 cm thickness between the two charcoal-rich layers with the lower sample dated at 2770 yr BP (99-T4a) and the upper sample dated at 2060 yr BP (99-T4b). The age of the upper sample is nearly identical to the 2080 yr BP age of the alluvial fan at site T1 (99-T1). The 1.7 m fluvial terrace at site T40 has an age of 1480 yr BP (99-T40), younger than the nearby alluvial fan at T1. Rounded chunks of charcoal at T40 suggest transport prior to deposition, thus the deposit is not necessarily related to the alluvial fan at T1, but possibly to some upstream source.

Fan accumulation rates

We can use the ^{14}C ages and inferences about genetic relations between fans and terraces to estimate accumulation rates for the alluvial fans along Boulder Canyon (Table 7). Fan morphology (Fig. 6) suggests that a considerable volume of alluvial material has been removed from fans T41 and T4, with eroded sediment deposited in adjacent terraces or transported farther downstream. Our volume estimates for fans T41 and T4 thus are minimums, and accumulation rates will also be minimum values. We do not calculate

accumulation rates for fan T2 since we have no charcoal dates to constrain accumulation. The volume at fan T1 is a maximum since we assume that it is smaller than our largest mapped fan, thus its accumulation rate is also a maximum. At site T4, we can infer from the graphic log (Fig. 17) that most of the alluvial material has accumulated since 2770 yr BP, the oldest age in the section. This assumption provides an accumulation rate of >0.3 $Mgha^{-1}yr^{-1}$. For the fan at T41, we can assume that approximately half of the fan's volume accumulated between 10 ka and ~ 9 ka, since half of depth of alluvial material is bounded by these ages. This assumption gives an accumulation rate of >0.35 $Mgha^{-1}yr^{-1}$. It is difficult to estimate accumulation rates for the fan at site T1 due to insufficient surveying of the fan. Nonetheless, if we assume that fan T1 is smaller than our largest mapped fan (50,000 m^3), we can provide an upper limit for accumulation rate by assuming that less than 50,000 m^3 of alluvial material has moved in the past 2080 yr BP, based on the charcoal age from within the fan. This gives an accumulation rate of <0.45 $Mgha^{-1}yr^{-1}$.

If we predict, instead, that deposition on fans is nonlinear over time after a major geomorphic disturbance such as a fire, we can assume that accumulation decreases rapidly in the 10 years following the event (conservative estimate based on Robichaud, 1999) rather than remaining constant over time. We thus calculate an average value for accumulation of fan material over a period of 10*x years, where x represents the number of events that contributed to fan formation as represented by charcoal-rich layers within a profile. For the fan at T4, two charcoal layers allow us to assume accumulation over a 20 year time period, with accumulation >39 $Mgha^{-1}yr^{-1}$. Two events leading to the accumulation at T41 result in an accumulation rate of >35 $Mgha^{-1}yr^{-1}$. A single exposure at fan T1 and the maximum estimate for the fan volume results in an accumulation rate of <96 $Mgha^{-1}yr^{-1}$. The range of accumulation rates, based on the assumption of

exponentially declining accumulation following fire events, thus is ~ 35 to <96 $Mgha^{-1}yr^{-1}$.

Discussion

History of Holocene geomorphic deposits in Middle Boulder Creek

Dated low terrace remnants and alluvial fans preserve local records of latest Pleistocene/earliest Holocene and late Holocene deposition in Boulder Canyon. Our mapping and ^{14}C ages suggest that terraces > 4m above the modern channel are early Holocene or older, and that surfaces between ~ 1 and 3 m are of late Holocene age. The map and temporal patterns of deposition suggest that stream incision through a late Pleistocene fill and downstream redeposition led to the formation of a basal fill terrace. Fire then destabilized several tributary catchments, contributing to periods of local deposition in the form of alluvial fans and genetically related fluvial terraces during latest Pleistocene/earliest Holocene time, and again during late Holocene time. None of the deposits we studied indicated a middle Holocene period of accumulation; however, middle Holocene deposits may simply not have been preserved in Boulder Canyon. Madole (1995) does report extensive middle Holocene alluvial deposition in the Southern Rocky Mountains.

Despite a range of assumptions made for each of the estimated accumulation rates for three of our alluvial fans, they each fall within the same order of magnitude for long-term accumulations averaged over 1000-3000 years, and for short-term averages that assume most accumulation occurs episodically within the first 10 years following a burn. The 0.2 to 0.4 $Mgha^{-1}yr^{-1}$ long-term estimates are very similar to Robichaud's (1999) 0.1 $Mgha^{-1}yr^{-1}$ measurement of rates of accumulation for fans several years after burning. When we assume a shorter-term, episodic accumulation history for our fans, our 35 to <96 $Mgha^{-1}yr^{-1}$, estimates also correlate well with Robichaud's >50 $Mgha^{-1}yr^{-1}$ measurement of accumulation rate in recently-burned catchments. The low end of our

estimates is also in general agreement with the upper limits of Bovis' (1974) measurements of soil movement on slopes within Boulder Canyon (0.2 to 0.002 $Mgha^{-1}yr^{-1}$). In order to accumulate material in alluvial fans rather than to transport sediment downstream, accumulation rates must have exceeded the amount of sediment normally transported by Front Range rivers (i.e.,1.5 $Mgha^{-1}yr^{-1}$ in Clear Creek). Fan formation therefore must have happened at rates closer to our episodic accumulation rates than to our long-term accumulation rates. Episodic erosion rates between 35 and 95 $Mgha^{-1}yr^{-1}$ following burns could have lead to periodic accumulation in alluvial fans

Links between forest fire frequency and climate regime in the Front Range

Ages of alluvial fans and fluvial terraces from the Middle Boulder Creek drainage support regional paleoclimatic, paleovegetational, and geomorphic evidence for frequent fires in late Holocene time. At least four fire events, recorded as charcoal-rich layers in fluvial terraces or by deposition of alluvial fans, occurred between 1480 and 2770 yr BP. The similar ages for charcoal in fluvial deposits at site T4 (2060 yr BP) and within the alluvial fan at site T1 (2080 yr BP) indicates that the charcoal could have been produced in a single event that led to deposition at both sites. The dry climate of the late Holocene probably had a strong influence on forest fire frequency.

Early Holocene fan accumulation likely reflects forest fires associated with short term oscillations in a climate regime characterized by warm temperatures and high precipitation. Reworked glaciofluvial sediment is the likely origin of the basal portion of the fluvial terrace at site T41, but the overlying charcoal-rich layers suggest that the sediment came from burned and destabilized slopes from 9 to 11 ka. Little evidence for late Pleistocene/early Holocene forest fires has been noted previously in the Front Range region. Assuming a close relationship between climate and forest fires, we might predict that the warm, wet period from 11,000 through 6000 yr BP was one characterized by few

fires, thus our deposit as well as Coe's 1998 data are anomalous. However, Veblen et al. (2000) state that some of the most extensive historic forest fires occur during warm, dry summers that had been preceded 2 to 4 years by high precipitation which allowed for the growth of vegetation to fuel fires. Climate records over the past ~100 years in Yellowstone National Park imply that "the intensity and interannual variability of summer precipitation are greater during warmer periods, enhancing the potential for severe short-term drought, major forest fires, and storm-generated fan deposition." (Meyer et al. 1995, p. 1211). Such patterns attest to the importance of climate-induced vegetation change in controlling forest fire frequency, though the change may not be discerned in paleoclimatic reconstructions based on palynology. As a result, we view the link between paleoclimatic reconstructions and forest fire frequency with some caution. Dry periods probably coincide with high forest fire frequency, but there is also a possibility of high forest fire frequency during other climate regimes in regions where vegetation is strongly affected by climate changes. The warm, wet early Holocene climate of the Colorado Front Range was probably interspersed with periods of drought, accounting for early Holocene fires and their associated fan deposition.

Alluvial fans in Boulder Canyon therefore suggest close linkage between climate regime and forest fire frequency, with periods of major accumulation in the Front Range occurring throughout the Holocene period. However, such linkages may be difficult to discern since most climate reconstructions do not provide the kind of resolution necessary to identify certain climate regimes associated with high forest fire frequency.

CONCLUSIONS

Alluvial fans and fluvial terraces preserve evidence of system responses to sediment budget perturbations related to past climate change, and preserve evidence of processes that have contributed to the evolution of the Colorado Front Range. Cosmogenic ^{26}Al, ^{10}Be, ^{36}Cl, and ^{14}C dating of geomorphic surfaces within and around Boulder Canyon provide for a detailed temporal perspective on processes contributing to the evolution of the Colorado Front Range. This thesis contributes a series of new ages that help constrain the glacial chronology in the Front Range region, a detailed analysis of fluvial response to glaciation, and perspective on other processes that presently contribute to the evolution of steep Front Range canyons. These results, coupled with work performed in other regions, lead to a host of new information concerning the geomorphic history of Boulder Canyon:

- Boulders from late Pleistocene glacial moraines near Nederland in the Colorado Front Range and near Twin Lakes Reservoir have model cosmogenic ^{10}Be, ^{26}Al, and ^{36}Cl exposure ages consistent with existing age estimates from sites in Wyoming, southwest Montana, and other regions of Colorado.
- Heights of Boulder Canyon terraces can be divided into intervals that correspond to Bull Lake, Pinedale, and Holocene events.
- No pre-Bull Lake deposits are preserved in Boulder Canyon.
- The height-age relationship of terraces reflects long-term net incision of Middle Boulder Creek with short-term fluctuations in base level during periods of rapidly changing stream load and power.
- Net river incision apparently occurred during transitions to interglacial periods.
- Middle to late Pleistocene incision rates represented by high terraces in Boulder Canyon are faster than early Pleistocene rates, possibly as a result of east to west migration of a knickpoint on Middle Boulder Creek.

- Extrapolation of incision rate based on the position and age of terraces suggests that canyon incision started ~ 2.5 Ma.
- Soil development, stratigraphic position, and age estimates suggests that terraces within Boulder Canyon can be correlated with alluvial surfaces on the High Plains east of the canyon.
- Low terraces (< 4 m above grade) and alluvial fans along Boulder Canyon between Nederland and Boulder record Holocene deposition resulting from forest fires.
- Forest fire occurrence in Boulder Canyon correlates with a dry late Holocene climate and with the warm and wet early Holocene climate.

These results provide new perspective on traditional work that has been performed both locally and regionally. Ages of geomorphic features from this thesis provide a basis for quantifying age estimates based on degree of soil development. Previous work in Boulder Canyon had overestimated the ages of many deposits, and had not recognized any Holocene record. A revised calibration for soil-based age estimates could lead to reinterpretation several other features in the region.

Future work in this region may entail a more thorough evaluation of the local glacial chronology using cosmogenic exposure age dating of several more glacial moraines. This could also help reveal whether or not there is evidence for multiple Pinedale advances, since the terrace record suggests at least two potential retreats. A more thorough investigation of terraces within the canyon and/or local history may offer insights on the low exposure ages derived from my soil profile at site T64, and could aid in supporting/refining the conclusions I have drawn from my data. Finally, results from this thesis would greatly benefit from corroboration with data from nearby catchments.

REFERENCES

Aitken, M. J., 1990, *Science-based dating in archaeology,* London, New York: Longman, p. 56-119.

Andrews, J.T., Carrara, P.E., King, F.B., and Struckenrath, R., 1975, Holocene environmental changes in the alpine zone, northern San Juan Mountains: evidence from bog stratigraphy and palynology: Quaternary Research, v. 5, p. 173-197.

Barber, L. B., 1983, Correlation of river terrace deposits along Boulder Creek east slope, Colorado Front Range: University of Colorado, 20 p.

Benedict, J. B., 1967, Recent glacial history of an alpine area in the Colorado Front Range, U.S.A. --I. Establishing a lichen-growth curve: Journal of Glaciology, v. 6, p. 817-832.

Benedict, J. B., 1968, Recent glacial history of an alpine area in the Colorado Front Range, U.S.A. -- II. Dating the glacial deposits: Journal of Glaciology, v. 7, p. 77-87.

Benedict, J. B., 1973, Chronology of cirque glaciation, Colorado Front Range: Quaternary Research, v. 3, p. 584-599.

Benedict, J. B., 1981, The Fourth of July Valley -- glacial geology and archeology of the timberline ecotone: Ward, Colorado, Center for Mountain Archeology Research Report 2, 139 p.

Bierman, P., 1993, Cosmogenic isotopes and the evolution of granitic landforms (Ph.D. thesis), University of Washington, 268 p.

Bierman, P. R., 1994, Using in situ produced cosmogenic isotopes to estimate rates of landscape evolution: A review from the geomorphic perspective, Journal of Geophysical Research, v. 99, n. B7, p. 13,885-13,896.

Bierman, P., and Gillespie, A., 1991, Range fires: A significant factor in exposure-age determination and geomorphic surface evolution: Geology, v. 19, p. 641-644.

Bierman, P., Gillespie, A., Caffee, M., and Elmore, D., 1995a, Estimating erosion rates and exposure ages with ^{36}Cl produced by neutron activation: Geochemica et Cosmochemica Acta, v. 59, p. 3779-3798.

Bierman, P. R., Gillespie, A. R. and Caffee, M., 1995b, First ^{10}Be , ^{26}Al, and ^{36}Cl age-estimates for earthquake recurrence intervals and debris flow fan deposition, Owens Valley, California. Geological Society of America Abstracts with Programs, v. 27, n.6, p. A-376.

Bierman, P.R., Davis, P. T., Marsella, K., Colgan, P., Mickelson, D.M., Larsen, P. and Caffee, M., 1998, What do glaciers take away? What do they leave behind?: Geological Society of America Abstracts with Programs , v. 30, n. 7, p. A-299.

Bierman, P.R., Marsella, K.A., Davis, P.T., Patterson, C., and Caffee, M., 1999, Mid-Pleistocene cosmogenic minimum-age limits for pre-Wisconsinan glacial surfaces in southwestern Minnesota and southern Baffin Island -- a multiple nuclide approach: Geomorphology, v. 27, p. 25-40.

Birkeland, P. W., Miller, D. C., Patterson, P. E., Price, A. B., and Shroba, R. R., 1999, Soil-geomorphic relationships near Rocky Flats, Boulder and Golden, Colorado area, with a stop at the Pre-Fountain Formation paleosol of Wahlstrom (1948): Geological Society of America Field Trip #18, 13 p.

Birkeland, P. W., and Shroba, R.R., 1974, The status of the concept of Quaternary soil-forming intervals in the western United States, *in* Mahaney, W.C., ed., Quaternary environments: Toronto, Atkinson College/York University Geography Monograph No. 5, p. 241-276.

Birkeland, P.W., Burke, R.M., and Shroba, R. R., 1987, Holocene alpine soils in gneissic cirque deposits, Colorado Front Range: U. S. Geological Survey Bulletin 1590, 21 p.

Bovis, M. J., 1974, Rates of soil movement in the Front Range, Boulder County, Colorado (Ph.D. thesis): University of Colorado, 235 p.

Brook, E. J., and Kurz, M. D., 1993, Surface-exposure chronology using in situ cosmogenic ^{3}He in Antarctic quartz sandstone boulders, Quaternary Research, v. 39, p. 1-10.

Brown, E. T., Brook, E. J., Raisbec, G. M., Yiou, F., and Kurz, M. D., 1992, Effective attenuation of cosmic rays producing ^{10}Be and ^{26}Al : Geochimica et Cosmochimica Acta, v. 55, p. 2269-2283.

Burbank, D. W., Leland, J., Fielding, E, Anderson, R. S., Brozovic, N., Reid, M. R., and Duncan, C., 1996, Bedrock incision, rock uplift and threshold hillslopes in the northwestern Himalayas: Nature, v. 379, p. 505-510.

Campbell, I. A. N.,1961, Apparent relationships between stream profiles and pediments near Boulder, Colorado: M. A. Thesis, Department of Geography, University of Colorado, 79 p.

Carrara, P. E., Mode, W. N., Rubin, Meyer, and Robinson, S. W., 1984, Deglaciation and postglacial timberline in the San Juan Mountains, Colorado: Quaternary Research, v. 21, p. 42-55.

Chadwick, O. A., Hall, R. D., and Phillips, F. M., 1997, Chronology of Pleistocene glacial advances in the central Rocky Mountains, Geological Society of America Bulletin, v.109, no. 11, p. 1443-1452.

Chapin, C. E., and Cather, S. M., 1994, Tectonic setting of the axial basins of the northern and central Rio Grande rifts, *in* G.R. Keller and S.M. Cather, eds., Basins of the Rio Grande Rift: Structure, stratigraphy, and tectonic setting: Geological Society of America Special Paper 291, p. 5-25.

Chapin, C. E., and Kelley, S. A., 1997, The Rocky Mountain Erosion Surface in the Front Range of Colorado, *in* D. W. Bolyard and S. A. Sonnenberg, eds., Geologic History of the Front Range, 1997 Rocky Mountain Section -AAPG Field Trip #7, p. 101-113.

Clapp, E., and Bierman, P., 1995, First geomagnetic-based, in situ produced cosmogenic isotope calibration program.: Geological Society of America Abstracts with Programs, v. 27, p. A-59.

Clark, D., Bierman, P.R., and Larsen, P., 1995, Improving in situ cosmogenic chronometers: Quaternary Research, v. 44, p. 366-376.

Colgan, P.M., Mickelson, D. M., Bierman, P. R., 2000, Deglacial timing, cosmogenic ^{10}Be and ^{26}Al evidence, south central Wisconsin, USA: Geological Society of America Bulletin, (in review).

Coe, J. A., Godt, J.W., Parise, M., 1998, Evaluation of stream and debris flow hazards on small fans along the Interstate-70 highway corridor, Central Colorado, U.S.A.: 23rd

General Assembly, European Geophysical Society, Nice, France, April, 1998, Annales Geophysicae, v. 16, Supplement IV, p. C1215.

Coe, J. A., Savage, B., and Crane, M., 1999, Vail rocks 99 37th rock mechanics symposium, geology and geologic hazards along the Interstate 70 corridor, Denver to Vail, Colorado, 29 p.

Davis, P. T., 1982, Chronology of Holocene glaciation, Arapaho cirque, Colorado Front Range: Abstracts for the XI Congress of the International Union for Quaternary Research, v. II, Moscow, p. 54.

Davis, P. T., 1987, late Pleistocene age for type Triple Lakes moraines, Arapaho Cirque, Colorado Front Range: Geological Society of America Abstracts with Programs, v. 19, n. 5, p. 270. Davis, R., and Schaeffer, O.A., 1955, Chlorine-36 in nature: Annals of the New York Academy of Science, v. 62, p. 105-122.

Davis, P. T., Birkeland, P. W., Caine, N., and Rodbell, D. T., 1992, New radiocarbon ages from cirques in Colorado Front Range: Geological Society of America Abstracts with Programs, v. 24, p. A-347.

Davis, W. M., 1911, The Colorado Front Range, a study on physiographic presentation: Association of American Geographers Annals, v. 11, p. 21-83.

Doerner, J. P., 1994, The late-Quaternary environmental history of Mt. Evans: pollen and stratigraphic evidence from Clear Creek, Colorado (Ph.D. thesis), Denver, Denver University, 216 p.

Dunai, T.J., 2000, Scaling factors for production rates of in situ produced cosmogenic nuclides: a critical reevaluation: Earth and Planetary Science Letters, v. 176, p. 157-169.

Dunne, J., Elmore, D., and Muzikar, P., 1999, Scaling factors for the rates of production of cosmogenic nuclides for geometric shielding and attenuation at depth on sloped surfaces: Geomorphology, v. 27, p. 3-11.

Elias, S. A., 1996, Late Pleistocene and Holocene seasonal temperatures reconstructed from fossil beetle assemblages in the Rocky Mountains: Quaternary Research, v. 46, p. 311-318.

Elias, S. A., 1999, Geologic records of past climatic episodes: analogs for future global warming and implications for the Front Range region: Geological Society of America Abstracts with Programs, v. 31, n. 7, p. A-442.

Elias, S. A., Carrara, P. E., Toolin, L. J., and Jull, A. J. T., 1991, Revised age of deglaciation of Lake Emma based on new radiocarbon and macrofossil analysis: Quaternary Research, v. 36, p. 307-321.

Epis, R. C., Scott, G. R., Taylor, R. B., and Chapin, C. E., 1980, Summary of Cenozoic geomorphic volcanic and tectonic features of central Colorado and adjoining areas: Colorado Geology, H. C. Kent and K. W. Porter, eds., Rocky Mountain Association of Geologists, Denver, Colorado, p. 135-156.

Fall, P. L., 1985, Holocene dynamics of the subalpine forest in central Colorado: American Association of Stratigraphic Palynologists, Contributions Series, v. 16, p. 31-46.

Fall, P. L., 1997, Timberline fluctuations and late Quaternary paleoclimates in the Southern Rocky Mountains, Colorado: Geological Society of America Bulletin, v. 109, n. 10, p. 1306-1320.

Gable, Dolores J., 1969, Geologic map of the Nederland quadrangle, Boulder and Gilpin Counties, Colorado: U. S. Geological Survey Geologic Quadrangle Map GQ-833, scale 1:24,000.

Gable, Dolores J., 1972, Geologic map of the Tungsten Quadrangle, Boulder, Gilpin, and Jefferson Counties, Colorado: U. S. Geological Survey Geologic Quadrangle Map GQ-978, scale 1:24,000.

Gable, D. J., and Madole, R. F., 1976, Geologic map of the Ward Quadrangle, Boulder County, Colorado, U. S. Geological Survey Map GQ-1277, scale 1:24,000.

Gosse, J. C., Evenson, E. B., Klein, J., Lawn, B., and Middleton, R., 1995, Precise cosmogenic ^{10}Be measurements in western North America – support for a global Younger Dryas cooling event: Geology, v. 23, p, 877-880.

Gregory, K. M., and Chase, C. G., 1994, Tectonic and climatic significance of a late Eocene low relief, high-level geomorphic surface, Colorado: Journal of Geophysical Research, v. 99, n. B10, p. 20141-20160.

Hancock, G. S., Anderson, R. S., Chadwick, O. A., and Finkel, R. C., 1999, Dating fluvial terraces with ^{10}Be and ^{26}Al profiles: application to the Wind River, Wyoming: Geomorphology, v. 27, p. 41-60.

Hanson, W. R., Chronic, J., and Matelock, J., 1978: Climatography of the Front Range urban corridor and vicinity, Colorado: U. S. Geological Survey Professional Paper1019, 59 p.

Hedge, C. E., 1967, Precambrian geochronology of the Central Front Range, Colorado: Geological Society of America, Rocky Mountain Section , 20th Annual Meeting, p. 39.

Hunt, C. B., 1954, Pleistocene and recent deposits in the Denver area, Colorado: U. S. Geological Survey Bulletin 996-C, p. 91-140.

Jacob, A. E., and Albertus, R. G., 1985, Thrusting, petroleum seeps, and seismic exploration, Front Range south of Denver, Colorado, *in* D. L. Macke and E. K., Maughan, eds., Rocky Mountain Field Trip Guide -1985: Rocky Mountain Section - DEPM, Denver, p. 77-96.

Jarrett, R. D., 1999, Geomorphic estimates of rainfall, floods, and sediment runoff: applied to the 1996 wildfire, Buffalo Creek, Colorado: Geological Society of America Abstracts with Programs, v. 31, n. 7, p. A-313.

Keattch, S. E., 1994, Lake sediment record of Holocene fire events in the Green Lakes valley, Colorado Front Range, U.S.A.: Geological Society of America Abstracts with Programs, v. 26, n. 7, p. A-303.

Knight, S. H., 1990, Illustrated history of the Medicine Bow Mountains and adjacent areas, Wyoming: Laramie, Geological Survey of Wyoming Memoir 4, 49p.

Kohl, C.P., and Nishiizumi, K., 1992, Chemical isolation of quartz for measurement of *in-situ* -produced cosmogenic nuclides: Geochimica et Cosmochimica Acta, v. 56, p. 3583-3587.

Kurz, M. D., 1986, Cosmogenic helium in a terrestrial igneous rock: Nature, v. 320, p. 435-439.

Lal, D., 1988, In situ-produced cosmogenic isotopes in terrestrial rocks: Annual Reviews of Earth and Planetary Science, v. 16, p. 355-388.

Lal, D., 1991, Cosmic ray labeling of erosion surfaces, in situ production rates and erosion models: Earth Planetary Scientific Letters, v. 104, p. 424-439.

Larsen, P.L., Bierman, P.R., and Caffee, M., 1995, Preliminary in situ production rates of cosmogenic ^{10}Be and ^{26}Al over the past 21.5 ky from the terminal moraine of the Laurentide ice sheet, north-central New Jersey.: Geological Society of America Abstracts with Programs, v. 27, p. A59.

Legg , T. E., and Baker, R. G., 1980, Palynology of Pinedale sediments, Devlins Park, Boulder Country, Colorado: Arctic and Alpine Research, v. 12, no. 3, p. 319-333.

Leonard, E. M., and Langford, R. P., 1994, Post-Laramide deformation along the eastern margin of the Colorado Front Range - a case against significant deformation: The Mountain Geologist, v. 31, p. 45-52.

Love, J. D., 1960, Cenozoic sedimentation and crustal movement in Wyoming: American Journal of Science, v. 258A, p. 204-214.

Machette, M. N., 1977, Geologic map of the Lafayette Quadrangle, Adams, Boulder, and Jefferson Counties, Colorado: U. S. Geological Survey Geologic Quadrangle Map GQ-1392, scale 1:24,000.

Madole, R. F., 1969, Pinedale and Bull Lake glaciation in upper St. Vrain drainage basin: Arctic and Alpine Research, v.1, p. 279-287.

Madole, R. F., 1972, Neoglacial facies in the Colorado Front Range: Arctic and Alpine Research, v. 4, p. 119-130.

Madole, R. F., 1976a, Glacial geology of the Front Range, Colorado: in Mahaney, W. C., ed., Quaternary stratigraphy of North America: Stroudsburg, Pennsylvania, Dowden, Hutchinson and Ross, Inc., p. 297-318.

Madole, R. F., 1976b, Bog stratigraphy, radiocarbon dates, and Pinedale to Holocene glacial history in the Front Range, Colorado: U. S. Geological Survey Journal of Research, v. 4, no. 2, p. 163-169.

Madole, R. F., 1980, Time of Pinedale deglaciation in north-central Colorado: Further considerations: Geology, v. 8 p. 118-122.

Madole, R. F., 1986, Lake Devlin and Pinedale glacial history, Colorado Front Range, Colorado: Quaternary Research, v. 25, p. 43-54.

Madole R. F., 1991, Colorado Piedmont Section *in* Quaternary geology of the Northern Great Plains, Morrison, R. B., ed., Quaternary nonglacial geology: Conterminous U. S.: Boulder, Colorado, Geological Society of America, The Geology of North America, v. K-2, p. 441-476.

Madole, R. F., 1995, Fire frequency during the Holocene in a small, forested drainage basin in the Southern Rocky Mountains: Geological Society of America Abstracts with Programs, v. 27 n. 6, p. A-171.

Madole, R. F., and Shroba, R. R., 1979, Till sequence and soil development in the North St. Vrain drainage basin, east slope, Front Range, Colorado, *in* F. G. Ethridge, ed., Field Guide, northern Front Range and northwest Denver Basin, Colorado: Fort Collins, Colorado State University Department of Earth Resources, p. 123-178.

Madole, R. F., VanSistine, D. P., and Michael, J. A., 1998, Pleistocene glaciation in the Upper Platte River drainage basin, Colorado: U. S. Geological Survey Geological Investigations Series I-2644.

Mahaney, W.C., 1974, Soil stratigraphy and genesis of neoglacial deposits in the Arapaho and Henderson cirques, central Colorado Front Range, *in* Mahaney, W.C., ed., Quaternary environments: Toronto, Atkinson College/York University Geography Monograph No. 5, p. 197-240.

Maher, L. J., Jr., 1972, Absolute pollen diagram of Redrock Lake, Boulder County, Colorado: Quaternary Research, v.2, p. 531-553.

Mears, B. Jr., 1993, Geomorphic history of Wyoming and high-level erosion surfaces, in A.W. Snoke, J. R. Steidtmann, and S.M. Roberts, eds., Geology of Wyoming: Geological Survey of Wyoming Memoir 5, p. 608-626.

Menounos, B., and Reasoner, M. A., 1997, Evidence for cirque glaciation in the Colorado Front Range during the Younger Dryas Chronozone: Quaternary Research, v. 48, p. 38-47.

Merritts, D. J., Vincent, K. R., and Wohl., E. E., 1994, Long-river profiles, tectonism, and eustasy: A guide to interpreting fluvial terraces, Journal of Geophysical Research, v. 99, no. B7, p. 14,031-14,050.

Meyer, G. A., 1999, Alluvial fan deposits as recorders of fire and geomorphic response: Geological Society of America Abstracts with Programs, v. 31, n. 7, p. A-312.

Meyer, G. A., Wells, S. G., and Jull, T. A. J., 1995, Fire and alluvial chronology in Yellowstone National Park: Climatic and intrinsic controls on Holocene geomorphic processes: Geological Society of America Bulletin, v. 107, p. 1211-1230.

Millspaugh, S. H., Whitlock, C., and Bartlein, P. J., 2000, Variations in fire frequency and climate over the past 17,000 yr in central Yellowstone National Park: Geology, v. 28, no. 3, p. 211-214.

Moore, F. E., 1960, Summary of Cenozoic history, southern Laramie Range, Wyoming and Colorado: GSA, RMAG, and Colorado Scientific Society publication, p. 217-222.

Moses, T., 1982, Early reduction in post-fire erosion rates in the Colorado Front Range: American Geomorphological Field Group, Field Trip Guidebook, p.140.

Nelson, A. R., Millington, A. C., Andrews, J. T., and Nichols, H., 1979, Radiocarbon-dated upper Pleistocene glacial sequence, Fraser Valley, Colorado Front Range: Geology, v. 7., p. 410-414.

Nelson, A. R., Shroba., R. R., and Scott, G. R., 1984, Quaternary deposits of the upper Arkansas River valley, Colorado: Boulder, Colorado, American Quaternary Association, 8th Biennial Meeting, August 16-17, unpublished guide for Field Trip #7, 57 p.

Nelson, A. R., and Shroba, R. R., 1998, Soil relative dating of moraine and outwash-terrace sequences in the northern part of the upper Arkansas valley, central Colorado, U. S. A.: Arctic and Alpine Research, v. 30, n. 4, p. 349-361.

Netoff, D. I., 1977, Soil clay mineralogy of Quaternary deposits in two Front Range-Piedmont transects, Colorado (Ph.D. thesis), University of Colorado, 169 p.

Nichols, H., 1982, Review of late Quaternary history of vegetation and climate in the mountains of Colorado: Ecological Studies of the Colorado Alpine, University of Colorado Institute of Arctic and Alpine Research Occasional Paper 37, p. 27-33.

Nishiizumi, K., Winterer, E.L., Kohl, C.P., Klein, J., Middleton, R., Lal, D., and Arnold, J.R., 1989, Cosmic ray production rates of ^{10}Be and ^{26}Al in quartz from glacially polished rocks: Journal of Geophysical Research, v. 94, p. 17907-17915.

Nishiizumi, K., Kohl, C.P., Arnold, J.R., Klein, J., Fink, D., and Middleton, R., 1991, Cosmic ray produced ^{10}Be and ^{26}Al in Antarctic rocks: exposure and erosion history: Earth and Planetary Science Letters, v. 104, p. 440-454.

Pazzaglia, F. J., Gardner, T. W., and Merritts, D. J., 1998, Bedrock fluvial incision and longitudinal profile development over geologic time scales determined by fluvial terraces, *in* Rivers Over Rock: Fluvial Processes in Bedrock Channels, Geophysical Monograph 107, American Geophysical Union, p. 207-235.

Petersen, K.L., and Mehringer, P.J., 1976, Postglacial timberline fluctuations, La Plata Mountains, southwestern Colorado: Arctic and Alpine Research, v. 8, p. 275-288.

Phillips, F. M., Zreda, M. G., Gosse, J. C., Klein, J., Evenson, E. B., Hall, R. D., Chadwick, O. A., Pankaj, S., 1997, Cosmogenic 36-Cl and 10-Be ages of Quaternary glacial and fluvial deposits of the Wind River Range, Wyoming, Geological Society of America Bulletin: v. 109; no.11; p. 1453-1463.

Pierce, K. L., Obradovich, J. D., and Friedman, I., 1976, Obsidian hydration dating and correlation of Bull Lake and Pinedale glaciations near West Yellowstone, Montana: Geological Society of America Bulletin, v. 87, p. 703-710.

Raisbeck, G. M., Yiou, and Bourles, D., 1995, Evidence for an increase in cosmogenic 10Be during a geomagnetic reversal, Nature, v. 315, p. 315-317.

Raynolds, R. G., 1997, Synorogenic strata in the central Front Range, Colorado, *in* Bolyard, D. W., and Sonnenberg, S. A., eds., Geologic History of the Colorado Front Range: RMS-AAPG Field Trip #7, p. 43-47.

Reedy, R. C., Arnold, J. R., and Lal, D., 1983, Cosmic ray record in solar system matter: Science, v. 219, p. 127-135.

Robichaud, P. R., 1999, Fire and erosion: what happens after the smoke clears... : Geological Society of America Abstracts with Programs, v. 31, n. 7, p. A-312.

Sarda, P., Staudacher, T., Allegre, C., and Lecomte, A., 1993, Cosmogenic neon and helium at Reunion: Measurement of erosion rate: Earth Planetary Scientific Letters, v. 119, p. 405-417.

Scott, G. R., 1960, Subdivision of the Quaternary alluvium east of the Front Range near Denver, Colorado: Geological Society of America Bulletin, v. 71, p. 1541-1543.

Scott, G. R., 1962, Geology of the Littleton Quadrangle, Jefferson, Douglas, and Arapahoe Counties, Colorado: U. S. Geological Survey Bulletin, 1121-L, 53 p.

Scott, G. R., 1963, Quaternary geology and geomorphic history of the Kassler Quadrangle, Colorado: U.S. Geological Survey Professional Paper 421-A, 70 p.

Scott, G. R., and Lindvall, R. M., 1970, Geology of new occurrences of Pleistocene bisons and peccaries in Colorado: U. S. Geological Survey Professional Paper 700B, p. B141-B149.

Scott, G. R., and Taylor, R. B., 1986, Map showing late Eocene erosion surface, Oligocene-Miocene paleovalleys and Tertiary deposits in the Pueblo, Denver, and Greeley 1°x2° quadrangles, Colorado: U. S. Geological Survey Miscellaneous Investigations Series Map I-1626, scale 1:250,000.

Short, S. K., 1985, Palynology of Holocene sediments, Colorado Front Range: Vegetation and treeline changes in the upper subalpine forest: American Association of Stratigraphic Palynologists Contributions Series, v. 16, p. 7-29.

Short, S. K., and Elias, S. A., 1987, New pollen and beetle analyses at the Mary Jane site, Colorado: Evidence for late glacial tundra conditions: Geological Society of America Bulletin, v. 98, p. 540-548.

Shroba, R. R., 1976, Soil development on Pinedale, Bull Lake, and pre-Bull Lake tills, Sawatch Range and Front Range, Cristo Range, New Mexico, and Wind River Range, Wyoming: Geological Society of America, Abstracts with Programs, v. 8, no. 5, p. 629.

Shroba, R. R., 1977, Soil development in Quaternary tills, rock-glacier deposits, and taluses, Southern and Central Rocky Mountains: University of Colorado, Ph.D. thesis, 424 p.

Shroba, R. R., Rosholt, J. N., and Madole, R. F., 1983, Uranium-trend dating and soil B horizon properties of till of Bull Lake age, North St. Vrain drainage basin, Front Range, Colorado, Geological Society of America Abstracts with Programs, v. 15, no. 5, p. 431.

Small, E. E., Anderson, R. S., Repka, J. L., and Finkel, R., 1997, Erosion rates of alpine bedrock summit surfaces deduced from in situ ^{10}Be and ^{26}Al: Earth and Planetary Science Letters, v. 150, p. 413-425.

Sonnenberg, S. A., and Bolyard, D. W., 1997, Tectonic history of the Front Range in Colorado, *in* Bolyard, D. W., and Sonnenberg, S. A., eds., Geologic History of the Colorado Front Range: RMS-AAPG Field Trip #7, p. 1-7.

Steven, T. A., Evanoff, E., and Yuhas, R. H., 1997, Middle and late Cenozoic tectonic and geomorphic development of the Front Range of Colorado, *in* Bolyard, D. W., and Sonnenberg, S. A., eds., Geologic History of the Colorado Front Range: RMS-AAPG Field Trip #7, p. 115-124.

Stone, J. O. H., Evans, J. M., Fifield, L. K., Allan, G. L., Cresswell, R. G., 1998, Cosmogenic chlorine-36 production in calcite by muons: Geochimica et Cosmochimica Acta, v. 62, n. 3, p. 433-454.

Stuiver, M., and Reimer, P. J., 1993, Extended ^{14}C database and revised CALIB radiocarbon calibration program, Radiocarbon, v.35, p. 215-230.

Szabo, B. J., 1980, Results and assessment of uranium-series dating of vertebrate fossils from Quaternary alluviums in Colorado: Arctic and Alpine Research, v. 12, n. 1, p. 95-100.

Tanaka, S., Sakamoto, R., Takagi, J., and Tsuchimoto, M., 1968, Search for Aluminum 26 induced by cosmic-ray muons in terrestrial rock: Journal of Geophysical Research, v. 73, p. 3303-3309.

Thilenius, J. F., 1975, Alpine range management in the western United States - principles, practice, and problems. The status of our knowledge: U. S. Department of Agriculture, Forest Service Research Paper, RM-157, 32 p.

Troll, C., 1973, The upper timberlines in different climatic zone: Arctic and Alpine Research, v. 5, p. A3-A18.

Veblen, T.T., Kitzberger, T., and Donnegan, J., 2000, Fire Regimes in Colorado: climatic and human influences on fire regimes in ponderosa pine forests in the Colorado Front Range: Ecological Applications, (in press) 39 p.

Vierling, L. A., 1997, Palynological evidence for Late- and Postglacial environmental change in central Colorado: Quaternary Research, v. 49, p. 222-232.

Weldon, R. J., 1986, Late Cenozoic geology of Cajon Pass: Implications for tectonics and sedimentation along the San Andreas fault, (Ph.D. thesis), California Institute of Technology, Pasadena, 400 p.

Whitlock, C., 1999, Holocene fire-climate-vegetation linkages based on lake-sediment records from the northwestern U.S.: Geological Society of America Abstracts with Programs, v. 31, n. 7, p. A-313.

Whitlock, C., and Bartlein, P. J., 1993, Spatial variations of Holocene climatic change in the Yellowstone region: Quaternary Research, v. 39, p. 231-238.

Whitlock, C., Bartlein, P. J., and Van Norman, K. J., 1995, Stability of Holocene climate regimes in the Yellowstone Region: Quaternary Research, v. 43, p. 433-436.

Wruck, C. T., Wilson, R. F., Bucknam, R. C., Jones, L. R., Mendes, P., and Gardner, M. E., 1967, Geology of the Boulder Quadrangle, Colorado, U. S. Geological Survey, unpublished map, scale 1:24,000.

Zreda, M.G., Phillips, F.M., Elmore, D., Kubik, P.W., Sharma, P., and Dorn, R.I., 1991, Cosmogenic chlorine-36 production rates in terrestrial rocks: Earth and Planetary Science Letters, v. 105, p. 94-109.

Zreda, M., Phillips, F., Kubik, P.W., Sharma, P., and Elmore, D., 1993, Cosmogenic ^{36}Cl dating of a young basaltic eruption complex, Lathrop Wells, Nevada: Geology, v. 21, p. 57-60.

Appendix A: Calibrated and uncalibrated ^{14}C ages

Sample	^{14}C age (yr BP)	corrected (+/- years)	Number of ranges	Calibrated age ranges (cal BP)											
				(lower)	(upper)	(fraction)	(lower)	(upper)	(fraction)	(lower)	(upper)	(fraction)	(lower)	(upper)	(fraction)
99-T4a	2770	100	1	2969	2763	1									
99-T4b	2060	100	2	2144	1912	0.967	1911	1896	0.033						
99-T1	2080	90	1	2150	1928	1									
99-T40	1480	100	4	1508	1504	0.044	1484	1453	0.133	1440	1437	0.043	1423	1295	0.78
99-T41a	9450	90	3	11061	11012	0.127	11009	10952	0.13	10779	10555	0.743			
99-T41b	8765	140	2	10110	10083	0.067	9918	9556	0.933						
99-T41c	10010	190	2	11915	11812	0.125	11761	11209	0.875						
Buffalo1	11180	300	1	13470	12894	1									
Buffalo2	13680	220	1	16768	16075	1									
Lake Devlin 2	12180	480	2	15228	13804	0.977	13629	13591	0.023						
Lake Devlin 3	12910	540	2	16111	14999	0.694	14859	14339	0.306						
Lake Devlin 4	19000	500	1	23215	21871	1									
Mary Jane site	13740	320	1	16935	16046	1									
Santanta Peak	12040	120	2	14939	14863	0.054	14316	13813	0.946						
Triple Lakes 2	2910	130	3	3236	3235	0.024	3212	2917	0.898	2913	2877	0.078			
Triple Lakes 1	5035	150	2	5916	5640	0.972	5629	5615	0.028						
Butterfly Lake 1	10410	1040	3	13391	10687	0.995	10648	10643	0.003	10604	10604	0.003			
Butterfly Lake 2	9915	760	2	12629	12459	0.075	12424	10499	0.925						

Note: intercal98 cannot be used to correct ages older than ~ 21,000 14C yr
Calibrated ages determined with the intercal98.14 calibration curve, and reported with 1 sigma ranges.

Appendix B. (continued)

Sample	^{26}Al model age[2] (ka)	Weighted average (ka)	^{10}Be/^{26}Al	^{10}Be measured[4] (10^6 atom g^{-1})	^{26}Al measured[5] (10^6 atom g^{-1})	^{10}Be model e (m Ma^{-1})
99-t75	102.9 ± 22.3	101.2 ± 21.4	6.04 ± 0.32	4.29 ± 0.10	25.884 ± 1.224	6.00 ± 1.34
99-t68	119.4 ± 26.1	121.8 ± 25.9	5.69 ± 0.31	4.59 ± 0.12	26.125 ± 1.260	4.78 ± 1.08
DC-91-3	nd	15.9 ± 3.3	nd	0.70 ± 0.03		
99-t76	16.9 ± 3.5	16.9 ± 3.5	6.04 ± 0.32	0.82 ± 0.02	4.966 ± 0.235	36.32 ± 7.82
99-t74	17.5 ± 3.6	17.5 ± 3.6	nd	nd	4.323 ± 0.207	nd
DC-91-2	15.3 ± 3.2	16.0 ± 3.3	nd	0.73 ± 0.02	4.25 ± 0.22	
99-t64-r	4.2 ± 0.9	4.0 ± 0.8	6.55 ± 0.57	0.14 ± 0.01	0.897 ± 0.065	161.24 ± 35.12
99-t64-0	2.8 ± 0.6	2.8 ± 0.6	6.01 ± 0.42	0.10 ± 0.00	0.621 ± 0.038	220.17 ± 47.39
99-t64-20	4.4 ± 1.0	4.3 ± 0.9	6.32 ± 0.79	0.13 ± 0.00	0.811 ± 0.097	177.26 ± 38.14
99-t64-40	2.6 ± 0.6	2.6 ± 0.6	nd	nd	0.384 ± 0.027	nd
99-t64-60	5.3 ± 1.1	5.4 ± 1.1	5.92 ± 0.41	0.11 ± 0.00	0.641 ± 0.039	210.09 ± 45.23
99-t64-80	5.8 ± 1.2	5.6 ± 1.2	6.53 ± 0.48	0.09 ± 0.00	0.564 ± 0.033	263.29 ± 57.08
99-t64-100	8.9 ± 1.8	8.3 ± 1.8	6.86 ± 0.51	0.10 ± 0.00	0.687 ± 0.045	227.39 ± 48.91
99-t64-120	16.4 ± 3.6	16.2 ± 3.4	6.21 ± 0.37	0.17 ± 0.01	1.032 ± 0.053	136.71 ± 29.37
99-t10-1	18.2 ± 3.8	19.0 ± 3.9	5.59 ± 0.35	0.27 ± 0.01	1.512 ± 0.085	62.03 ± 13.34
99-t10-1	12.0 ± 2.5	12.6 ± 2.6	5.59 ± 0.35	0.27 ± 0.01	1.512 ± 0.085	62.03 ± 13.34
99-t18	16.2 ± 3.3	16.0 ± 3.2	6.19 ± 0.36	0.29 ± 0.01	1.774 ± 0.092	54.26 ± 11.67
99-t26-1	nd	13.8 ± 2.8	nd	0.26 ± 0.01	nd	57.48 ± 12.36
99-t43	11.8 ± 2.5	11.8 ± 2.4	6.01 ± 0.42	0.43 ± 0.01	2.558 ± 0.167	51.20 ± 11.00
99-t60-1	32.7 ± 6.8	36.3 ± 7.5	4.97 ± 0.28	1.34 ± 0.04	6.678 ± 0.320	15.20 ± 3.32
99-t71-1	22.9 ± 4.8	22.7 ± 4.7	6.20 ± 0.34	0.56 ± 0.01	3.477 ± 0.167	28.04 ± 6.05
99-t71-2	28.3 ± 5.9	29.2 ± 6.0	5.61 ± 0.33	0.56 ± 0.01	3.152 ± 0.168	27.65 ± 5.97
99-t72	131.8 ± 28.4	129.8 ± 27.5	6.03 ± 0.35	2.34 ± 0.08	14.133 ± 0.667	6.41 ± 1.44

Appendix B. (continued)

Sample	^{26}Al model e (m Ma^{-1})	measured ^{36}Cl/Cl (x 10^{-15})	radiogenic ^{36}Cl/Cl[5] (x 10^{-15})	σ (cm^2 g^{-1})	FR ^{10}Be	FR ^{26}Al	thickness correction[6]	geometric correction[7]	depth correction[8]
99-t75	5.64 ± 1.36	nd	nd	nd	6.00	36.0	1.03	1.00	1.00
99-t68	4.82 ± 1.18	nd	nd	nd	6.03	36.8	1.01	1.00	1.00
DC-91-3		350 ± 11	19	0.00776			1.01	1.00	1.00
99-t76	35.76 ± 7.90	nd	nd	nd	6.00	36.0	1.05	1.00	1.00
99-t74	34.62 ± 7.66	nd	nd	nd	6.00	36.0	1.01	1.00	1.00
DC-91-2		339 ± 13	19	0.00705			1.01	1.00	1.00
99-t64-r	147.42 ± 33.20	nd	nd	nd	6.00	36.0	1.02	0.99	1.00
99-t64-0	223.26 ± 49.40	nd	nd	nd	6.03	36.8	1.00	0.99	1.00
99-t64-20	170.84 ± 41.76	nd	nd	nd	6.03	36.8	1.00	0.99	0.81
99-t64-40	361.14 ± 80.83	nd	nd	nd	6.03	36.8	1.00	0.99	0.65
99-t64-60	216.35 ± 47.85	nd	nd	nd	6.03	36.8	1.00	0.99	0.53
99-t64-80	245.76 ± 54.21	nd	nd	nd	6.03	36.8	1.00	0.99	0.43
99-t64-100	201.80 ± 44.95	nd	nd	nd	6.03	36.8	1.00	0.99	0.35
99-t64-120	134.09 ± 29.39	nd	nd	nd	6.03	36.8	1.00	0.99	0.28
			nd						
99-t10-1	67.42 ± 13.93	nd	nd	nd	6.03	36.8	1.02	0.90	0.55
99-t10-1	67.42 ± 14.93	nd	nd	nd	6.03	36.8	1.02	0.90	0.83
99-t18	53.18 ± 11.75	nd	nd	nd	6.03	36.8	1.04	0.97	0.73
99-t26-1	nd	nd	nd	nd	6.03	36.8	1.02	0.77	1.00
99-t43	51.65 ± 11.60	nd	nd	nd	6.03	36.8	1.02	1.00	1.00
99-t60-1	18.39 ± 4.13	nd	nd	nd	6.03	36.8	1.03	1.00	1.00
99-t71-1	27.27 ± 6.06	nd	nd	nd	6.03	36.8	1.02	0.97	1.00
99-t71-2	29.24 ± 6.53	nd	nd	nd	6.00	36.0	1.02	0.97	0.73
99-t72	6.05 ± 1.45	nd	nd	nd	6.00	36.0	1.03	0.97	0.73

Appendix B. (continued)

Notes:

1: From relative soil development

2: Calculated using Nishiizumi et al. (1989) production rate estimates of ^{10}Be = 6.03 atomsg^{-1} yr^{-1}; ^{26}Al = 36.8 atoms$g^{-1}yr^{-1}$; also samples at 40° N; density = 2.7 gcm^{-3}(rock), 1.5 gcm^{-3} (soil); latitude = 40° N; attenuation length = 165 gcm^{-2}.

3: Average (weighted) calculated considering uncertainty of each measurement.

4: uncertainty is counting statistics and carrier (2%) only

5: uncertainty is counting statistics and stable Al (4%) only

6: made integrating flux through sample thickness using $\rho = 2.7$, $\Lambda = 165$ g cm^{-2}

7: made using technique of Dunne (1999) for exposure geometry

8: using $\rho = 1.5$ for depth correction on buried samples